Universitat Autònoma de Barcelona

Tesis Doctoral

MESENCHYMAL STROMAL CELL THERAPY FOR CARTILAGE REGENERATION: *IN VIVO* TESTING IN A REFINED PRECLINICAL SHEEP MODEL OF CHONDRAL AND OSTEOCHONDRAL LESIONS

Carla Sofia Freire Ribeiro da Fonseca

2015

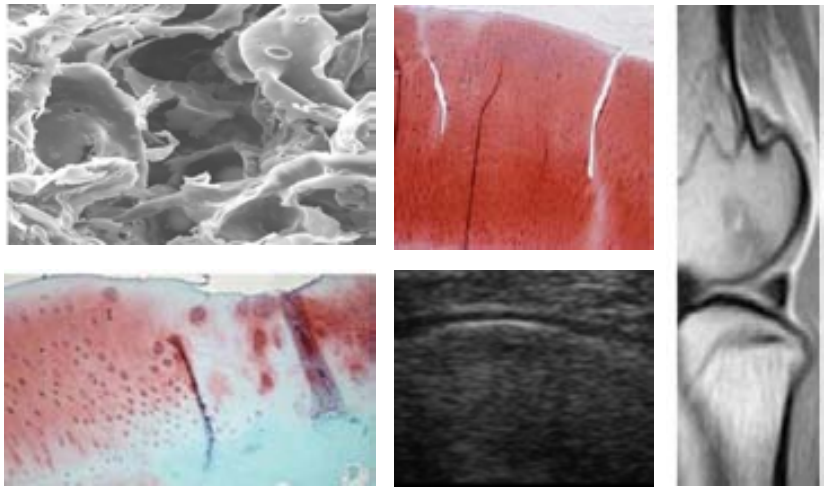

Universitat Autònoma de Barcelona

Facultat de Veterinària

Departament de Medicina i Cirurgia Animals

Programa de Doctorat en Medicina i Sanitat Animal

MESENCHYMAL STROMAL CELL THERAPY FOR CARTILAGE REGENERATION: *IN VIVO* TESTING IN A REFINED PRECLINICAL SHEEP MODEL OF CHONDRAL AND OSTEOCHONDRAL LESIONS

Tesi que presenta

Carla Sofia Freire Ribeiro da Fonseca

per optar al títol de doctora

Directors de tesi:

Félix Angel García Arnás

Jordi Joan Cairó Badillo

2015

A mis padres, Arlindo y Laura.

A mi hermano Bruno.

A mis tios Emilia y Necas.

A mi compañero Jorge.

AGRADECIMIENTOS

Tengo como gran referencia en mi vida personal y profesional a mi padre, Hombre cuyo gusto por la naturaleza, medicina y ciencia han influenciado decisivamente mi vida y mi camino. Con su gusto y espirito perfeccionista en el trabajo, el suelea decir muy frecuentemente que el trabajo une a las personas. De los proyectos de investigación que han dado origen a esta tesis, que han envuelto la labor de muchos y diversos profesionales, han nascido lazos de unión muy especiales, que han resultado de la ilusión por la descubierta y de la construcción de un objetivo común.

La mayor riqueza de estos años, es sin duda la gran calidad humana y profesional del equipo que he tenido el privilegio de integrar. Por eso, a todos ellos quiero aquí transmitir mis más sinceros agradecimientos.

Antes de todo quiero agradecer a mis directores de tesis, Félix García y Jordi Cairó, por la confianza que han depositado en mí, por todos los enseñamientos transmitidos, y por me hubieren abierto las puertas al mundo de la investigación.

Quero también agradecer a Marta Caminal y a David Peris, mis compañeros y amigos, sin los cuales este trabajo no hubiera sido posible.

A Quim Vives, Arnau Pla y a Francesc Godià por todo su trabajo.

A todos mis compañeros del Departamento de Medicina y Cirugía Animales, y muy en especial a Otilia Bambo, Xavier Moll y Anna Morist por su colaboración en el trabajo experimental.

A Rosa Rabanal e a Pere Jordi Fábregas por el criterioso trabajo de análisis histopatológico.

Al Dr. Josep Barrachina, David Codina y Carlos Guinot por las largas horas compartidas en quirófano.

A Christian de la Fuente, a Yvonne Espada y a Elisabet Dominguez por su colaboración en el estudio por imagen.

A todo el equipo del Servei de Granjes Experimentals de la UAB, en especial a Ramón Costa, Josep Ruiz de la Torre, Adela, Ramón, Josep y Valeriano por todo el apoyo en el trabajo experimental con los animales.

Quiero también agradecer a toda mi familia, muy en especial a mis padres, por su incentivo y por todo su apoyo. Sin ellos nunca hubiera podido empezar esta etapa. Quiero también agradecer a Jorge, mi compañero, por todo su amor y enorme incentivo en el finalizar de esta fase.

Por fin, unas palabras de profundo reconocimiento a todos los animales que entraran en el estudio.

Cuando terminé la licenciatura en veterinaria, mi padre me ha regalado su fonendoscopio, diciéndome que estaba seguro que yo como veterinaria recibiría de mis pacientes signos de reconocimiento más sinceros que ellos (médicos) recibían muchas veces por parte de sus pacientes. Es verdad que al largo de estos años he recibido por parte de mis pacientes signos de reconocimiento muy especiales, que sin duda compensan todo el esfuerzo y dedicación que la profesión veterinaria exige. Pero en el área del animal de laboratorio, quien merece todo el reconocimiento son los animales, a quien utilizamos para buscar la respuesta a problemas muy concretos.

Las ovejas son unos animales de una estoicidad e inteligencia tan grande como su dulzura. Espero que el resultado de la investigación de estas nuevas terapias, ensayadas en esta especie, pueda un día venir a beneficiar no solo la clase de animales humanos como también la de animales no humanos.

INDEX

ABBREVIATIONS

1- ABBREVIATIONS

ACI- autologous chondrocyte implantation

ASC- adipocyte-derived mesenchymal stromal cell

BM-MSC- bone marrow-derived mesenchymal stromal cell

Co-MSC- chondrocyte-derived mesenchymal stromal cell

ECM- extra-cellular matrix

FDA- Food and Drug Administration

MACI- matrix-associated autologous chondrocyte implantation

MRI- magnetic resonance imaging

MSC- mesenchymal stromal cell

OA- osteoarthritis

PCL- polycaprolactone

PDO- polydioxanone

PFF- poly-propylene fumarate

PGA- polyglycolic acid

PLA- polylactic acid

PLGA- polylactic-poliglicolic acid

POE- polyorthoesters

STZ- superficial tangential zone

US- ultrasonography

ABSTRACT

2- ABSTRACT

One of the widest spread musculoskeletal diseases concerns the joints and involves the lesion of articular cartilage, being the knee one of the most affected joints.

Cartilage lesions can be divided on two different types: partial-thickness cartilage lesions (chondral lesions) which do not penetrate the underlying subchondral bone, and full-thickness cartilage lesions (osteochondral lesions) which penentrates the subchondral bone.

Actually there is no effective treatment for the chondral or osteochondral lesions, although a large investigation effort is being made in this issue. The present tendency is to develop new cell- and tissue-engineering-based methods that may overcome the size limitations of current technologies. For this purpose, the use of animal experimental models is of extreme importance, because they are a reliable source of information between the *in vitro* assays and the human therapy application.

Several animal models are used for cartilage repair strategies testing, from small to large animal models. Small animal models (rodents or rabbits) are recommended for mechanism or proof of principle studies when data regarding toxicity, formulation, dose response or safety are needed before further pivotal studies. However large animal models (dog, pig, goat, sheep or horses) are necessary for truly translational research aimed at gaining regulatory approval for clinical use in humans.

This work presents the study of an animal experimental model for the evaluation of the knee's cartilage regeneration with cellular therapies approach. The aim was the development of a refined animal model to assess the efficacy and safety of mesenchymal stromal cellular therapies with a possible future application in human medicine, and settle the basis for the clinical trials.

INTRODUCTION

3- INTRODUCTION

3.1- Epidemiology of Osteoarthritis

Musculoskeletal conditions are the most common cause of severe long-term pain and physical disability, and they affect hundreds of millions of people around the world. Osteoarthritis (OA) is one of the four major musculoskeletal conditions and is characterized by focal areas of loss of articular cartilage within synovial joints, which are associated with hypertrophy of bone (osteophytes and subchondral bone sclerosis) and thickening of the capsule. The course of the disease varies but is often progressive. Symptoms can be relieved and function improved, especially by joint replacement, but progression cannot be prevented yet (Woolf and Pfleger 2003).

Worldwide estimates are that 9.6% of men and 18% of women aged ≥60 years have syntomatic osteoarthritis. Radiographic studies of United States of America and European populations aged ≥45 years show higher rates for osteoarthritis of the knee: 14.1% for men and 22.8% for women (Woolf and Pfleger 2003).

Being OA a disease that causes significant pain and disability and leads in many cases to lasting joint damage, all countries need to focus on preventive and treatment strategies to reduce the burden it causes in the community (Brooks 2003).

3.2- Form and function of hyaline articular cartilage

Hyaline cartilage is an avascular tissue that contains only one cellular type (the chondrocyte) sparsely distributed in an extracellular matrix.

It is a viscoelastic material with variable load-bearing properties, associated with different positions and activities. Its complex organization and ultra-structure composition determines its ability to minimize surface friction on articular surfaces, high lubrication, shock absorption, and wear resistance while bearing large repetitive loads throughout a lifetime. These characteristics are clearly unmatched by any synthetic material (Flik, Verma *et al.* 2007).

Hyaline cartilage has a characteristic composition and architecture, and four distinct zones can be recognized (Figure 1 and Figure 2).

- Lamina splendens: consists in the superficial layer, made of tightly packed collagen fibers parallel to the articular surface and a cellular layer of flattened chondrocytes. Type IX collagen is found in this layer between type II bundles that provides resistance to shear. It is thought that this layer limits passage of large molecules between synovial fluid and cartilage, and it is known that preservation of this superficial layer is critical to protect the deeper zones.

- Transitional layer (intermediate zone): composed by spherical chondrocytes, proteoglycans and obliquely oriented collagen fibers that resist compressive forces but also serve as a transition between the forces in the surface and the compressive forces placed in the deeper layers.

- Deep zone: consists of collagen fibers and chondrocytes oriented perpendicular to the articular surface, which resist compressive loads.

- Calcified layer: is the tidemark that separates subchondral bone from the calcified cartilage and provides complex adhesive properties of the cartilage to bone.

Collectively, these highly specialized layers produce the superior loading and minimal friction characteristics of hyaline cartilage that make it particularly difficult to restore or duplicate once it is damaged or lost (Alford and Cole 2005).

The extra-cellular matrix of hyaline articular cartilage is also divided into regions, based on proximity to the chondrocyte, differing in content and in collagen fibril diameter and organization:

- Peri-cellular matrix: surrounds completely the chondrocyte, forming a thin layer around the cell membrane. Contains proteoglycans and non-collagenous matrix components but little or no collagen fibrils. This matrix region may play a functional biomechanical role for signal transduction within cartilage during loading.

- Territorial matrix: surrounds the peri-cellular region and contains thin collagen fibrils that form a fibrillar network at its periphery, which possibly provides mechanical protection for the chondrocyte during loading.

- Inter-territorial region: encompasses the entire matrix between the territorial matrices of the individual cells, and is the largest of all regions. In this zone reside large collagen fibrils and the majority of the proteoglycans. The collagen fibrils within the inter-territorial zone change orientation depending on the zone of articular cartilage: they are parallel to the surface in the superficial zone, obliquely in the middle zone, and perpendicular to the articular surface in the deep zone (Figure 2) (Flik, Verma *et al*. 2007).

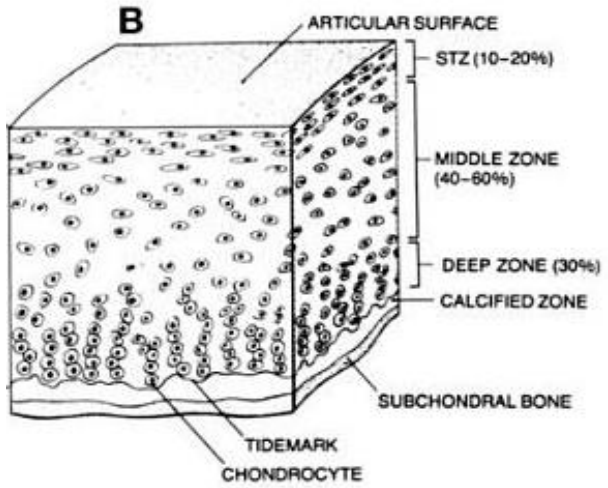

Figure 1- Schematic view of a section of normal articular cartilage structure. There are four zones: the superficial tangential zone (STZ), the middle zone, the deep zone, and the calcified zone. The cells in the superficial zone have an ellipsoidal shape and lie parallel to the surface; the cells of the other zones have a more spherical shape. In the deep zone, the chondrocytes align themselves in columns perpendicular to the surface (Flik, Verma *et al*. 2007).

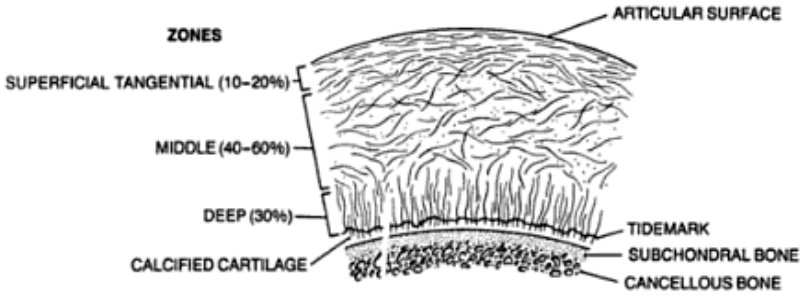

Figure 2- Schematic view of the inter-territorial matrix collagen fibril orientation and organization in normal articular cartilage. In the superficial tangential zone the fibrils lie nearly parallel to the surface. In the middle zone, they assume a more random alignment. In the deep zone, they lie nearly perpendicular to the articular surface (Flik, Verma *et al*. 2007).

The extracellular matrix of hyaline cartilage makes up approximately 95% of the tissue by volume and is mainly composed of type II collagen, but types V, VI, IX, X, XI, XII and XIV are also present in smaller amounts.

Sulphated proteoglycan macromolecules constitute 12% of articular cartilage weight. Keratin sulphate and chondroitin sulphate on the glycosaminoglycans carry a negative charge that creates a high affinity for water that helps cartilage resist compressive loads and causes the aggrecans to repel one another, resulting in maximal volume expansion.

The chondrocytes are of mesenchymal stem cell origin and are responsible for synthesizing the matrix. They constitute 2% of the total volume of adult articular cartilage. They are mainly anaerobic, and they survival depends on the proper chemical and mechanical environment, including growth factors, mechanical loads, hydrostatic pressures and piezoelectric forces (Alford and Cole 2005).

3.3- Response to Injury

The highly specific microscopic anatomy and interdependent physiology of articular cartilage can be disrupted by small, superficial injuries, even without immediate cartilage loss (Alford and Cole 2005).

- Partial thickness injuries:

Superficial damage will injure chondrocytes, limit their metabolic capacity for repair and lead to decreased proteoglycan concentration, increased hydration and altered fibrillar organization of collagen (Mankin 1982; Mow, Setton et al. 1990; Mankin, Mow *et al*. 1994). These alterations will lead to increased force transmission to the underlying subchondral bone, which increases its stiffness and, in turn, causes impact loads to be more readily transmitted to the partially damaged cartilage. This vicious cycle is thought to contribute to the progression of partial-thickness articular cartilage injuries.

The avascular nature of articular cartilage means that pure cartilage injuries do not cause hemorrhage or fibrin clot formation, or provoke an immediate inflammatory response. The chondrocytes respond by proliferating and increasing the synthesis of matrix macromolecules near the injury site, but the new matrix and proliferating cells cannot restore the surface (Mankin 1982).

- Full-thickness injuries:

A full-thickness injury to articular cartilage that penetrates subchondral bone provides access to cells, blood supply, and theoretically a higher capacity for repair (Goldberg and Caplan 1998).

Localized bleeding initiates a cascade beginning with hematoma formation, stem cell migration, and synthesis of type I cartilage, resulting in fibrocartilage rather than the hyaline cartilage produced by the chondrocyte. This repair tissue has inferior stiffness, inferior resistance and poorer wear characteristics than normal hyaline articular cartilage (Nehrer, Spector *et al.* 1999).

3.4- Current treatment options

The first arthroscopic treatment of chondral injuries was to debride the cartilage to reduce mechanical symptoms and inflammation that may arise from inflammatory mediators. Early cartilage repair techniques penetrated the subchondral bone to recruit pluripotential mesenchymal marrow stem cells that would differentiate and form fibrocartilage. Recently, autograft and allograft osteochondral plugs with true hyaline cartilage and subchondral bone have become popular. Biologic replacement with autologous chondrocyte implantation has led to more advanced biologically derived solutions to cartilage restoration (Alford and Cole 2005). The present direction involves synthetic implants and single-stage biologically active carriers or matrices.

- Arthroscopic lavage and debridement

Debridement of friable inflammatory tissue was popularized 6 decades ago as a method of reducing mechanical symptoms. Arthroscopic joint lavage without debridement provides short-term benefits in 50% to 70% of patients.

In carefully selected patients with a specific history of low-energy trauma, mechanical symptoms, minimal misalignment, stable ligaments, and low body mass index, arthroscopic debridement may be of some use, but in general, arthroscopic debridement and lavage alone have shown to have no significant lasting benefit in arthritic knees without specific localized mechanical symptoms (Harwin 1999).

- Marrow stimulation techniques

Techniques designed to stimulate the subchondral bone marrow rely on the differentiation of primitive mesenchymal cells to produce fibrocartilage, which is repair cartilage. Unlike hyaline cartilage, which contains primarily type II collagen, fibrocartilage is primarily composed of type I collagen, with marked differences in biomechanical and structural properties. After these techniques (drilling, abrasion arthroplasty, microfracture), the extent of fill is rarely more than 75% of the total volume of the chondral defect, and the biomechanical properties of the repair fibrocartilage are inferior to those of hyaline cartilage (Alford and Cole 2005).

- Cartilage replacement techniques

Osteochondral auto-grafts involve the transfer of intact hyaline cartilage and subchondral bone, and heal to the surrounding recipient tissue. Osteochondral auto-grafts are small bone plugs covered with normal hyaline articular cartilage that are removed from a relatively non-weight bearing surface and transferred in a single stage to the chondral defect. The key to this technique is chondrocyte viability because only living chondrocytes can produce and maintain the extracellular matrix of proper load-bearing capacity. The disadvantages of this technique include donor site morbidity and limited available graft volume. In addition, it is technically difficult to position the plugs to re-create the contour of curved surfaces (Alford and Cole 2005).

Fresh osteochondral allografts provide larger constructs of subchondral bone and viable cartilage from cadaveric donors. It is generally recommended that fresh articular cartilage allograft be transplanted within days of harvest, with the understanding that the longer the wait, the greater the death of cartilage cells. The urgent nature of using osteochondral grafts as they become available creates logistical challenges of obtaining the correct size graft at a time and place that the patient is available for surgery (Alford and Cole 2005).

- Biologic techniques

Autologous chondrocyte implantation (ACI) is a two-stage procedure in which an arthroscopic biopsy of normal hyaline cartilage is cultured in vitro, and the resulting chondrocytes are then re-implanted, by arthrotomy, into a cartilage defect beneath an autologous periosteal patch. This flap is used in

order to seal the chondrocyte suspension, increasing the cellular retention. However, complications at a relatively high rate such as hypertrophy and arthrofibrosis, caused by the periosteal flap, led to the development of matrix-associated ACI techniques (MACI) without the need of a periosteal flap. The tendency is to develop new cell- and tissue-engineering-based methods that may also overcome the size limitations of current ACI technologies and be applied to larger defects, like the cell-based-polymer therapy (Alford and Cole 2005).

These new techniques should be developed in order to pass from ACI to MACI, and from arthrotomy to arthroscopic surgical techniques.

3.5- Cartilage tissue engineering

Tissue engineering applies the knowledge of biology, cell transplantation, materials science and bioengineering to construct biological substitutes that can restore and maintain normal function in diseased or injured tissues (Vacanti and Upton 1994; Lu, Peter et al. 2000; Hollister 2005). In this strategy, a biodegradable three-dimensional (3D) porous scaffold is often used as a matrix to support cell adhesion, to guide new tissue formation, and to restore organ function. Tissue engineering is a potential alternative for the treatment of osteochondral defects, as it can be effectively used to regenerate cartilage, bone and cartilage-bone interface (Nukavarapu and Dorcemus 2013). Natural and synthetic polymeric biomaterials have been widely used for cartilage tissue engineering. It is well known that cell function on a scaffold is related to the chemical properties of the scaffold material, as the scaffold surface chemistry affects cell adhesion, morphology and activity (Singhvi, Kumar et al. 1994; Yousefi, Hoque et al. 2014).

Scaffold materials

Biomaterials used in tissue engineering can be categorized into four major groups: natural polymers, synthetic polymers, metallic materials, and inorganic materials such as ceramics and bioactive glasses (Place, George et al. 2009; Okamoto and John 2013).

Natural polymers like glycosaminoglycan, collagen, starch, hyaluronic acid, chitosan, alginate, and biodegradable bacterial plastics such as polyhydroxyalkanoates (PHA) are excellent biomaterials that support cell adhesion and regeneration while offering biocompatibility. One of the major constraints of natural polymers is that their mechanical properties are weaker when compared to ceramics and metallic materials (Yang and Temenoff 2009).

Synthetic biodegradable polymers used in tissue engineering include polyglycolic acid (PGA), polylactic acid (PLA), poly(L-lactic-co-glycolic acid) (PLGA), polycaprolactone (PCL), polydioxanone (PDO), poly(propylene fumarate) (PFF), polyorthoesters (POE), polyphosphazenes and polyanhydrides (Puppi, Chiellini *et al.* 2010; Dhandayuthapani, Yoshida *et al.* 2011; Liu, Holzwarth *et al.* 2012). The advantages that synthetic biodegradable polymers offer lie in their range of chemistries, ease of processing and controlled molecular weight distribution that can be tailored to the target application (Mano and Reis 2007; Yousefi, Hoque *et al.* 2014).

PLGA is a scaffold widely used on cartilage engineering. It is of easy production, and it is possible to modify characteristics. PLGA is non immunogenic and has been approved by the Food and Drug Administration (FDA) for clinical use.

Cell-free approaches

Published studies reveal that for small and confined osteochondral lesions, it might be sufficient to use a cell-free approach with appropriate scaffolds (e.g., adequate biomechanical properties and the capacity to resorb/remodel). Although in the case of more extended injuries, the delivery of growth factors is necessary for local cell recruitment. The use of a cell-based approach becomes mandatory if the wound bed is further compromised. Therefore, in most practical cases the scaffolding material alone cannot initiate biological responses that could support the regeneration process (Yousefi, Hoque *et al.* 2014).

Mesenchymal stromal cells as cell sources for cartilage regeneration

Currently, chondrocytes are the only identified cell source for the transplantation purposes. This cell source has important limitations, related to donor site availability and morbidity. Given the limitations of cartilage as a cell source, investigating an alternative cell source may provide improved treatment options with superior results (Tang, Carasco *et al.* 2012).

Mesenchymal stromal cells (MSC) have raised as a promising cell source candidate for cartilage regeneration in the treatment of articular cartilage defects (Baksh, Song *et al.* 2004).

MSC populations were first identified within the stromal compartment of bone marrow. Initially considered as supporting milieu for the maintenance and differentiation of the hematopoietic stem cells, it was later demonstrated by Friedenstein *et al.* (1968) that these cells had stem cell properties including clonal expansion by self-renewal and osteogenic differentiation (Friedenstein, Petrakova *et al.* 1968).

Interest in the application of MSCs for the development of articular cartilage cell therapies was renewed by the work of Pittenger *et al*. (1999) who demonstrated the multipotent differentiation of MSCs into three cell lineages of adipocytes, osteoblast and chondrocytes (Pittenger, Mackay *et al.* 1999).

MSC are a rare cell type but have been isolated from a multitude of tissues including bone marrow (Im, Kim *et al.* 2001; Murphy, Fink *et al.* 2003; Zhou, Liu *et al.* 2006; Koga, Muneta *et al.* 2008; Guo, Park *et al.* 2010), placenta (Timmins, Kiel *et al.* 2012), umbilical cord (Yang, Huang *et al.* 2012), skeletal muscle (Jackson, Lozito *et al.* 2010), synovium (Shirasawa, Sekiya *et al.* 2006; Jones and Pei 2012), synovial fluid (Jones, Crawford *et al.* 2008) and adipose tissue (Hennig, Lorenz *et al*. 2007; Yoshimura, Muneta *et al*. 2007; Koga, Muneta *et al.* 2008; Mizuno, Tobita *et al.* 2012). In contrast to mature chondrocytes, MSCs can be expanded *ex vivo* to relatively high cell numbers making them an attractive cell source for autologous cell therapies (Hardingham, Oldershaw *et al.* 2006; Khan, Malik *et al.* 2009; Oldershaw 2012).

MSC characteristics which increased interest in the scenario of cell-based therapy, as an alternative cell source, include the fact that MSC play an important role in the homeostasis and regeneration of tissues, are able to differentiate under appropriate stimuli *in vitro* into various cell lineages such as chondrocytes and osteoblasts, and are more abundant than chondrocytes without showing dedifferentiation phenomenon and the need for healthy cartilage biopsy to harvest cells (Caplan 2005). Moreover, MSCs have a trophic, anti-inflammatory and immunosuppressive action, by modulating T and B cells and inducing the expression of anti-inflammatory factors, such as interleukin 10 (IL-10), IL-1 receptor antagonist (IL-1RA) or prostaglandin E2 (PGE2) (Abumaree, Al Jumah *et al.* 2012; Veronesi, Maglio *et al.* 2013).

3.6- Preclinical studies

The treatment of articular cartilage defects is evolving rapidly, both for surgical treatments and for the specific field of cartilage repair products that contain living cells.

Prior to initiation of human trials, several types of information must be gathered in non-clinical models. Studies to provide a scientific and medical rationale for evaluating the experimental products in humans, to support an initial human dose and to evaluate potential toxicities are well-accepted components of most pharmaceutical development programs. Due to their inherent complexity, products containing cells require substantial additional information. These data may be gathered through numerous different studies, including the following assessments:

-interactions between cellular and device components of a combination product;

-biocompatibility analysis of the device component;

-analysis of the contributions of different components of a product to its biological action;

-evaluation of potential immune responses to the product;

-exploration of potential clinical or surrogate endpoints

Various experimental systems are usually combined to assemble a data set sufficiently comprehensive to allow sound decisions regarding conduct of initial clinical studies, and the selected models should reflect the type of information needed for the product in question (FDA Cellular 2005).

One of the most basic requirements in any pharmaceutical development program is data to provide reasonable assurance of the product´s safety. In addition to conventional safety studies that assess potential toxicities in a context designed to model the clinical indication, many cellular products need to be evaluated for their potential to undergo unanticipated undesired changes in their characteristics, such as malignant transformation.

Models designed to address this concern should evaluate a number of cells sufficient to detect rare events with reasonable statistical confidence. It is also important to assess the potential for adverse events in models approximating the human clinical situation.

Proof-of-concept studies should mimic the intended clinical indication as closely as possible. This is needed not only to allow the most reliable evaluation of the therapeutic potential of the experimental product, but also to assess the likely duration of clinical effect. The latter consideration is of special importance, because given the risks inherent in any cellular therapy, failure of the intervention after a brief interval of benefit could be viewed either as a late-occurring toxicity or a treatment failure. For joint lesions, this issue presents a special problem, because the model needs do resemble a human patient not only in applicable cell biology and pathophysiology, but also in joint mechanics and anatomy (FDA Cellular 2005).

Immunological considerations

Though the articular space is thought to be an area of relative immune privilege in both animals and humans due to the relative lack of local microvasculature and relative hypocellularity of articular cartilage and synovial fluid that bathes the articular surface, rheumatoid arthritis and other inflammatory arthritis suggest that this is not absolute, and therefore immune re-

sponse to both cellular and device components of component products may occur in the articular space. The testing of cellular products derived from human cells in animal models thus poses a special concern, as these cells are xenogenic to all animal species, and therefore at risk for xenotransplant rejection.

Immunological reactions to human product in animals often necessitate that preclinical studies be performed with animal cellular products that are analogous to the intended clinical product, rather than the actual human product. The determination that a specific animal cell is analogous to the intended clinical product is made on the basis of some combination of morphology, biochemical or molecular biological characteristics, ontogeny, and function. Ideally this determination would be multifaceted and involve not just *in vitro* measures of cell identity, but also incorporate detailed understanding of the *in vivo* activity of both the animal analog and putative human correlated cell. Implicit in the use of analogous animal cells as a means to assess biological activity and/or safety of a human cellular clinical product that is composed at least in part of human cells is the assumption that cells from the two species will respond similarly to the stresses imposed in the *in vivo* articular environment. The data obtained from testing analogous animal cells will provide a partial basis from which to make a risk/benefit analysis that is integral to review of preclinical data prior to initiation of clinical trials. The degree of understanding of the relationship between an animal cell and its human correlate is an important factor in determining the strength of the extrapolations from findings in animals to the potential risks in humans (FDA Cellular 2005).

Animal models of cartilage repair

Animal models are an essential research tool in many biomedical projects, because they act as the bridge between *in vitro* studies and human clinical trials. Their use is required for regulatory approval for clinical use of biologics, devices, and methods (Cook, Hung et al. 2014).

Research using animal models provides important knowledge of pathological conditions that can eventually lead to the development of more effective clinical treatment of diseases in both humans and animals (An and Friedman 1999).

Animal models of cartilage repair are categorized as small animal models (mice, rats and rabbits) and large animal models (dog, pig, sheep, goat and horse).

Rodents

Rodent models are cost-effective in providing proof of concept data to serve as a bridge between in vitro experiments and more costly large animal preclinical studies. Chondrogenesis has been extensively studied in murine models by several biomaterial and cells implantation (Lammi, Lammi *et al.* 2001; Dausse, Grossin *et al.* 2003; Matsumoto, Kubo *et al.* 2008). However, rodent joints are of small size, have thin cartilage, and open growth plates are present through advancing age, which are likely to increase the intrinsic healing potential of cartilage. This fact can confound repair and regeneration studies in this models (Chu, Szczodry et al. 2010).

Mice

The availability of athymic, transgenic and knock-out strains are advantages that make mice potential valuable models for mechanistic *in vivo* studies. Immunocompromised mice allow the performace of studies involving allogenic or xenogenic cells and tissues (Chu, Szczodry *et al.* 2010). There are also mice strains in which OA occurs spontaneously (Bendele, McComb *et al.* 1999), and transgenic and knock-out mice to study how the overexpression or the absence of a particular gene or protein impacts cartilage regeneration and repair (Helminen, Kiraly *et al.* 1993; Serra, Johnson *et al.* 1997; Helminen, Säämänen *et al.* 2002; Majumdar, Askew *et al*. 2007; Wu, Kim *et al*. 2008). The improved understanding of the molecular basis for cartilage regeneration may generate new treatment options for further study in larger animal models (Chu, Szczodry *et al.* 2010).

Rats

The larger size of the rat, comparing to mice, improves the feasibility and reproducibility of studies involving creation of cartilage defects (Anraku, Mizuta *et al.* 2008; Anraku, Mizuta *et al.* 2009). In addition, athymic rats are available. The ability to create osteochondral defects within which xenogenic cells can be implanted provides a unique opportunity to study the repair potential of human cells within the diarthrodial environment (Pagnotto, Wang *et al. 2007)* or of other xenogenic cells, as murine cells (Matsumoto, Kubo *et al.* 2008). The successful use of murine cells in athymic rats raises the possibility of studying the effects of different genes and proteins on cartilage repair by using cells from transgenic and knockout mice (Chu, Szczodry *et al.* 2010). The rat model also provides a cost effective means for initial testing

of the in vivo degradation characteristics and safety profile of new biodegradable scaffolds and polymers (Ferretti, Marra *et al.* 2006).

Rabbits

The rabbit model has been widely used on cartilage regeneration research (Furukawa, Eyre et al. 1980; Shapiro, Koide et al. 1993; Chu, Coutts et al. 1995; Chu, Dounchis et al. 1997; Kawamura, Wakitani et al. 1998; Han, Chu et al. 2003). This is a practical animal model for early stages of therapy evaluation due to reasonable joint size for surgical procedures, ease of handling and relative cost effectiveness. However, this animal model has lost favor in recent years due to high potential for spontaneous healing, sizable variation from human joint loading conditions, and thin cartilage which make the interpretation of experimental results problematic (Chu, Szczodry *et al*. 2010).

In fact, endogenous healing potential has been described on rabbits (Wei, Gao *et al*. 1997), while cartilage in humans, if left untreated, have little to no spontaneous repair. This makes difficult to evaluate the translational potential of treatments using this model (Chu, Szczodry *et al.* 2010).

The loading conditions in the lapine knee are due to the high degree of knee flexion: therefore they use the trochlea groove as partial weight bearing surface, which in the connection with low body weight creates much different loading conditions than in humans or large animals (Ahern, Parvizi *et al.* 2009).

Regarding cartilage thickness, it is documentated that the lapine model has a mean cartilage thickness on the trochlear groove of 0.44 ± 0.08 mm and of 0.3 ± 0.07 mm on the anteromedial femoral condyle (Räsänen and Messner 1996), which limits the size and depth of articular cartilage defects

that can be made (Chu, Szczodry *et al.* 2010). The most commonly reported depth of experimental osteochondral defects induced on rabbits is of 3mm (Wei, Gao *et al.* 1997; Buma, Pieper *et al.* 2003; Han, Chu *et al*. 2003), which means that more than 80% of the defect volume is located within the subchondral bone (Chu, Szczodry *et al*. 2010).

Dogs

The dog has been used in studies of articular cartilage repair (Oates, Chen *et al.* 1995; Shortkroff, Barone *et al.* 1996; Breinan, Minas *et al.* 1997; van Dyk, Dejardin *et al*. 1998; Breinan, Minas *et al.* 2001; Cook, Patron *et al.* 2003). They lack significant intrinsic ability to heal cartilage defects, as happens with humans, and they can more closely model the human situation than rodent or lapine models. Dogs suffer naturally from cartilage pathology as osteochondritis dissecans and OA (Shortkroff, Barone *et al.* 1996).

In medium to large dogs, the thickness of the cartilage ranging from 0.95 to 1.3 mm (Ahern, Parvizi *et al.* 2009) is greater than that of rodents or lapine models, which renders the possibility to create and study partial thickness cartilage injuries. However, canine cartilage is still relatively thin and articulation size small when compared to humans, and consequently repair studies in canine models generally use small diameter osteochondral defects (Bouwmeester, Kuijer *et al.* 2002; Hunziker 2002). Advantages of this model is that the relatively exposed stifle joint facilitates arthroscopic approach of the tibio-femoral joint (Feczkó, Hangody *et al.* 2003), and that dogs are well suited to study protocols requiring specific exercise and rehabilitation protocols or bandages (Chu, Szczodry *et al*. 2010).

However, the strong bond between dogs and humans, and their status as family pets have highlighted ethical concerns regarding their use as ani-

mal models on research. Therefore this animal model is used only if the study protocol, due to specific particularities, cannot be done using another animal species (Chu, Szczodry *et al*. 2010).

Pigs

The porcine joint size, weight bearing requirements and cartilage thickness more closely imitate the human condition than the canine and smaller models (Chiang, Kuo *et al*. 2005; Vasara, Hyttinen *et al*. 2006; Jiang, Chiang *et al*. 2007). However, the porcine model has been relatively underused in cartilage research. This is in part due to housing requirements of adult swine, which are heavy and large when adults, making them difficult to handle in research facilities (Swindle, Smith *et al*. 1988; Newman, Turner *et al.* 1995). Miniature swine breeds maintain an adult weight and size comparable to adult human males; however the size of the mini-pig stifle joint remains smaller than humans. Adult pigs, as with humans, have limited capability for endogenous repair of chondral and osteochondral defects (Chu, Szczodry *et al.* 2010). Pig cartilage has a thickness around 1.5 mm (Frisbie, Cross *et al*. 2006), which allows the creation of full and partial-thickness cartilage defects, with defect volumes closely corresponding to the ones observed in clinical human defects. Arthroscopic evaluation of the knee is feasible (Pan, Li *et al*. 2003; Zelle, Zantop *et al*. 2007). This model is not well adapted to protect weight bearing or to perform exercise protocols (Chu, Szczodry *et al*. 2010).

Minipigs have potential to be a large animal model for studying the use of allograft and xenograft tissues for cartilage repair. Prolonged tolerance to large musculoskeletal allografts was reported using a short course of cyclosporine (Bourget, Mathes *et al*. 2001). Transgenic pigs have also been

developed to express human regulators of complement activation, indicating a possibility for transgenic work in large animals (Hancock 1997). These exciting findings have interesting implications for the potential use of xenograft tissue in joint reconstruction and osteochondral transplantation (Yang and Sykes 2007; Chu, Szczodry *et al.* 2010).

Goats

The caprine model is commonly used in cartilage research (Butnariu-Ephrat, Robinson *et al*. 1996; Niederauer, A Slivka *et al.* 2000; Jackson, Lalor *et al*. 2001; Murphy, Fink *et al.* 2003; Kangarlu and Gahunia 2006). The advantages of this model are joint size, cartilage and subchondral bone thickness and consistency, accessibility for arthroscopic procedures, and limited intrinsic cartilage healing capacity (Jackson, Lalor *et al.* 2001; Ahern, Parvizi *et al.* 2009). The caprine joint is larger than the canine joint, and the proportion of cartilage to subchondral bone and subchondral bone consistency in goats is reported to be closer to humans than small animal, canine or sheep models (Jackson, Lalor *et al.* 2001; Ahern, Parvizi *et al.* 2009). When compared to other large animal models, goats are relatively inexpensive and easy to handle (Chu, Szczodry *et al.* 2010). The larger size of the joints facilitates creation of chondral and osteochondral defects in goats, and allows arthroscopic examination of the knee (Brehm, Aklin *et al.* 2006). However exercise protocols or protected weight bearing are difficult to implement in goats, making them less well suited for studies where these factors are important (Chu, Szczodry *et al.* 2010). The cartilage thickness on the medial femoral condyle ranges from 0.8 to 2.0 mm, providing an opportunity to study the healing of partial and full-thickness cartilage defects (Brehm, Aklin *et al.* 2006). However, despite the size of the goat stifle joint, the cartilage defects are, by volume, in the lower range of commonly ob-

served cartilage defects in humans (Ahern, Parvizi *et al*. 2009), and the tibio-femoral joint is still significantly smaller in goats when compared to humans (Chu, Szczodry *et al.* 2010).

Sheep

The ovine model is commonly used in cartilage research (Martini, Fini *et al.* 2001; Erggelet, Neumann *et al.* 2007; Munirah, Samsudin *et al.* 2007; Ahern, Parvizi *et al.* 2009). The knee anatomy is similar to humans (Allen, Houlton *et al.* 1998), and it is recognized the possibility of minimally invasive surgical approaches on this model. However, published research in the area reveals the habitual use of invasive methodology on the experimental procedures (Munirah, Samsudin *et al.* 2007; Jubel, Andermahr *et al*. 2008; Milano, Deriu *et al.* 2012).

Articular cartilage thickness of sheep is of variable thickness. Published literature refers cartilage thickness ranging from 0.4-1mm (Lu, Hayashi *et al.* 2000), 0.45mm (Frisbie, Cross *et al.* 2006) and 1.68mm as average thickness for the medial femoral condyle (An and Freidman 1998). The subchondral bone is very dense and hard (Ahern, Parvizi *et al.* 2009).

The critical size cartilage defect on sheep has been reported as 7mm. The location of the cartilage defects in the ovine model has involved the medial femoral condyle (Pearce, Hurtig *et al.* 2001; Dorotka, Windberger *et al.* 2005; Tytherleigh-Strong, Hurtig *et al.* 2005; Uhl, Lahm *et al.* 2005; Frosch, Drengk *et al.* 2006), both femoral condyles (Siebert, Miltner *et al.* 2003; Von Rechenberg, Akens *et al.* 2003; Tibesku, Szuwart *et al*. 2004), and the femoral trochlea (Kandel, Grynpas *et al.* 2006).

Sheep are readily available, easy to handle and are relatively inexpensive model suitable for testing new approaches in cartilage regeneration and repair (Ahern, Parvizi *et al.* 2009).

Horses

Similar to humans, horses suffer from cartilage problems ranging from osteochondritis dissecans to cartilage injury and OA. Largely due to racing industry, the clinical treatment of cartilage injuries in horses is well developed (Nixon, Fortier *et al*. 2004). Consequently, the injury and repair of articular cartilage are better known in horses than in most other animal models.

The equine model is highly beneficial for preclinical evaluation of the efficacy of new repair techniques and technologies, as it allows for the closest correlation with humans among all animal models commonly employed in cartilage research. Cluster analysis of studies involving single cartilage defects on the distal femur placed horses as the only animal model in the same group with humans in regard to defect dimension (Ahern, Parvizi *et al*. 2009). Cartilage thickness in horses is reported to be in range of 1.75-2mm, which is closest to human cartilage thickness (2.35 mm) among all animal models. Therefore, full and partial cartilage thickness defects can be readily and successfully created with very close correlation to clinically relevant sized defects in human cartilage (Hendrickson, Nixon *et al*. 1994; Hidaka, Goodrich *et al.* 2003; Strauss, Goodrich *et al.* 2005; Ahern, Parvizi *et al.* 2009). Evaluation of chondral and osteochondral defects of 15 to 20 mm, which are similar to the sizes requiring treatment in humans, is possible in the equine model (Convery, Akeson *et al*. 1972; Hidaka, Goodrich *et al.* 2003).

Similar to humans, equine articular cartilage shows a loss of function and a low intrinsic capability for repair (Convery, Akeson *et al*. 1972; Koch and Betts 2007). It is reported that large defects (9 mm) made on weight bearing areas of femoral condyles in Shetland ponies do not heal after 9 months (Clar, Cummins *et al.* 2005). Additionally, horse models with large joint dimension, thick articular cartilage layers, and fully extended, upright stifle joints during gait should be considered, as they are quite similar to human knee anatomy (Gotterbarm, Breusch *et al.* 2008).

The dimensions of the equine stifle joint allow the use of arthroscopic techniques (Wilke, Nydam *et al*. 2007). The availability of complementary clinical data offers additional advantages for translation of basic research to preclinical study in horses (Chu, Szczodry *et al*. 2010).

The horse is the largest of the animal models commonly available for cartilage research, weighting around 500 kg. Equine joint loading conditions and the consequent hardness of the equine subchondral bone are of some concern (Murray, Vedi *et al*. 2001), as well as the difficulty to maintain protection of weight bearing in this model. Therefore, the location of the experimental cartilage defect should be carefully considered to avoid early overloading: the lateral trochlea of the femur has been frequently used for cartilage repair studies in the equine model (Ahern, Parvizi *et al*. 2009).

The major disadvantage of equine models include high expense and the need of highly specialized and equipped facilities to conduct experiments on equines, but horses should be considered as a good translational model for studying new cartilage treatments prior to human clinical trials (Chu, Szczodry *et al*. 2010).

The importance of large animal models in translational research

The combination of overall increased stifle size, less effective native cartilage repair, and longer lifespan are advantages of large animal models of human clinical indications. Larger animals allow for the testing of cellular products and associated attachment devices that more closely approximate the size and design of the intended clinical product. The two primary benefits of large animals are the ability to model a clinically useful duration of response (durability) to products more closely, and the potential to incorporate minimally invasive or non-invasive endpoints into a product development strategy prior to clinical trials.

One key requirement for successful implementation of cell-based therapies for joint surface repair is durability of clinical benefit. Due to biology of cartilage repair in large animals, studies of eight to twelve weeks duration (maximal length in rabbits) are only adequate to provide information on the biocompatibility and early cellular viability in larger animals. Longer-term studies of at least six to twelve months duration are needed to assess the true success of cartilage repair. This study duration is similar to what is generally thought by the orthopedic community to be needed for initial clinical indications of activity in humans. The ability to use large animals to test not just the cartilage repair product, but also the feasibility of various diagnostic modalities such as imaging, biomechanical tests, arthroscopy, and arthroscopic biopsy for the in situ evaluation of the product could prove to be beneficial in an overall product development scheme that includes these modalities in clinical trial design.

The most frequently used large animal model in cartilage repair studies is the goat, because of her reasonable cartilage thickness, relatively large stifle size and ease of use, cost and availability. Some investigators

made also extensive use of sheep, whose stifle resembles that of goats in many aspects (FDA Cellular 2005).

Preclinical imaging

It is recognized that the implementation of preclinical imaging represents a keystone in the refinement of animal models allowing longitudinal studies and enabling a powerful, non-invasive and clinically translatable way for monitoring disease progression in real time (Tremoleda, Khalil *et al.* 2011). The use of imaging modalities holds significant potential for the assessment of disease pathogenesis and therapeutic efficiency overtime in animal models of musculoskeletal disorders, minimizing the use of conventional invasive methods and animal redundancy (Tremoleda, Khalil *et al.* 2011).

Magnetic resonance imaging (MRI) is a non-invasive imaging technology extensively used in clinics for assessment of articular cartilage in joint disorders, and has also been used in the ovine model of cartilage repair (Uhl, Lahm *et al.* 2005; Goebel, Orth *et al.* 2012).

In humans, musculoskeletal ultrasound (US) plays an important role in detecting the minimal soft tissue changes (McCune, Dedrick *et al.* 1990; Grassi, Lamanna *et al*. 1999; Court-Payen 2004; Naredo, Cabero *et al.* 2005). US has the ability to differentiate intra and extra-articular soft tissue structures, is a quick, readily available, inexpensive and non-invasive imaging technique (Abraham, Goff *et al.* 2011) which is particularly adapted in longitudinal in vivo experimental model studies (Boulocher, Duclos *et al*. 2008) .

OBJECTIVES

4- OBJECTIVES

General objective:

The general objective of this research work was the development of a refined preclinical animal model of partial thickness and full thickness cartilage defects to test and assess new approaches in regenerative medicine, using mesenchymal stromal cells.

The aim was to obtain nonclinical data sufficient to establish a scientific rationale for clinical investigation of the experimental product, and to demonstrate an acceptable safety profile of the experimental product prior to initiating a human clinical study.

Detailed objectives:

1-Development of the animal experimental model:

- Develop a minimally invasive surgical procedure for experimental osteochondral lesion induction and assay product implantation
- Study the behavior and resistance to arthroscopic implantation of the tissue engineered constructs
- Study the efficacy of the PLGA scaffolds seeded with Co-MSC in the regeneration of osteochondral lesions
- Develop the complementary exams to assess the evolution of the lesion and of the treatment, in a non-invasive methodology

2-Test different sources of MSC in the preclinical ovine model: MSC derived from fat, bone barrow and cartilage seeded in PLGA scaffolds:

- To study the efficacy of these cellular therapies in osteochondral lesions regeneration
- Assess the safety of these cellular therapies in cartilage lesions in the sheep knee

3-Study the efficacy and safety of BM-MSC in the regeneration of chronic chondral lesions

4-Detail the refinement strategies developed on the preclinical ovine model, regarding experimental lesion modelling and non-invasive imaging techniques for longitudinal assessment.

SCIENTIFIC PUBLICATIONS

5.1- STUDY 1

AN ARTHROSCOPIC APPROACH FOR THE TREATMENT OF OSTEOCHONDRAL FOCAL DEFECTS WITH CELL-FREE AND CELL-LOADED PLGA SCAFFOLDS IN SHEEP.

Fonseca C, Caminal M, Peris D, Barrachina J, Fàbregas PJ, Garcia F, Cairó JJ, Gòdia F, Pla A, Vives J.

Cytotechnology. 2014 Mar; 66(2):345-54.

Cytotechnology
DOI 10.1007/s10616-013-9581-3

METHOD IN CELL SCIENCE

An arthroscopic approach for the treatment of osteochondral focal defects with cell-free and cell-loaded PLGA scaffolds in sheep

C. Fonseca · M. Caminal · D. Peris · J. Barrachina · P. J. Fàbregas · F. Garcia · J. J. Cairó · F. Gòdia · A. Pla · J. Vives

Received: 17 October 2012 / Accepted: 30 April 2013

Abstract Osteochondral injuries are common in humans and are relatively difficult to manage with current treatment options. The combination of novel biomaterials and expanded progenitor or stem cells provides a source of therapeutic and immunologically compatible medicines that can be used in regenerative medicine. However, such new medicinal products need to be tested in translational animal models using the intended route of administration in humans and the intended delivery device. In this study, we evaluated the feasibility of an arthroscopic approach for the implantation of biocompatible copolymeric poly-D,L-lactide-*co*-glycolide (PLGA) scaffolds in an ovine preclinical model of knee osteochondral defects. Moreover this procedure was further tested using ex vivo expanded autologous chondrocytes derived from cartilaginous tissue, which were loaded in PLGA scaffolds and their potential to generate hyaline cartilage was evaluated. All scaffolds were successfully implanted arthroscopically and the clinical evolution of the animals was followed by non invasive MRI techniques, similar to the standard in human clinical practice. No clinical complications occurred after the transplantation procedures in any of the animals. Interestingly, the macroscopic evaluation demonstrated significant improvement after treatment with scaffolds loaded with cells compared to untreated controls.

C. Fonseca, M. Caminal and D. Peris contributed equally to this work.

Electronic supplementary material The online version of this article (doi:10.1007/s10616-013-9581-3) contains supplementary material, which is available to authorized users.

C. Fonseca · F. Garcia
Departament de Medicina i Cirurgia Animals, Àrea de Medicina i Cirurgia Animal, Facultat de Veterinària, Edifici V, Campus de la UAB, 08193 Bellaterra, Cerdanyola del Vallès, Spain

M. Caminal · A. Pla (✉) · J. Vives (✉)
Divisió de Teràpies Avançades/XCELIA, Banc de Sang i Teixits, Edifici Dr. Frederic Duran i Jordà, Passeig Taulat, 116, 08005 Barcelona, Spain
e-mail: apla@bst.cat

J. Vives
e-mail: jvives@bst.cat

D. Peris · J. J. Cairó · F. Gòdia · J. Vives
Grup d'Enginyeria Cel lular i Tissular, Departament d'Enginyeria Química, Escola d'Enginyers, Universitat Autònoma de Barcelona, Edifici Q, Campus de la UAB, 08193 Bellaterra, Cerdanyola del Vallès, Spain

J. Barrachina
Hospital ASEPEYO Sant Cugat, Avinguda Alcalde Barnils, 54-60, Sant Cugat del Vallès, 08174 Barcelona, Spain

P. J. Fàbregas
Unitat d'Anatomia i d'Embriologia, Departament de Ciències Morfològiques, Facultat de Medicina, Universitat Autònoma de Barcelona, 08193 Bellaterra, Cerdanyola del Vallès, Spain

Published online: 15 May 2013

Keywords Preclinical animal model · Expanded chondrocytes · Regenerative medicine · Arthroscopy · Osteochondral defect

Introduction

Articular cartilage focal defects represent a common condition affecting the knee and play a significant role in the subsequent development of degenerative joint disease. The response to injury depends on the severity and depth of the lesion, but in general the healing potential is very limited. In this scenario, chondral lesions involving the subchondral bone usually result in fibrocartilage scar tissue refilling, which has poorer biomechanical and biochemical features compared to hyaline cartilage (Alford and Cole 2005).

Since the simultaneous regeneration of both cartilage and subchondral bone can be approached by the use of porous biopolymeric scaffolds that can contribute to (1) preserve the structure of the lesion area and (2) absorb bone marrow from the focal osteochondral injury, permitting bone remodelling and differentiation of neighbouring stem cells, we evaluated its use in a preclinical model of osteochondral injury. In particular, a large animal model was chosen in order to evaluate the viability of an arthroscopic approach for the implantation of a copolymeric poly-D,L-lactide-*co*-glycolide (PLGA) scaffold using standard instrumentation and techniques in human clinical practice. This is an important point, since there is a great deal of interest in the possibility of using arthroscopy in preclinical animal models for the development of new techniques and investigate the performance of novel implants in situ using minimally invasive approaches (Allen et al. 1998).

An osteochondral defect was created in the medial femoral condyle of the ovine stifle joint, since sheep is a representative animal model for studying a range of orthopaedic conditions and treatments because of its similar size and anatomy to the human knee. Although no animal model is completely ideal, sheep is a reasonable experimental animal for surrogate orthopaedic research directed at efficacy, safety, and mechanism of action (Simon and Aberman 2010) and, in fact, it has been previously used in several other studies for the treatment of chondral and osteochondral lesions (as reviewed in Ahern et al. 2009).

Materials and methods

Animals

The surgical procedures were developed in five cadavers that were euthanized for reasons unrelated to the current study. For the in vivo study, six healthy 2-year old ewes of the Ripollesa-Lacona breed were obtained from *Servei de Granges i Camps Experimentals* (SGCE, Bellaterra, Spain). During the pre- and post-operative procedures, animals were housed together, fed a standard diet and allowed access to water ad libitum. All animal care and experimental procedures were approved by the Universitat Autònoma de Barcelona's Ethical Committee on Human and Animal Experimentation (Ref. No. CEAAH 501), and registered by the Departament de Medi Ambient de la Generalitat de Catalunya (Reg. No. 3666).

Study design

Two surgical procedures were performed in each animal. The first procedure involved an arthrotomy to harvest a cartilage biopsy for subsequent chondrocyte isolation and expansion (Suppl. Fig. 1A and 1B). The second procedure was performed after 4 weeks, and involved creation of a standardized osteochondral defect bilaterally in the medial femorotibial condyles via an arthroscopic approach (Suppl. Fig. 1D and 1F). Each of the osteochondral lesions produced in the 12 knees were included in one of any of the three treatments detailed next and described in Table 1: (a) 4 knees received scaffold seeded with expanded

Table 1 Study design

Animal ID	Time point (weeks)	Left knee	Right knee
F6	12	S	CS
F12	12	L	CS
F14	12	S	L
F16	20	CS	S
F17	20	L	CS
F44	20	L	S

Experimental plan used to evaluate the effect of treatment with cell-seeded and cell-free PLGA scaffold to osteochondral defects on the medial femorotibial condyles

CS cell-seeded scaffold, *S* scaffold, *L* untreated lesion

cells; (b) 4 knees received scaffolds without cells and (c) 4 knees were not treated. After surgery, sheep were allowed to move freely. Animals were divided in two identical groups, according to the two time points (12 and 20 weeks post-treatment, respectively).

Anaesthesia and post-operative care

All procedures were performed using aseptic techniques and under general anaesthesia. After premedication with an intramuscular (IM) injection of 0.01 mg/kg of buprenorphine (Buprex, Schering-Plough, S.A., Alcobendas, Spain) and 0.2 mg/kg of midazolam (Dormicum, Roche, Madrid, Spain), intravenous (IV) access was established at cephalic vein. Sheep were pre-oxygenated and induced with 4 mg/kg IV propofol (Propofol-Lipuro 1 %, BBraun Melsungen AG, Melsungen, Germany). The animals were under general anaesthesia intubated and maintained on isoflurane 2 % (Isoflo, Abbott laboratories Ltd, Abbott Park, IL, USA) with 100 % oxygen. Esophageal intubation was made to prevent ruminal bloat. A continuous infusion of Ringer lactate (Ringer lactate, BBraun Melsungen AG) was administered at 10 mL/kg/h during surgery. Intra-operative monitoring consisted of electrocardiography, pulse oximetry, non invasive blood pressure and capnography. All animals received one dose of subcutaneous (SC) meloxicam (Metacam, Boehringer-Ingelheim, Sant Cugat, Spain) 0.2 mg/kg daily for 10 days and a single dose of transdermal fentanyl (Durogesic, Janssen-Cilag, Madrid, Spain) 100 μg for post-operative pain relief. For peri-operative infection prophylaxis the animals received 22 mg/kg of cefazolin IM (Kurgan, Normon Laboratories, Madrid, Spain) every 12 h during 10 days.

Isolation, culture and scaffold-seeding of articular chondrocytes

The right shoulder joint was aseptically prepared and exposed with a craniolateral approach to the shoulder (Suppl. Fig. 1A). An approximately 3 cm-long incision was made in the skin and subcutaneous tissue, extending from the acromion process to the proximal humerus. The acromial portion of the deltoideus muscle was retracted caudally, and a lateral incision of the articular capsule was made between the glenoid rim and the humeral head. The humerus was rotated internally and an articular cartilage layer of 1 mm thick and 6 mm long was harvested from the head of humerus, using a curette. Cartilage was pierced and used as a source of chondrocytes (Suppl. Fig. 1). To do this, cartilage was washed and soaked with phosphate-buffered saline solution (PBS, HyClone, Logan, UT, USA) and immediately processed in the laboratory. The fragments of cartilage were minced, washed three times in PBS, and digested with 0.2 % (w/v) Collagenase B (Roche) for 24 h. Cells and tissue were resuspended in 10 mL of DMEM (Dulbecco's modified Eagle's medium, GIBCO-BRL/Life Technology, Carlsbad, CA, USA) supplemented with 10 % (v/v) foetal calf serum (FCS, Biological Industries, Kibbutz Beit Haemek, Israel) and centrifuged at 400 g for 5 min. Cells were washed in PBS and cultured in a T-25 flask in DMEM medium containing 10 % (v/v) FCS, in a humidified 5 % CO_2 incubator. After cell attachment and mesenchymal-morphology conversion, cells were scaled-up by seeding T-150 flasks at 2,500 cell/cm^2. Cell number and viability were determined by the haemocytometer-based trypan blue dye exclusion assay.

The cells were cultured in low glucose DMEM medium supplemented with Streptomycin (0.167 g/L, Sigma-Aldrich, St. Louis, MO, USA), Kanamycin (0.075 g/L, Sigma-Aldrich) and 10 % foetal calf serum (FCS, Biological Industries). Cells were passaged until passage 4 under a humidified atmosphere of 5 % carbon dioxide at 37 °C, using 0.25 % trypsin (GIBCO-BRL) and counted with a haemocytometer. The cultured chondrocytes obtained from each sheep were reseeded onto three-dimensional PLGA scaffolds in a minibioreactor (Hexascreen Culture Technologies S.L., Cerdanyola del Vallès, Spain) (Suppl. Fig. 1). Briefly, 3×10^6 cells were inoculated in each minibioreactor, where a PLGA scaffold was fixed using a 25G needle, and stirred at 200 rpm for 24 h incubation time in a total final volume of 12 mL. The amount of inoculum was determined in pilot experiments indicating the maximum load of cells absorbed by the scaffold (data not shown).

Scanning electron microscopy

Samples were fixed in 2.5 % glutaraldehyde and 2 % paraformaldehyde in PBS (pH 7) and dehydrated in ethanol series (15 min in each 30–50–70–90–100–100 %) to absolute ethanol and immediately

transferred to acetone before being critical-point dried and gold-coated using a Sputter Coater (K550, Coating Attachment, Emitech, Ashford, U.K.). Samples were examined with an HITACHI S-570 electron microscope (Tokyo, Japan) at a voltage of 15 kV.

Scaffolds

PLGA scaffolds were manufactured in-house following a solution-casting/salt-leaching technique using PLGA particles with an inherent viscosity of 0.55–0.75 dL/g (Lactel) as described elsewhere (Mikos et al. 1994). Briefly, polymeric PLGA particles were first dissolved in chloroform. Then, sieved salt particles ranging 300–500 μm were dispersed in the polymer solution at a 9:1 ratio (NaCl:PLGA). The mixture was casted into a mould with a cylindrical shape, with a diameter of 4 mm and with 7 mm high. After the evaporation of the solvent, the salt particles were extracted by washing the polymer with distilled water for 48 h. Then the scaffolds were dried first at air temperature for 24 h and then vacuum dried for 24 h. Finally, the scaffolds were gamma sterilized (20 kGy) and stored at −20 °C.

Osteochondral defect creation and arthroscopic implantation

The creation of osteochondral defects and the introduction of the test items were performed arthroscopically (Suppl. Fig. 1). Each joint was approached via a stab incision lateral to the distal aspect of the patellar ligament, allowing the insertion of the arthroscope with camera for the visualization of the medial condyle. A mechanical shaver was used to remove the fat pad allowing a clearer view. For this purpose, a second stab incision was made medial to the distal aspect of the patellar ligament to allow the shaver insertion. Once cleaned, the shaver was removed. A mosaicplasty instrument set (Smith and Nephew Inc, Memphis, TN, USA), consisting of a donor and a receptor cannulae, was used to create the lesion and to place the scaffold (Suppl. Fig. 1D). For this purpose, the cylindrical hollow punch with an inner diameter of 2.7 mm (donor cannula) was placed through the second stab incision, previously used. This instrument was used to perform a cylindrical osteochondral lesion of diameter 3.5 and 5 mm depth in the caudal aspect of the medial femoral condyle of each knee. The scaffold of cylindrical shape and 4 mm diameter and 7 mm high was placed through the receptor canula, filling the lesion by the application of moderate force to the syringe piston (Suppl. Fig. 1F). The joints were irrigated by saline solution (NaCl-0.9, BBraun Medical SA) at room temperature during surgery.

Magnetic resonance imaging

MRI examination was performed on both knees of each animal under general anaesthesia, using a 0.2 T unit with open permanent magnet (Vet-MR, Esaote S.p.a., Genova, Italy). First group of animals was examined at 11 weeks post-treatment and the second group, at 19 weeks post-treatment.

Animals were positioned in sternal recumbency with the leg extended and symmetrically placed inside a dual phased array coil.

Sequences included axial, coronal and sagittal: sagittal high resolution spin echo T1 (TR/TE 590/26, DFOV 20 cm, slice thickness 4 mm) and high resolution spin echo T1 coronal (TR/TE 690/26, DFOV 22 cm, slice thickness 3 mm); sagittal sequences in Gradient echo (TR/TE 600/22, FA = 40°, DFOV 22 cm, slice thickness 4 mm); sagittal STIR imaging (TR/TE/TI 1560/24/75, DFOV 23 cm, slice thickness 4 mm) and coronal STIR imaging (Short T1 Inversion Recovery) for fat suppression (TR/TE/TI 1840/24/75, DFOV 23 cm, slice thickness 3 mm); axial PD/T2 Turbo Multiecho imaging (TR/TE 2800/28 and 2800/90, DFOV 22, slice thickness 4 mm).

Macroscopic assessment

The animals from the two experimental groups were sedated with an IM injection of 0.02 mg/kg of midazolam and euthanised by IV injection of 12 mg/kg pentobarbital (Dolethal 20 mg/100 mL, Vetoquinol S.A., Paris, France).

Both stifle joints were harvested, grossly evaluated blindly by CF, JB and FG, and photographed. The gross appearance of repaired tissues was assessed in accordance with the International Cartilage Repair Society (ICRS) classification (van den Borne et al. 2007). Biologically acceptable regeneration was defined as having smooth, firm repair tissue that filled the defect and appeared attached to the adjacent cartilage. Samples were excised in blocks including all the implanted tissue and the surrounding native tissue, and were fixed in a 4 % PFA (paraformaldehyde, Sigma-Aldrich) solution, for histological analysis.

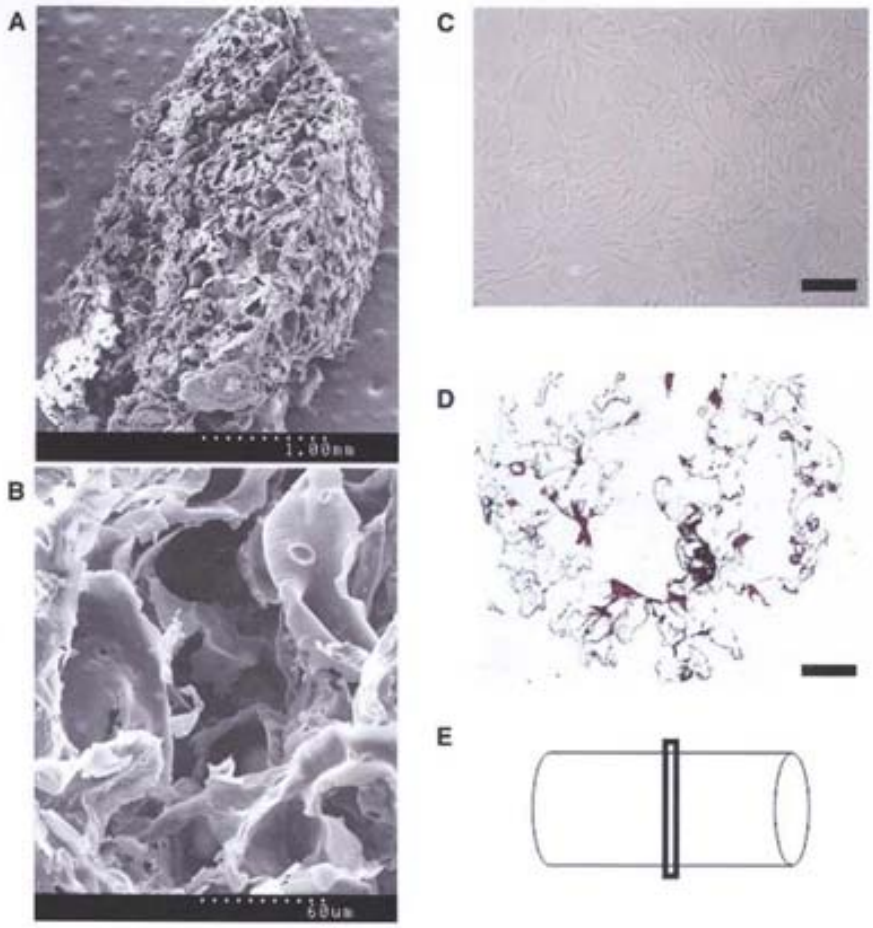

Fig. 1 SEM images from macroporous PLGA scaffolds. **a**, **b** Cell-free scaffold at low and high magnification, respectively. **c** Ovine chondrocytes in culture are stretched cells with fibroblastic appearance. **d** Cross-section from an H&E stained cell-seeded scaffold, as shown in **e**, where the schematic shows the structure of the scaffold with a cylindrical shape of 4 mm diameter and 7 mm long. *Scale bars* **c** = 200 μm; **d** = 600 μm

Histological evaluation and immunohistochemical procedures

Condyles were fixed in 4 % PFA solution at room temperature for 2 weeks, decalcified with 5 % formic acid for 4–6 weeks and embedded in paraffin for subsequent histological and immunohistochemical procedures. Microtome sections 4 μm thick were cut in sagittal plane sections and stained with haematoxylin/eosin (H&E, Sigma-Aldrich) and Safranin O (Sigma-Aldrich). The success of the treatment was evaluated blindly by PJF following the Histological scoring Grading Scale on at least 4 sequential histological sections (Mainil-Varlet et al. 2001).

The presence of Collagen type II and Sox9 was detected by immunohistochemical techniques using polyclonal antibodies (MAB 8887, Chemicon (EMD Millipore Corporation, Billerica, MA, USA); and AB5535, Chemicon, respectively). Briefly, paraffin sections were deparaffinized and hydrated. For collagen type II, sections were also treated with 0.1 % Pepsin (Sigma-Aldrich) in HCl 0.01N for 20 min. For both collagen type II and sox9, endogenous peroxidase activity was blocked with hydrogen peroxide for 30 min and washed in 3 % bovine serum albumin (BSA, Sigma-Aldrich) in Phosphate Buffered Saline (PBS, Sigma-Aldrich). The sections were then incubated with either the antibody against collagen type II (dilution 1:200) or sox9 (dilution 1:200) overnight at 4 °C. Antibody binding was visualized by using Universal LSAB™ 2 Kits (Dako, Glostrup, Denmark) in combination with diaminobenzidine (DAB) according to the manufacturer's instructions. The sections were counterstained with haematoxylin.

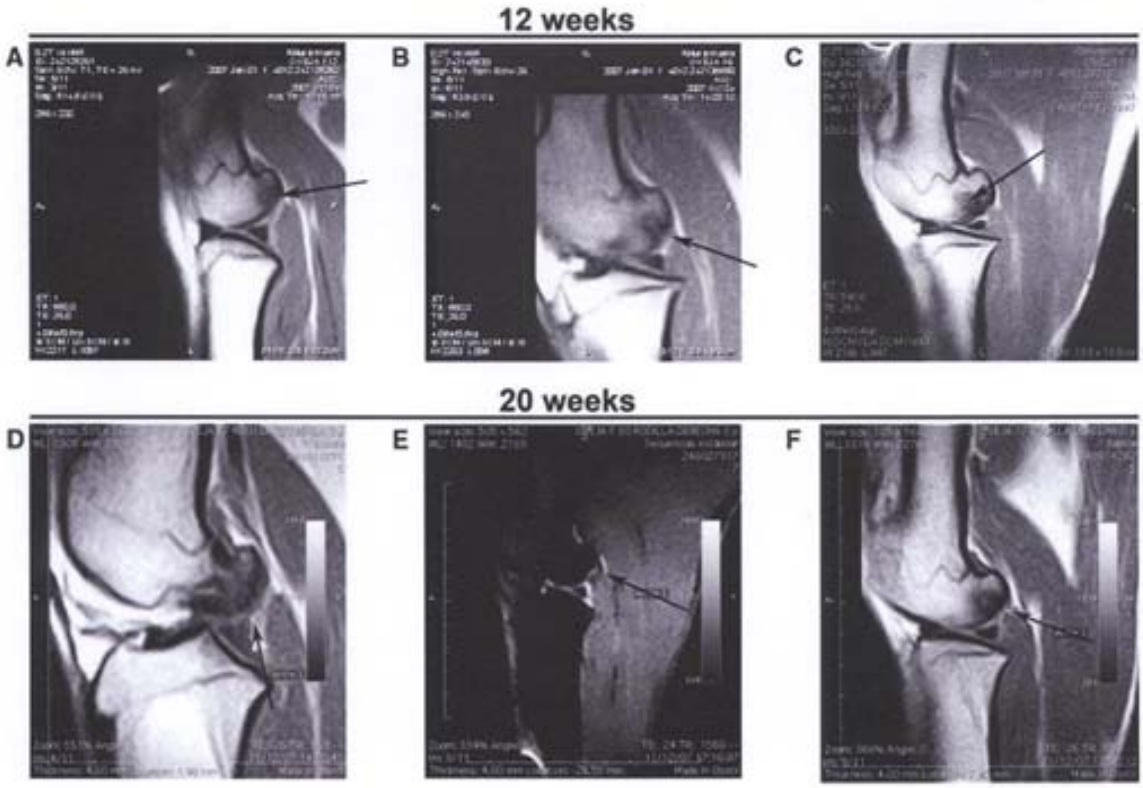

Fig. 2 MRI images. The top images were taken at 12 weeks after arthroscopy: **a** untreated knee (sample F12left). **b** Defect treated with cell-free PLGA scaffold (sample F6left), where an incomplete osteointegration of the implant is shown by an *arrow*; and **c** osteochondral defect treated with cell-seeded PLGA scaffold (sample F6right), where the *arrow points* to an oedema-like signal in the subchondral bone. *Bottom images* were taken from samples recovered 20 weeks post arthroscopy: **d** untreated knee (sample F17left), where the *arrow points* at the irregular articular surface. **e** Lesion treated with cell-free PLGA scaffold (sample F30right), where the *arrow points* to the erosion on the articular surface; and **f** lesion treated with cell-seeded PLGA scaffold (sample F17right), where the *arrow* indicates the continuity of the surface

Statistical analysis

To verify the comparability of the treatment groups, comparisons with regard to macroscopic evaluation and histological grade were performed using a non-parametric Kruskal–Wallis statistical analysis ($n = 4$) with the GraphPad Prism program (GraphPad software).

Results

Production of scaffolds and cell/scaffold constructs

Scanning electron microscopy was used to assess the microstructure of the porous PLGA scaffolds produced. They displayed high interconnectivity of pores, and a 3D structure that facilitated migration of cells within the scaffold (Fig. 1a, b).

Autologous chondrocytes were expanded in vitro yielding a therapeutic dose of 3×10^6 cells/scaffold (Fig. 1c). Each PLGA scaffold and its corresponding dose of chondrocytes were incubated together in a single-use bioreactor resulting in colonization rates of more than 70 %: that is a number of cells seeded ranging between 2.2×10^6 and 2.4×10^6 cells/scaffold, as determined by indirect counting of non-seeded cells present on the supernatant. Histological analysis of seeded scaffolds showed cells consistently distributed within the PLGA structure and tightly attached to the surface (Fig. 1d).

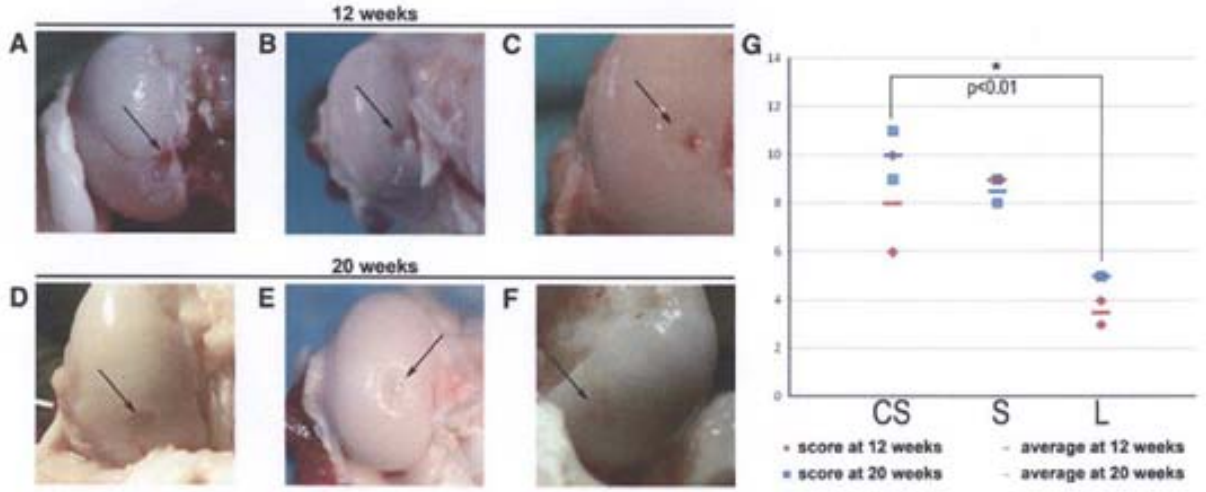

Fig. 3 Macroscopic aspect of knees. The top images were taken at 12 weeks post arthroscopy: **a** knee displaying a condyle (sample F12left) suffering arthritis as a consequence of the untreated osteochondral lesion; **b** lesion treated with cell-free PLGA scaffold and showing a good integration of the implant (sample F6left) and merely displaying a slight erosion on the surface; and **c** defect treated with cell-seeded PLGA scaffold (sample F6right), where the *arrow marks* the integration site of the repair tissue next to the border zone of the native tissue, which appears almost identical. *Bottom images* show macroscopic findings at 20 weeks post arthroscopy: **d** untreated lesion in sample F17left, where the *arrow marks* the defect site; **e** lesion treated with cell-free PLGA scaffold in sample F30right, where a repair tissue (*arrow*) appears below the level of the native articular cartilage; and **f** cell-seeded PLGA scaffold treatment in sample F17r, offering repair tissue well integrated (*arrows*), and levelled with the surrounding native articular cartilage. **g** *Graphical* representation of the scores obtained at 12 and 20 weeks grouped together according to each treatment, where the average from each group is also graphically represented to highlight the similarity in their values. A significant statistical difference ($p < 0.01$) was observed between the group treated with cell-seeded scaffold compared to the untreated lesion. *CS* cell-seeded scaffold, *S* scaffold, *L* untreated lesion

Experimental lesion, test item implantation and clinical outcome

Bilateral arthroscopy was well tolerated and all animals were able to stand on all four limbs and walk immediately after surgery. No clinical complications occurred after the transplantation procedures in any of the animals.

MRI evaluation at 11 and 19 weeks (prior to euthanasia at 12 and 20-week post-surgery, respectively) revealed osteochondral sclerotic lesions in all untreated knees (Fig. 2a, d). Most of the defects treated with scaffold constructs, either with or without cells, presented continuity of the surface, which was not observed in the untreated group (Fig. 2).

Macroscopic assessment and histological results

Animals were euthanized at 12 and 20 weeks post-treatment, and the repair process was evaluated macroscopically. No evidence of infection or fibrinous overgrowth on the joint surface was observed. Taken together, both scores from groups euthanized at 12 and 20 weeks, knees treated with cell-seeded scaffolds presented the best macroscopic results and showed differences that were statistically significant ($p < 0.01$) compared to untreated controls (CS = 9.0 ± 2.1; S = 8.8 ± 0.5; L = 4.3 ± 1.0; Fig. 3g).

At the histological level, a repetitive pattern was observed on the surface of the perilesional zone in all samples, consisting in a marked decrease in cellular density, low intensity of Safranin O staining and presence of clusters of chondrocytes, preferentially in the most superficial layers and the more numerous, the closer to the area of the lesion (Fig. 4).

Although macroscopically fibrous tissue was only observed in specimens from the 20-week time point, all 12 and 20-week untreated knees displayed at the histological level some amount of fibrous repair tissue of low quality lacking continuity of the cartilage surface surrounding the damaged area.

Collagen II positive immunostaining displayed a uniform sheet pattern distribution on the superficial cartilage in those lesions that were treated with cell-

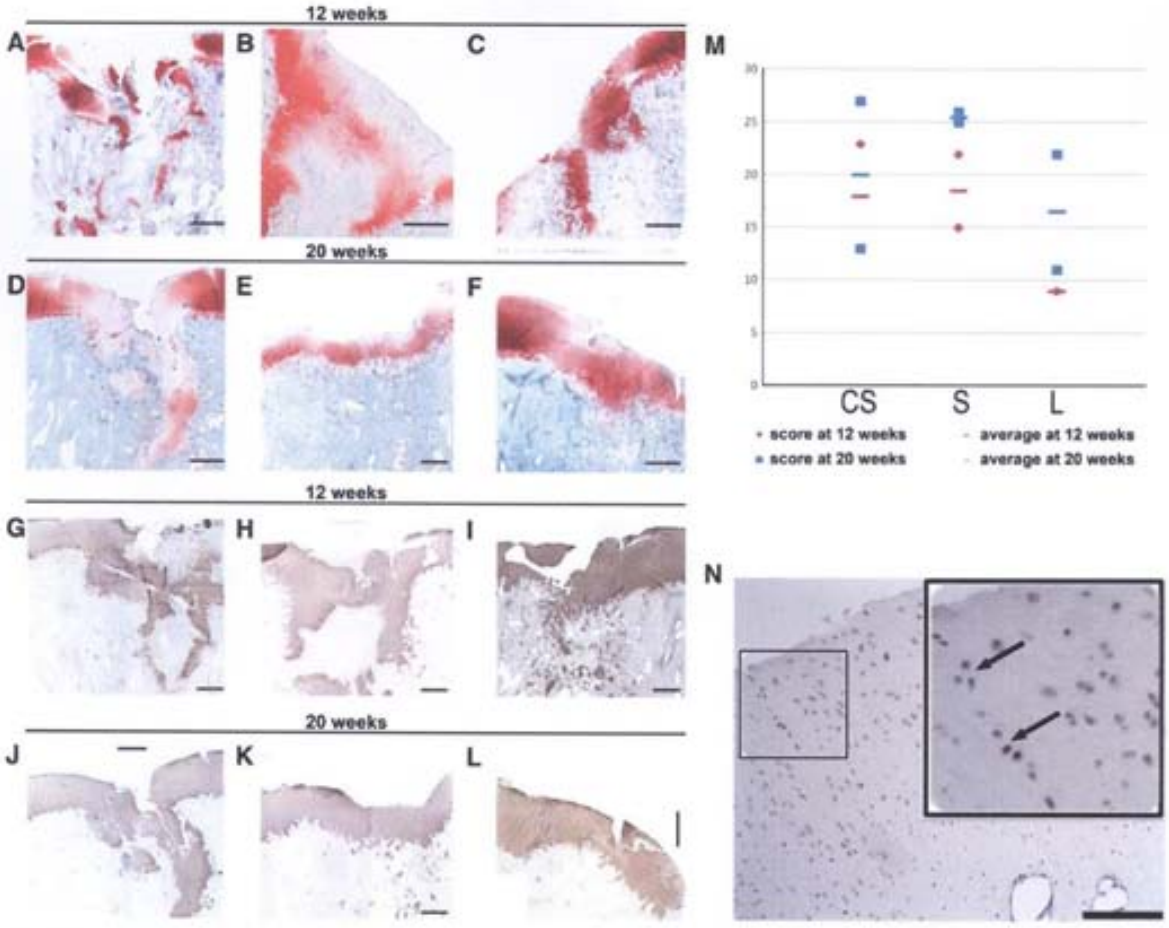

Fig. 4 Histochemical analysis of paraffin sections of cartilage specimens. In the left top panels, images from samples taken at 12 and 20 weeks post-operatively stained with Safranin O. In the *left bottom panels*, Collagen II immunostainings from samples taken at 12 and 20 weeks post-operatively. **a**, **g** Untreated knee (sample F12left); **b**, **h** defect treated with cell-free PLGA scaffold (F14left); **c**, **i** defect treated with cell-seeded PLGA scaffold (sample F6right); **d**, **j** untreated knee (sample F17left); **e**, **k** defect treated with cell-free PLGA scaffold (F16right); **f**, **l** defect treated with cell-seeded PLGA scaffold (sample F17right). **m** Graphical representation of the scores obtained at 12 and 20 weeks grouped together according to each treatment, where the average from each group is also graphically represented to highlight the similarity in their values. **n** Section from a knee treated with PLGA scaffolds loaded with chondrocytes (sample F16left) and stained for Sox9 (inset: zoomed view with *arrows* pointing to Sox9 positive cells). *CS* cell-seeded scaffold, *S* scaffold, *L* untreated lesion. *Scale bar* 600 μm

free scaffolds (at 20 weeks post-treatment; Fig. 4k) and cell-seeded scaffolds (both at 12 and 20-week post-treatment; Fig. 4i, l). Expression of Sox9 was observed in cells present within the hyaline cartilage (Fig. 4n). In all samples, Sox9 signal was found in most superficial cells of native hyaline cartilage and in clusters of chondrocytes located superficially in the perilesional area.

Taken together the scores from the histology and immunohistochemistry for each treatment, no statistically significant differences ($p > 0.01$) were found among any of the experimental groups (CS = 19.0 ± 7.1; S = 22.0 ± 5.0; L = 10.5 ± 9.0; Fig. 4m).

Discussion

In the orthopaedic field, special attention is given to cartilage repair using tissue-engineering techniques

due to the complexity of pathologies involving two types of distinct tissues: articular cartilage and subchondral bone. Accordingly, the use of either natural based polymers or synthetic materials in the manufacture of biocompatible scaffolds is currently a hot topic. Indeed, numerous studies have focused on the design of complex scaffolds, including the combination of two distinct layers or a gradient scaffold (reviewed by Rodrigues et al. 2011). In the present study, PLGA was chosen because it is one of the few synthetic materials approved by the FDA as scaffolding material for clinical applications and it has been previously used in articular cartilage treatment, emerging as a valuable chondrocyte and MSC delivery vehicle (Sittinger et al. 1996; Uematsu et al. 2005). Furthermore, the method followed for the manufacture of the scaffolds permitted to set a porosity level that allowed the ingrowth of host tissue as well as supporting the preloading with in vitro-expanded chondrocytes. Importantly, the scaffold structure allowed arthroscopic implantation making it an attractive material for clinical use and highlights the need for the use of large animal models in the development of new cartilage repair techniques; in particular, those species with size and physiology similar to humans. We used skeletally mature 2-year-old sheep (Kilborn et al. 2002), and the osteochondral defects were modelled in weight bearing areas. For this purpose, the experimental defects were located in the central/posterior region of the medial femoral condyle, with the aim of represent the clinical situation faced in humans. We chose to harvest cartilage cells from the shoulder, so both knees of each animal could be used in the study, in the same comparable conditions without additional lesions on the surrounding area that might influence the outcome of the treatments.

The use of chondrocytes allowed a significant improvement with respect to untreated controls at the macroscopic level, although this observation was not confirmed histologically, probably due to the short observation time. Therefore, it was not clear whether the addition of chondrocytes into the PLGA scaffolds could significantly accelerate the regeneration mechanisms.

To our knowledge, this is the first report of arthroscopic implantation of the PLGA scaffolds in the sheep knee. Published studies used arthrotomy procedures to implant the tissue engineered constructs (Córdoba et al. 2007; Erggelet et al. 2007; Niederauer et al. 2000), because the difficulty of holding in place the implant without invasive procedures. The biomechanical characteristics of some of the constructs, as the ones made of chondrocytes and fibrin are too soft to hold in the defect site independently of the use of a periosteum patch. The need of development of this minimally invasive technique in the sheep knee has been mentioned by some authors (Munirah et al. 2007; Sha'ban et al. 2008) and the regulatory authorities require the use of the intended route of administration in humans and the intended delivery device in preclinical studies. This surgical technique has the recognized advantage of decreased morbidity associated with arthrotomy, more ethical experimental procedure and a final study that matches the clinical situation faced in human patients. On the other side there are two limitations that need to be acknowledged in the present study. Although the clinically accepted range of MRI covers from 0.2T to 3T (Ghazinoor et al. 2007), the use of low-field MRI in this study made the detection of small cartilage abnormalities very challenging. The second point concerns to the sample size and the proximity of the two time endpoints for the euthanasia, which gave similar results, making possible to combine data for each treatment from both the 12- and 20-week groups for the statistical analysis. Future studies should evaluate the effects of a full regeneration process at later end-points (i.e., up to 12 months), other cell sources, and the appropriate therapeutic dose.

Acknowledgments The authors would like to acknowledge critical review and helpful comments of the original manuscript by Dr. Joan Garcia; Anna Morist, Anna Garrit and Cristian de la Fuente for technical assistance; and José Luís Ruiz, Ramón Costa and the crew of the "Servei de Granges i Camps Experimentals" of the UAB (Bellaterra, Spain) for their careful assistance to animal management. The project MEDCEL (PSE-010000-2007-4) was supported by the Spanish Ministry of Education and Science (MEC).

References

Ahern BJ, Parvizi J, Boston R, Schaer TP (2009) Preclinical animal models in single site cartilage defect testing: a systematic review. Osteoarthr Cartil 17:705–713

Alford JW, Cole BJ (2005) Cartilage restoration, part 1: basic science, historical perspective, patient evaluation, and treatment options. Am J Sports Med 33:295

Allen MJ, Houlton JEF, Adams SB, Rushton N (1998) The surgical anatomy of the stifle joint in sheep. Vet Surg 27:596–605

Córdoba FEV, Martínez CV, López VM, Butrón HL, Marín BR, Villaseñor EE, Castrejón HV, Arrieta LS, Morales RE, de León CIP (2007) Resultados en la reparación experimental de lesiones osteocondrales en un modelo porcino mediante ingeniería de tejidos. Acta Ortopédica Mexicana 21: 217–223

Erggelet C, Neumann K, Endres M, Haberstroh K, Sittinger M, Kaps C (2007) Regeneration of ovine articular cartilage defects by cell-free polymer-based implants. Biomaterials 28:5570–5580

Ghazinoor S, Crues JV 3rd, Crowley C (2007) Low-field musculoskeletal MRI. J Magn Reson Imaging 25:234–244

Kilborn SH, Trudel G, Uhthoff H (2002) Review of growth plate closure compared with age at sexual maturity and lifespan in laboratory animals. Contemp Top Lab Anim Sci 41:21–26

Mainil-Varlet P, Rieser F, Grogan S, Mueller W, Saager C, Jakob RP (2001) Articular cartilage repair using a tissue-engineered cartilage-like implant: an animal study. Osteoarthr Cartil 9:S6–S15

Mikos AG, Thorsen AJ, Czerwonka LA, Bao Y, Langer R, Winslow DN, Vacanti JP (1994) Preparation and characterization of poly(L-lactic acid) foams. Polymer 35: 1068–1077

Munirah S, Samsudin OC, Chen HC, Salmah SH, Aminuddin BS, Ruszymah BH (2007) Articular cartilage restoration in load-bearing osteochondral defects by implantation of autologous chondrocyte–fibrin constructs: an experimental study in sheep. J Bone Joint Surg Br 89:1099–1109

Niederauer GG, Slivka MA, Leatherbury NC, Korvick DL, Harroff HH, Ehler WC, Dunn CJ, Kieswetter K (2000) Evaluation of multiphase implants for repair of focal osteochondral defects in goats. Biomaterials 21: 2561–2574

Rodrigues MT, Gomes ME, Viegas CA, Azevedo JT, Dias IR, Guzon FM, Reis RL (2011) Tissue-engineered constructs based on SPCL scaffolds cultured with goat marrow cells: functionality in femoral defects. J Tissue Eng Regen Med 5:41–49

Sha'ban M, Kim SH, Idrus RB, Khang G (2008) Fibrin and poly(lactic-*co*-glycolic acid) hybrid scaffold promotes early chondrogenesis of articular chondrocytes: an in vitro study. J Orthop Surg Res 3:17

Simon TM, Aberman HM (2010) Cartilage regeneration and repair testing in a surrogate large animal model. Tissue Eng B Rev 16:65–79

Sittinger M, Reitzel D, Dauner M, Hierlemann H, Hammer C, Kastenbauer E, Planck H, Burmester GR, Bujia J (1996) Resorbable polyesters in cartilage engineering: affinity and biocompatibility of polymer fiber structures to chondrocytes. J Biomed Mater Res 33:57–64

Uematsu K, Hattori K, Ishimoto Y, Yamauchi J, Habata T, Takakura Y, Ohgushi H, Fukuchi T, Sato M (2005) Cartilage regeneration using mesenchymal stem cells and a three-dimensional poly-lactic-glycolic acid (PLGA) scaffold. Biomaterials 26:4273–4279

van den Borne MPJ, Raijmakers NJH, Vanlauwe J, Victor J, de Jong SN, Bellemans J, Saris DBF (2007) International Cartilage Repair Society (ICRS) and Oswestry macroscopic cartilage evaluation scores validated for use in autologous chondrocyte implantation (ACI) and microfracture. Osteoarthr Cartil 15:1397–1402

5.2- STUDY 2

CARTILAGE RESURFACING POTENTIAL OF PLGA SCAFFOLDS LOADED WITH AUTOLOGOUS CELLS FROM CARTILAGE, FAT, AND BONE MARROW IN AN OVINE MODEL OF OSTEOCHONDRAL FOCAL DEFECT.

M. Caminal, D. Peris, C. Fonseca , J. Barrachina , D. Codina , R.M. Rabanal, X. Moll , A. Morist , F. García , J.J. Cairó , F. Gòdia , A. Pla , J. Vives.

Cytotechnology. 2015. Published online 17 January 2015.

Cytotechnology
DOI 10.1007/s10616-015-9842-4

ORIGINAL RESEARCH

Cartilage resurfacing potential of PLGA scaffolds loaded with autologous cells from cartilage, fat, and bone marrow in an ovine model of osteochondral focal defect

M. Caminal · D. Peris · C. Fonseca · J. Barrachina · D. Codina · R. M. Rabanal · X. Moll · A. Morist · F. García · J. J. Cairó · F. Gòdia · A. Pla · J. Vives

Received: 11 February 2014 / Accepted: 8 January 2015

Abstract Current developments in tissue engineering strategies for articular cartilage regeneration focus on the design of supportive three-dimensional scaffolds and their use in combination with cells from different sources. The challenge of translating initial successes in small laboratory animals into the clinics involves pilot studies in large animal models, where safety and efficacy should be investigated during prolonged follow-up periods. Here we present, in a single study, the long-term (up to 1 year) effect of biocompatible porous scaffolds non-seeded and seeded with fresh ex vivo expanded autologous progenitor cells that were derived from three different cell sources [cartilage, fat and bone marrow (BM)] in order to evaluate their advantages as cartilage resurfacing agents. An ovine model of critical size osteochondral focal defect was used and the test items were implanted arthroscopically into the knees. Evidence of regeneration of hyaline quality tissue was observed at 6 and 12 months post-treatment with variable success depending on the cell source. Cartilage and BM-derived mesenchymal stromal cells (MSC), but not those derived from fat, resulted in the best quality of new cartilage, as judged qualitatively by magnetic resonance imaging and macroscopic assessment, and by histological quantitative scores. Given the limitations in sourcing cartilage tissue and the risk of donor site morbidity, BM emerges as a preferential source of MSC for novel cartilage resurfacing therapies of osteochondral defects using copolymeric poly-D,L-lactide-co-glycolide scaffolds.

Keywords Preclinical animal model · Regenerative medicine · Arthroscopy · Osteochondral defect · Progenitor cells

M. Caminal and D. Peris have contributed equally to this work.

Electronic supplementary material The online version of this article (doi:10.1007/s10616-015-9842-4) contains supplementary material, which is available to authorized users.

M. Caminal · A. Pla · J. Vives (✉)
Divisió de Teràpies Avançades/XCELIA, Banc de Sang i Teixits, Edifici Dr. Frederic Duran i Jordà, Passeig Taulat, 116, 08005 Barcelona, Spain
e-mail: jvives@bst.cat

D. Peris · J. J. Cairó · F. Gòdia
Grup d'Enginyeria Cel·lular i Tissular, Departament d'Enginyeria Química, Escola d'Enginyeria, Universitat Autònoma de Barcelona, Edifici Q, Campus de la UAB, 08193 Bellaterra, Cerdanyola del Vallès, Spain

C. Fonseca · R. M. Rabanal · X. Moll · A. Morist · F. García
Departament de Medicina i Cirurgia Animals, Àrea de Medicina i Cirurgia Animal, Universitat Autònoma de Barcelona, Edifici V, Campus de la UAB, 08193 Bellaterra, Cerdanyola del Vallès, Spain

J. Barrachina · D. Codina
Hospital ASEPEYO Sant Cugat, Avinguda Alcalde Barnils, 54-60, Sant Cugat del Vallès, 08174 Barcelona, Spain

Published online: 17 January 2015

Introduction

Articular cartilage focal defects represent a common condition affecting the knee and play a significant role in the subsequent development of degenerative joint disease (Huey et al. 2012). The self-healing response to chondral lesions involving the subchondral bone results in fibrocartilage, which has poorer biomechanical and biochemical characteristics compared to native hyaline cartilage (Alford and Cole 2005).

In an attempt to develop tissue engineering strategies, responsive seed cells and supportive scaffolds are sought as they are the critical components for successful resurfacing of articular cartilage. The only approved cell culture-based medicine available today employs autologous articular chondrocytes, which has shown mixed results in humans (Batty et al. 2011) and increases the risk of secondary osteoarthritis due to the procedure followed for tissue harvesting (which requires taking a biopsy of macroscopically intact cartilage from a non-weight bearing part of the joint) (De Bie 2007; Vanlauwe et al. 2011; Zaslav et al. 2009). Recently, much research has invested in searching for alternative cell sources (Oldershaw 2012) including amongst others mesenchymal stromal cells (MSC), which can be readily isolated and expanded in vitro from bone marrow (BM-MSC) or adipose tissue (ASC) (Lee and Im 2010; Pittenger et al. 1999). MSC not only hold high expansion and differentiation capacity but also the potential to recapitulate chondrogenesis when implanted in osteochondral defects (Caplan 1991). Indeed this has been extensively reported in the recent literature [please refer to Veronesi et al. (2014) and Tang et al. (2012) for comprehensive reviews on BM-MSC and ASC in preclinical studies], highlighting the broad use of small animal models in early research stages but also the limited number of studies on large, skeletally mature animal models with prolonged follow-up time periods and undergoing surgical approaches similar to human clinical practice (i.e. arthroscopy) (Hurtig et al. 2011).

In the present work, (A) the feasibility and long-term safety of a cell-based therapy was investigated and (B) the potential of cartilage resurfacing capacity of three different ovine cell sources in combination with poly-D,L-lactide-co-glycolide (PLGA) three-dimensional scaffolds was compared in a large animal model of single-site critical size osteochondral defects.

Materials and methods

Animals

Eight healthy 3-year old ewes of the Ripollesa-Lacona breed were supplied by *Servei de Granges i Camps Experimentals* (SGCE, Bellaterra, Spain). During the pre- and post-operative procedures, animals were housed together, fed a standard diet and allowed access to water ad libitum. All animal care and experimental procedures were approved by the Universitat Autònoma de Barcelona's Ethical Committee on Human and Animal Experimentation (Ref. No. CEAAH 501), and registered by the Departament de Medi Ambient de la Generalitat de Catalunya (Reg. No. 3666).

Study design

Two surgical procedures were performed in each animal. The first procedure involved the harvesting of tissues from three different sources (cartilage, BM and fat) for subsequent cell isolation and expansion. The second procedure was performed arthroscopically 4 weeks later and involved the creation of a standardized critical size osteochondral defect bilaterally in the medial and lateral femorotibial condyles. Each of the osteochondral defects produced in the medial and lateral femorotibial condyles were included randomly in either one of any of the three treatment or control groups (Table 1). After surgery, animals were allowed to move freely. Animals were further divided in two new groups, according to the two time end-points (6 and 12 months post-treatment, respectively). Each condyle was considered as an experimental unit, having four experimental units in each animal. A full necropsy was performed on all animals from the 12-month group.

Anaesthesia and post-operative care

All procedures were performed using aseptic techniques and under general anaesthesia. After premedication with an intramuscular (IM) injection of 0.01 mg/kg of buprenorphine (Buprex, Schering-Plough, S.A.) and 0.2 mg/kg of midazolam (Dormicum, Roche), intravenous (IV) access was established at cephalic vein. Animals were pre-oxygenated and induced with 4 mg/kg IV propofol (1 % Propofol-Lipuro, BBraun

Table 1 Study design

Sheep ID	Left (l) knee		Right (r) knee		Clinical follow-up (months)
	MC/dose	LC/dose	MC/dose	LC/dose	
F57	ASC-S 4.5×10^6	Chond-S 4.0×10^6	BM-MSC-S 3.2×10^6	BM-MSC-S 4.9×10^6	6
F58	BM-MSC-S 1.4×10^6	L	ASC-S 3.5×10^6	Chond-S 3.9×10^6	6
F63	Chond-S 1.3×10^6	BM-MSC-S 1.4×10^6	ASC-S 1.0×10^6	Chond-S 1.0×10^6	6
F64	Chond-S 2.4×10^6	BM-MSC-S 5.0×10^6	S	S	6[a]
F44	Chond-S 1.1×10^6	BM-MSC-S 4.9×10^6	S	S	12
F52	ASC-S 1.0×10^6	L	Chond-S 4.2×10^6	BM-MSC-S 3.2×10^6	12
F59	BM-MSC-S 1.4×10^6	L	ASC-S 2.6×10^6	Chond-S 3.7×10^6	12
F61	BM-MSC-S 4.9×10^6	Chond-S 0.7×10^6	Chond-S 1.1×10^6	ASC-S 1.1×10^6	12

Experimental plan used for the evaluation of the effect of different treatments on osteochondral defects on the medial and lateral femorotibial condyles. Dose of cells is indicated when appropriate

MC medial condyle, *LC* lateral condyle, *ASC-S* scaffold seeded with adipose tissue-derived MSC, *BM-MSC-S* scaffold seeded with bone marrow-derived MSC, *Chond-S* scaffold seeded with progenitor cells expanded from cartilage biopsies, *S* cell-free scaffold; *L* untreated lesion

[a] Animal F64 was found dead at month 4 after treatment

Melsungen AG). The animals were intubated and maintained on 2 % isoflurane (Isoflo, Abbott laboratories Ltd) mixed with oxygen. Esophageal intubation was made to prevent ruminal bloat. A continuous infusion of Ringer lactate (Ringer lactate, BBraun Melsungen AG) was administered at 10 mL/kg/h during surgery. Intra-operative monitoring consisted of electrocardiography, pulse oximetry, non invasive blood pressure and capnography. All animals received one daily dose of subcutaneous 0.2 mg/kg meloxicam (Metacam, Boehringer) daily for 10 days and a single dose of transdermal 100 µg fentanyl (Durogesic, Janssen-Cilag) for post-operative pain relief. For peri-operative infection prophylaxis, all animals received 22 mg/kg of cefazolin IM (Kurgan, Normon Laboratories) and thereafter every 12 h for 10 days.

Isolation of cells, culture and seeding of scaffolds

Bone marrow was aspirated from the sternum of the animal models and were used for the isolation of the BM-MSC as described elsewhere (Caminal et al. 2014a; Vélez et al. 2012). An articular cartilage layer of 1 mm thick and 6 mm long was harvested from the head of humerus, using a curette. Then cartilage was pierced and used as a source of chondrocytes. Intra-abdominal fat tissue was used as a source of ASC. Tissues were washed and soaked with phosphate-buffered saline solution (PBS, HyClone) and immediately processed in the laboratory. The fragments of fat and cartilage were minced, washed three times in PBS, and digested with 0.2 % (w/v) Collagenase (Sigma-Aldrich) I or II (respectively) for 24 h. Cells and tissues were resuspended in 10 mL of Dulbecco's modified Eagle's medium (DMEM, Gibco) supplemented with 10 % (v/v) foetal calf serum (FCS, Biological Industries) and centrifuged at 400 *g* for 5 min. Cells were washed in PBS and cultured in a T-25 flask in DMEM containing 10 % (v/v) FCS, in a humidified 5 % CO_2 incubator. Cells were scaled-up by seeding T-150 flasks at 2,500 cell/cm^2. Cell number and viability were determined by the

haemocytometer-based trypan blue dye exclusion assay. Glucose and lactate concentrations in supernatants were determined using an YSI 2700 automated analyser (Yellow Springs Instruments). Generation time (t_d, days), cell growth rate (μ, days^{-1}), specific consumption (q_{Glc}, nmol/10^6 cells/h) and production rates (q_{lac}, nmol/10^6 cells/h) of extracellular metabolites (glucose and lactate, respectively) were calculated as described elsewhere (Schop et al. 2009).

ASC, MSC and chondrocyte progenitors were cultured in low glucose DMEM medium supplemented with streptomycin (0.167 g/L, Sigma-Aldrich), kanamycin (0.075 g/L, Sigma-Aldrich) and 10 % FCS. Ex vivo expanded cells were then loaded onto three-dimensional PLGA scaffolds that were manufactured in-house following a solution-casting/salt-leaching technique using PLGA particles with a viscosity of 0.55–0.75 dL/g (Lactel), as described elsewhere (Fonseca et al. 2014). Briefly, polymeric PLGA particles (at 50:50 or 75:25 ratio of PLA:PGA, respectively) were first dissolved in chloroform. Then, sieved salt particles ranging 74–147 μm (for small pores), 300–500 μm (for large pores) and a combination of both (for mixed size pores) were dispersed in the polymer solution at a 9:1 ratio (NaCl:PLGA). The mixture was casted into a cylindrical mould, with a diameter of 4 and 7 mm high. After the evaporation of the solvent, the salt particles were extracted by washing the polymer with distilled water for 48 h. Then the scaffolds were dried at air temperature for 24 h and then vacuum dried for 24 h. Finally, the scaffolds were gamma sterilized (20 kGy) and stored at −20 °C.

For the manufacture of cell:scaffold constructs, 5×10^6 fresh cells (not previously cryopreserved) and scaffolds were incubated for 24 h at 37 °C in stirred minibioreactors (Hexascreen Culture Technologies S.L.) in a final volume of 12 mL of DMEM supplemented with 10 % FCS. Degradation assays were conducted placing the scaffolds in DMEM using a cell culture incubator. Then, samples were taken, lyophilised and weighted, and plotted in order to determine the weight percent of initial polymer.

Differentiation assay

Multipotentiality of isolated cells was determined using StemPro differentiation media (Gibco). Safranin O (Sigma), Oil Red O (Sigma), Alkaline Phosphatase (Takara Bio Inc.) and Von Kossa (Silver nitrate, Sigma) stainings were performed to determine the outcome of the differentiation assays.

Flow cytometry

Flow cytometric analyses were performed as reported elsewhere (Caminal et al. 2014b) in order to evaluate the expression of CD44 (G44-26, BD Biosciences), CD90 (5E10, BD Biosciences), CD105 (MHCD1 0504, Invitrogen), CD140a (αR1, BD Biosciences), CD166 (3A6, BD Pharmingen) in a FACSCalibur flow cytometer (BD Biosciences). PE-conjugated IgG1 (X40, BD Biosciences) and FITC-conjugated IgG2bk (27-35, BD Biosciences) antibodies were used as isotype controls. Fc-binding receptors were blocked with normal mouse IgG (10400C, Life Technologies).

RT-PCR

Total RNA was extracted using RNeasy Mini columns (Qiagen) according to the manufacturer's instructions. RNA samples were subjected to reverse transcription-PCR (RT-PCR) analysis in a single-step procedure using the Titan One Tube RT-PCR System (Roche). Reverse transcription was carried out at 50 °C with specific primers, followed by hot-start PCR in the same tube. Primers used were: GAPDH: 5′-CGGATTTGGTCGTATTGG-3′ forward and 5′-TCAAAGGTGGAGGAGTGG-3′ reverse (861 bp); type-I collagen 5′-CCACCAGTCACCTGCGTACA-3′ forward and 5′-GGAGACCACGAGGACCAGAA-3′ reverse (460 bp); type-II collagen 5′-ACGGTGGACGAGGTCTGACT-3′ forward and 5′-GGCCTGTCTCTCCACGTTCA-3′ reverse (141 bp); aggrecan 5′-CCGCTATGACGCCATCTGCT-3′ forward and 5′-TGCACGACGAGGTCCTCACT-3′ reverse (375 bp); biglycan 5′-CCATGCTGAACGATGAGGAA-3′ forward and 5′-CATTATTCTGCAGGTCCAGC-3′ reverse (204 bp); and TGF-β 5′-CGGCAGCTGTACATTGACTT-3′ forward and 5′-AGCGCACGATCATGTTGGAC-3′ reverse (271 bp).

Scanning electron microscopy (SEM)

Samples were fixed in 2.5 % glutaraldehyde and 2 % paraformaldehyde in PBS (pH 7) and dehydrated in ethanol series (15 min in each 30–50–70–90–100–100 %) to absolute ethanol and immediately

transferred to acetone before being critical-point dried and gold-coated using a Sputter Coater (K550, Coating Attachment, Emitech Ashford). Samples were examined with an HITACHI S-570 electron microscope at a voltage of 15 kV.

Osteochondral defect creation and arthroscopic implantation

Osteochondral defects were created and test items were implanted arthroscopically. Each joint was approached via a stab incision lateral to the distal aspect of the patellar ligament, allowing the insertion of the arthroscope with its camera for the visualization of the medial condyle. A mechanical shaver was used to remove the fat pad and thus allowing a clearer view. For this purpose, a second stab incision was made medial to the distal aspect of the patellar ligament to allow the shaver insertion. Then the shaver was removed and a mosaicplasty instrument set consisting of a donor and a receptor cannulae (Smith and Nephew Inc), was used to create the defect and to place the scaffold using the cylindrical hollow punch with an inner diameter of 2.7 mm (donor cannula) placed through the second stab incision. This instrument was used to perform a cylindrical osteochondral lesion of diameter 3.5 and 5 mm depth in the caudal aspect of the medial and lateral femoral condyles of each knee. Cylindrical scaffolds were placed through the receptor cannula, filling the lesion by the application of moderate force to the syringe piston. The joints were irrigated by saline solution (NaCl-0.9, BBraun Medical SA) at room temperature during surgery.

Magnetic resonance imaging (MRI)

MRI examination was performed on both knees of each animal under general anaesthesia at 6 or 12 months, according to the experimental group, using a 0.2 T unit with open permanent magnet (Vet-MR, Esaote S.p.a.) as described previously (Fonseca et al. 2014).

Histological evaluation and immunohistochemical procedures

All animals were sedated with an IM injection of 0.02 mg/kg of midazolam and euthanised by IV injection of 12 mg/kg pentobarbital (Dolethal 20 mg/100 mL, Vetoquinol S.A.). Both stifle joints were harvested and condyles fixed in 4 % paraformaldehyde solution at room temperature for 2 weeks, decalcified with 5 % formic acid for 4–6 weeks and embedded in paraffin for subsequent histological and immunohistochemical procedures. Microtome sections 4 µm thick were cut in the sagittal plane and stained with either haematoxylin/eosin (H&E, Sigma-Aldrich) or safranin O (Sigma-Aldrich). The success of the treatment was evaluated blindly following a histological scoring grading scale (Mainil-Varlet et al. 2003) (Suppl. Table 1) on at least 4 sequential histological sections including the areas depicted in Suppl. Figure 1.

The presence of type-II collagen was detected immnunohistochemically using polyclonal antibodies (MAB 8887, Chemicon). Briefly, paraffin sections were deparaffinised, hydrated, and then treated with 0.1 % Pepsin (Sigma-Aldrich) in 0.01 N HCl for 20 min. Endogenous peroxidase activity was blocked with hydrogen peroxide for 30 min and washed in 3 % bovine serum albumin (BSA, Sigma-Aldrich) in PBS. Sections were incubated with the primary antibody (dilution 1:200) overnight at 4 °C. Antibody binding was visualized by using Universal LSAB^{TM}2 Kits (Dako) in combination with diaminobenzidine (DAB) according to the manufacturer's instructions and counterstained with haematoxylin.

Results

Autologous progenitor cells were harvested from ASC, BM and cartilage followed by in vitro expansion (Fig. 1a–c). A total of 600 cm^2 (that is four T-150 flasks per cell line) were used in the scale up. The yield ranged 2.1–8 × 10^4 chondrocyte progenitor cells/cm^2, 0.8–5.4 × 10^4 BM-MSC/cm^2, and 0.5–5.2 × 10^4 ASC/cm^2. MSC showed fibroblastic morphology, trilineage potency and expressed CD44, CD90, CD105, CD140a and CD166 surface markers (Fig. 1d, f–h). Expanded cells from cartilage tissue expressed low levels of type-II collagen, as opposed to native articular cartilage used as control, and displayed trilineage potential (Fig. 1e, i–k) Expanded chondrocyte progenitors and ASC displayed higher metabolism than BM-MSC, although similar cell growth rates were observed in the three cell types (Table 2), which were subsequently used for seeding three-dimensional

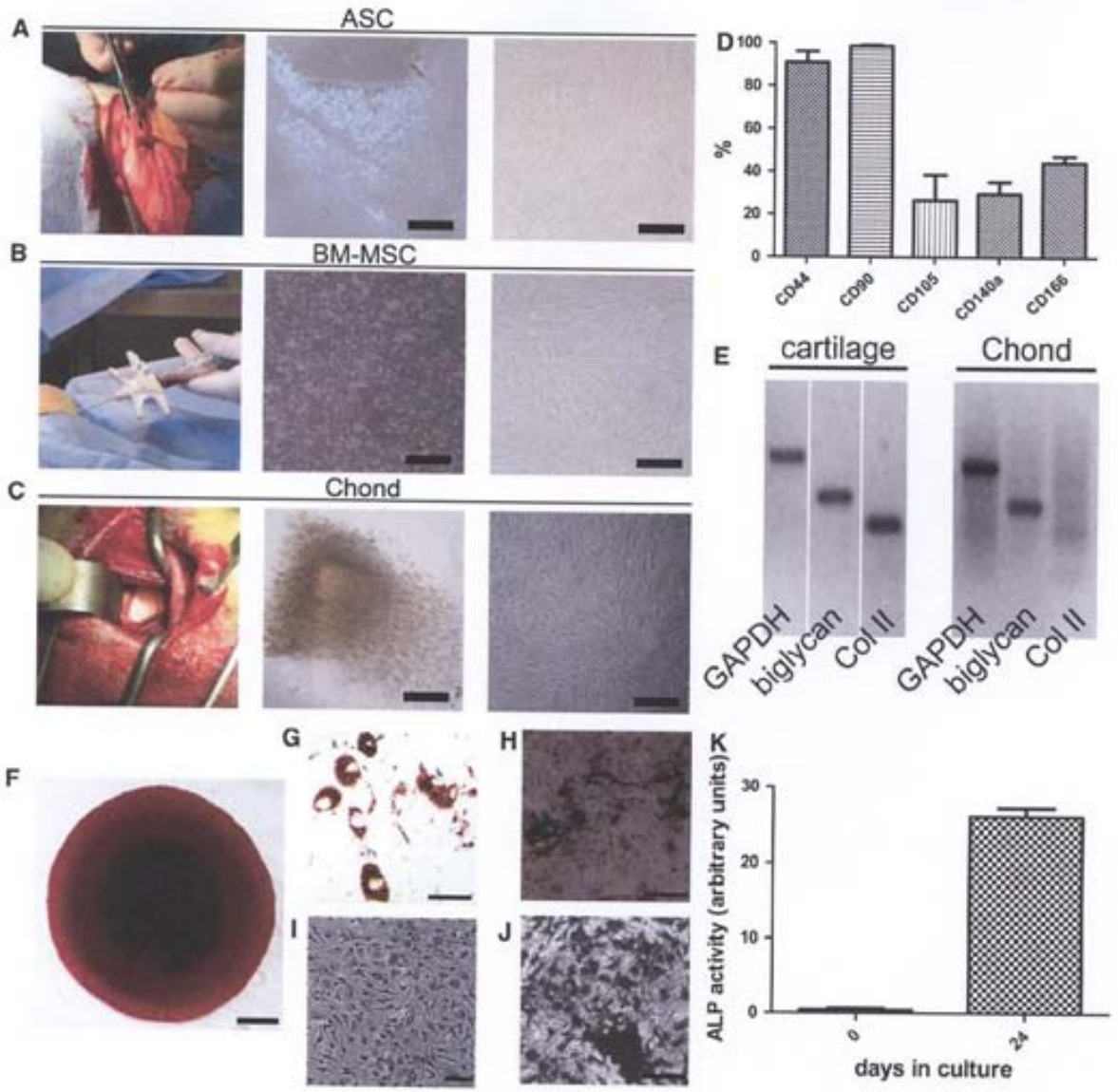

Fig. 1 Harvesting of tissues, cell expansion and characterisation. First, tissue was harvested from fat (**a**), bone marrow (**b**) and cartilage (**c**). Then, enzymatic disaggregation was performed for fat and cartilage, and mononuclear cells were isolated from bone marrow and then plated in T-flasks. Finally, ASC, BM-MSC and dedifferentiated chondrocytes were expanded in vitro. Immunophenotype profile of MSC using antibodies that cross-reacted with ovine samples (**d**) and RT-PCR from cultures of expanded cells from cartilage compared to native cartilage tissue (**e**). Multipotentiality of MSC and progenitor cells expanded from cartilage tissue as determined in chondrogenesis (**f**), adipogenesis (**g**, **i**, respectively) and osteogenesis (**h**, **j**, **k**) assays. *Col II* type-II collagen. *Scale bars* = 200 μm

scaffolds. Prior to do this, the degradation profile of different scaffold designs (PLA:PGA ratio and pore size) and cell seeding kinetics were tested with expanded chondrocyte progenitors (Fig. 2). With respect to the degradation profile, no changes in mass were detected within the first 5 weeks. However, at 7 weeks, mass was reduced to half of its initial value in PLGA 50:50 with large pore size (Fig. 2a). Only PLGA scaffolds with large pore sizes (in the range 300–500 μm) were homogeneously colonised with cells, whereas scaffolds with smaller pores displayed cells only on the external surface (Fig. 2b–d). The

Table 2 Cell growth and metabolic parameters

Cell type	μ (days^{-1})	t_d (days)	q_{Glc} (nmol/10^6 cells/h)	q_{lac} (nmol/10^6 cells/h)	$Y_{lac/Glc}$
Chond	0.37	1.85	7.61	15.74	1.78
ASC	0.34	2.07	9.17	17.86	1.88
BM-MSC	0.39	1.76	1.36	4.00	1.80

Values of the cell growth rate (μ), generation rate (t_d), specific consumption rate of the carbon source (q_{Glc}), production rate of lactate (q_{lac}) and molar lactate/glucose yield ($Y_{lac/Glc}$)

ASC adipose tissue-derived MSC, *BM-MSC* bone marrow-derived MSC, *Chond* cells derived from cartilage tissue

scaffold used for subsequent studies was PLGA 50:50. In order to confirm the biocompatibility of the scaffolds prior to their use in vivo, these were seeded with expanded chondrocyte progenitors and the metabolic activity of cells loaded onto the PLGA scaffolds was determined by measuring glucose consumption and lactate production for the next 12 days (Fig. 2e). Steady consumption of glucose and production of lactate was observed along the culture time indicative of a viable cell culture. Histological analysis of the scaffolds confirmed the presence of viable cells consistently distributed within the PLGA structure (Fig. 2f). Then, each PLGA scaffold and 5×10^6 -cells expanded from either fat, BM or cartilage were incubated in single-use bioreactors resulting in the seeding of an average of 2.28×10^6 ASC (range 1–4.5 $\times$ 10^6 cells), 2.34×10^6 expanded chondrocyte progenitor cells (range 0.7–4 $\times$ 10^6 cells) and 3.37×10^6 BM-MSC (range 1.4–5 $\times$ 10^6 cells), as determined by indirect counting of non-seeded cells present in the supernatant (Table 1).

Experimental lesion, test item implantation and clinical outcome

Bilateral arthroscopy was well tolerated and all animals were able to stand on all four limbs and walk immediately after surgery. No clinical complications occurred after the transplantation procedures in any of the animals with the exception of F64 (from the 6-month group), that was found dead at month 4 after treatment. The necropsy performed on this animal revealed pneumonia as a most probable cause of death, which was not related to the treatment (Supplemental Fig. 2).

All the constructs remained firmly adhered at the implantation site and PLGA was fully resorbed at the two end-time points of the study, as revealed by macroscopical observation and confirmed by histological analysis, consistent with the degradation rate observed in vitro (Fig. 2a). A full necropsy was performed on all animals from the 12-month group in order to exclude any potential long-term toxicity that may be caused by the treatment. No infections, fibrinous overgrowth on the joint surface or signs of other potential adverse effects were observed in any of the organs.

Untreated and cell-free controls

Major findings in the untreated control group included the presence of fissures extending to the subchondral bone and MRI analyses revealed signs of bone oedema (Fig. 3a). Spongy bone increased its thickness and invaded the cartilage surface. Wide areas of the articular surface were refilled with fibrocartilage and presented focuses of vascularisation (Fig. 3b). The presence of poteoglycans was restricted to the deepest zone, around the columnar-distributed chondrocytes but not on the surface (Fig. 3c). Type-II collagen staining accumulated in S1 but was fainter in D1 (Fig. 3d; Suppl. Figure 1).

With respect to cell-free scaffold controls, at 6 months post-treatment, the presence of a fibrous matrix was restricted to the deepest zone (Table 3; Fig. 3e–h). Integration in S1 and S2 territories was irregular and subchondral bone presented residual calcified cartilage in D1. At 12 months post-treatment, irregularities were observed on the surface at the defect site, not levelled with the surrounding tissue and presenting deep depressions and fissures. MRI analysis showed wider lesions than the defect modelled initially with a marked irregularity in the subchondral bone.

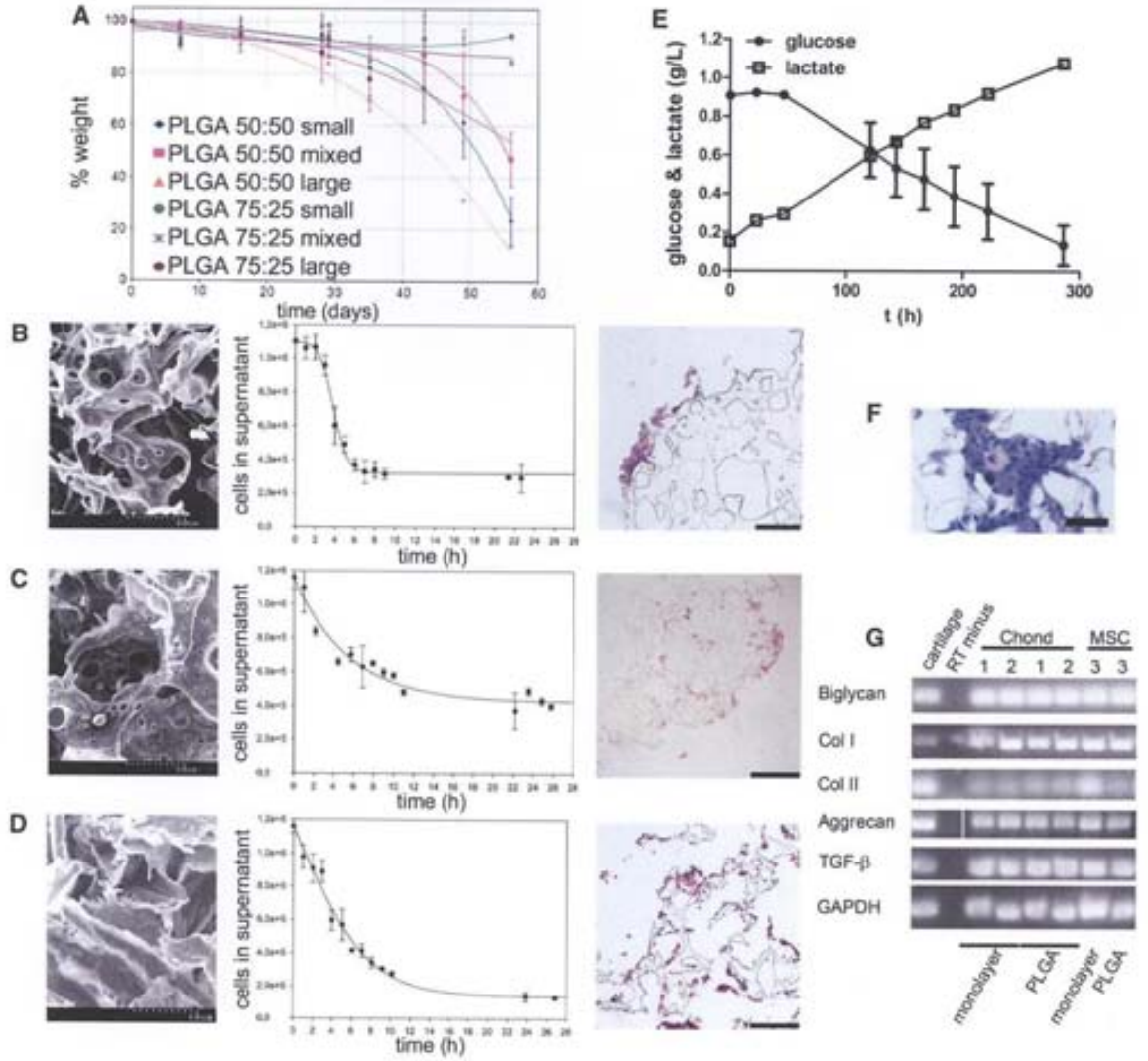

Fig. 2 Characterisation of PLGA scaffolds. In **a**, degradation profile of PLGA scaffolds at 50:50 and 75:25 PLA:PGA ratios and manufactured with different pore size (small, large and mixed). SEM images of the surface of non-seeded scaffolds and Haematoxylin and Eosin-stained histological analyses of cell-seeded PLGA 50:50 scaffolds manufactured with different pore sizes (**b**: small pore sizes in the range 74–147 μm and 74.96 ± 0.15 % porosity; **c**: mixed pore sizes in the range 74–147 and 300–500 μm and 81.73 ± 0.02 % porosity; and **d**: large pore sizes in the range 300–500 μm and 77.06 ± 0.04 % porosity) after 24-h incubation time. Biocompatibility of PLGA scaffolds loaded with cells expanded from cartilage tissue as determined by glucose consumption and lactate production in culture (**e**). In **f**, paraffin section of a cell-seeded PLGA 50:50 scaffold after 12 days in culture. In **g**, chondrogenesis assay for expanded cells from cartilage (samples 1 and 2) and MSC (sample 3) differentiated for 12 days in vitro either in monolayer or loaded onto PLGA scaffolds. *Col I* type-I collagen; *Col II* type-II collagen. *Scale bars* = 400 μm, except in **e** = 200 μm

Scaffolds seeded with chondrocytes expanded from cartilage biopsies

At 6 months post-treatment, proteoglycan and type-II collagen content did not match the expression levels observed in neighbouring normal tissue, and the integration was only partial at the S1/D1 border. In S1 and D1, chondrocytes were grouped in clusters as if migrating to the lesioned area. Cystic empty cavities with broad fibrous focuses were observed within the

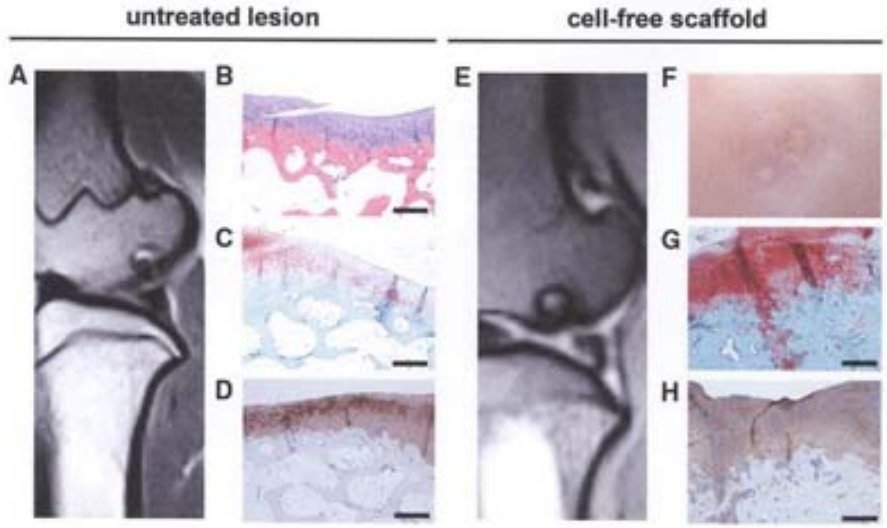

Fig. 3 Untreated and cell-free scaffold control groups. MRI image from F58l (**a**), Haematoxylin and Eosin staining of a section from F52l (**b**), safranin O staining of a section from animal F52l (**c**) and immunohistochemical staining for type-II collagen on a tissue section from animal F59l (**d**). MRI image from F44r (**e**), macroscopic view of the defect site on condyle F44r (**f**); safranin O staining (**g**) and immunohistochemical staining for type-II collagen (**h**) on sequential sections of condyle F44r. *Scale bars* = 500 μm

Table 3 Summary of scores for each condyle according to the treatment applied

	6 months					12 months					
Controls	L	F58l	S	F64r[a]	F64r[a]	L	F44r	F44r	S	F59l	F52l
		12		n.d.	n.d.		7	8		8	13
		Hyaline		n.d.	n.d		Mixed	Hyaline		Mixed	Mixed
ASC-S	F57l	F63r	F58r			F52l	F61r	F59r			
	8	3	7			9	9	7			
	Mixed	Mixed	Mixed			Mixed	Mixed	Mixed			
BM-MSC-S	F57r	F57r	F58l	F63l	F64l[a]	F52r	F59l	F44l	F61l		
	7	4	4	3	n.d.	10	8	10	17		
	Mixed	Mixed	Mixed	Mixed	n.d.	Hyaline	Mixed	Hyaline	Hyaline		
Chond-S	F57l	F63l	F63r	F58r	F64l[a]	F52r	F61l	F61r	F59r	F44l	
	4	8	4	11	n.d.	10	11	7	9	8	
	Mixed	Mixed	Mixed	Hyaline	n.d.	Hyaline	Hyaline	Mixed	Mixed	Hyaline	

This summary includes histological evaluation (maximum score = 18 points) and the overall classification of the type of new tissue generated in the defect (either hyaline or mixed hyaline/fibrocartilage). The code used for animal identification corresponds to animal number (i.e.: F6) followed by the r (right) or l (left) knee (i.e.: F6r), according to the experimental groups described in Table 1

ASC-S scaffold seeded with adipose tissue-derived MSC, *BM-MSC-S* scaffold seeded with bone marrow-derived MSC, *Chond-S* scaffold seeded with progenitor cells derived from cartilage tissue, *S* cell-free scaffold, *L* untreated lesion, *nd* not determined

[a] Animal F64 was found dead at month 4 after treatment

spongy bone. In some cases, lesions appeared fully repaired at the macroscopic level and displayed shiny smooth white tissue of great similarity to the surrounding intact articular cartilage, whilst others presented deep depressions of the surface with a colour that differed from the native adjacent tissue (Table 3). MRI analyses revealed subchondral bone lesions with sclerotic aspect and small osseous

oedemas, as evidenced by STIR hypersignal. At 12 months, S1 appeared uniform and levelled in most cases (Fig. 4b). S1 and S2 were made of hyaline cartilage with columnar chondrocytes in the deep zone of S1 and grouped on the surface areas (Fig. 4c). Subchondral bone in D1 and D2 was similar to normal tissue in S3, evidencing complete bone regeneration (Table 4). Type-II collagen content and safranin O staining extent and intensity was higher in all specimens from the 12-month group compared to the 6-month treatment group.

Scaffolds seeded with adipose tissue-derived mesenchymal stromal cells

At the 6 month time point, massive surface depressions were observed macroscopically on the defect site. MRI analyses confirmed the presence of sclerotic lesions affecting the subchondral lamina. Better results were obtained at 12 months. Histologically, the surface appeared irregular in some samples with vertical fissures that deepened into the middle region of the articular cartilage, but presenting good integration to the perilesional zones S2 and S3 (Fig. 4g, h). Hyaline-like tissue predominated, although fibrous tissue was also present in some areas at the integration border of the subchondral bone and the surface (Fig. 4g). Subchondral bone in D1 and D2 presented increased thickness with large trabeculae and the tidemark (which is the basophilic line between calcified and uncalcified cartilage) disappeared (Fig. 4h). MRI analyses did not evidence any noteworthy improvement, and it was possible to detect lesions with pseudonodular morphology in some specimens (Fig. 4e).

Scaffolds seeded with bone marrow-derived mesenchymal stromal cells

At 6 months post-treatment, MRI analyses did not reveal extensive lesions, but craters were observed on the caudomedial aspect in line with the results obtained histologically. At the end of 12 post-transplantation months, the defects were completely regenerated with white, shiny, and smooth tissue similar to the intact articular cartilage, although some fissures were also observed. MRI analyses showed the presence of smaller lesions than in other treatment groups, as demonstrated by T1 and T2 hiposignal, and absence of canvas STIR sequences (Fig. 4i). No morphological alterations were observed on the condylar surface, which was compatible with a regenerated lesion. Histologically, the extracellular matrix (ECM) was of hyaline nature in S1, with chondrocytes

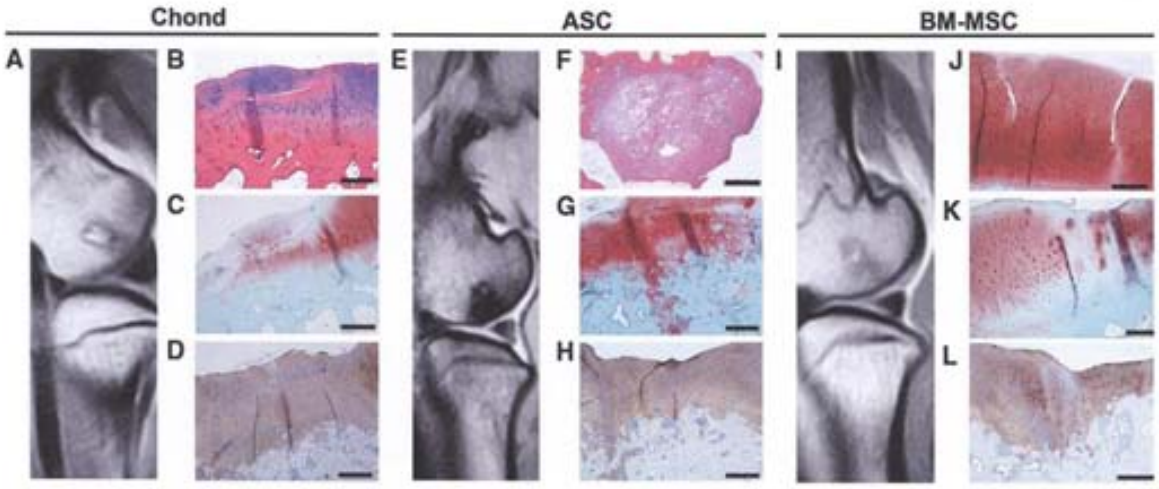

Fig. 4 MRI and histological analyses at 12 months post-treatment with PLGA scaffolds loaded with cells. MRI image of condyle F61l (**a**); Haematoxylin and Eosin staining (**b**) and safranin O staining of lateral condyle F61l (**c**); immunohistochemical staining for type-II collagen on medial condyle F61r (**d**). MRI image of condyle F59r (**e**); Haematoxylin and Eosin staining of condyle F52r (**f**); safranin O (**g**) and immunohistochemical staining for type-II collagen (**h**) staining of condyle F59r. MRI image of condyle F61l (**i**) and safranin O staining of condyles F61l (**j**) and F52r (**k**) and immunohistochemical staining for type-II collagen of condyle F52r (**l**). *Scale bars* = 500 μm, except **f** = 1,000 μm and **k** = 200 μm

Table 4 Histological results at 12 months post-treatment

	ASC	BM-MSC	Chondrocytes
I. Surface	=	+	=
II. Matrix	=	+	+
III. Cell distribution	+	+	+
IV. Cell viability	−	=	=
V. Subchondral bone	=	+	+
VI. Calcification of cartilage	−	−	−
Proteoglycans	−	+	−
Collagen type II	−	−	−

Comparison of the scores that define the quality of the neotissue (according to the ICRS histological grading system) resulting from treatment with three cell sources compared to the controls treated with cell-free scaffolds

ASC adipose-derived MSC, *BM-MSCS* bone marrow-derived MSC, = same as control, + higher than control, − lower than control

organised individually and in columns (Fig. 4j). Subchondral bone also showed normal aspect. In some specimens, though, the lesion was found partially levelled but thinner with the presence of fissures on the surface (Fig. 4l). Proteoglycan and type-II collagen contents were poor in S1, with scarce cellularity in relation to adjacent native cartilage (Fig. 4h; Table 4).

Discussion

In the orthopaedic field, special attention is given to novel tissue-engineering techniques for the repair of damage on hip, knee and elbow joints, due to the complexity of treating pathologies that involve two types of tissue (namely, subchondral bone and avascular articular cartilage) (Capito and Spector 2003). Despite of the extensive literature on the use of stem cell therapies at the research stage, only ex vivo expanded chondrocytes have been approved by the regulatory authorities for human use and have thus become the *gold standard* in cell therapy for cartilage resurfacing of focal injuries (Vanlauwe et al. 2011).

In the present study, scaffolds of PLGA (a copolymer made of PLA and PGA) were used as a vehicle of three different cell types that were tested side-to-side under the same experimental conditions in order to assess cartilage resurfacing capacity at 6 and 12 months post-implantation on critical size osteochondral defects. PLGA was chosen because (A) its proven biocompatibility, (B) the feasibility of three-dimensional molding of the constructs in the shape of the experimental defects, (C) it allowed minimally invasive arthroscopic implantation and (D) its degradation rate, which was compatible with the expected deposition of ECM by the cells loaded on the scaffolds (Villalobos Córdoba et al. 2007; Niederauer et al. 2000; Sittinger et al. 1996; Uematsu et al. 2005). Moreover, the use of porous PLGA scaffolds permitted the retention of the cells at the defect site and promoted homogeneous distribution throughout the graft.

We observed that PLGA scaffolds at a ratio of 50 (PLA):50 (PGA) preserved their integrity up to 5 weeks in vitro, which is compatible with the time taken by the cells to synthesize the new ECM [from 9 to 20 days, according to the work performed by Barry and collaborators (Barry et al. 2001)] that substitutes the scaffolding material (Middleton and Tipton 2000). Furthermore, PLGA-based constructs allow arthroscopic implantation, making this biomaterial even more attractive for clinical use, since the arthroscopic technique reduces morbidity, surgical time, patient recovery and secondary complications typically derived from open surgery that are routinely performed in tissue engineering strategies for cartilage repair (Villalobos Córdoba et al. 2007; Erggelet et al. 2007; Niederauer et al. 2000). Although in some samples the tide mark was faint or disappeared, it is remarkable that none of the specimens showed detachment of neocartilage from subchondral bone, indicating that the integration between the two layers resisted the load bearing forces in all treatment groups and highlighting the suitability of PLGA scaffolds in the treatment of osteochondral defects.

With respect to cell types, the differentiation potential of MSC into chondrocytes and osteoblasts makes these cells very attractive for the simultaneous regeneration of bone/cartilage lesions. Additionally, MSC can be expanded extensively in vitro whilst chondrocytes hold a limited culture growth capacity and display phenotypic instability during the course of their expansion in monolayer culture. Such phenotypic instability (also called "dedifferentiation") is characterised by a shift of cellular morphology from a rounded to the typical fusiform

fibroblastic shape, among other features (Schnabel et al. 2002), as we also observed in the present study (Fig. 1i). Considering the advantages of using BM-MSC and provided that both chondrocytes and BM-MSC gave similar results with respect to the quality of the new tissue, our results may suggest that BM-MSC as the preferred cell source in cell-therapies aiming at osteochondral repair using PLGA scaffolds. On the other hand, we observed that ASC were not as effective as BM-MSC to regenerate osteochondral defects neither at 6 nor at 12 months post-treatment. Different expression profiles in ASC and BM-MSC may explain why the latter differentiate more efficiently into bone and cartilage, whereas ASC differentiate better into adipocytes as reported previously by Liu and collaborators (Liu et al. 2007) thus supporting our observations in the present study.

The safety of the implantation of autologous cell:scaffold constructs was demonstrated by the absence of local or systemic adverse effects during the clinical follow-up and by a full necropsy performed at 12 months post-treatment. With respect to the efficacy, the presence of cartilage of hyaline quality 1 year after treatment with either BM-MSC or chondrocytes is a key point since current surgical approaches typically result in a short-term clinical success but eventually fail due to poor mechanical properties of the mixed matrix that is generated. For example, even though fibrocartilaginous repair tissue from microfracture results in initially enhanced clinical knee-function scores at earlier assessment time points, it later degrades, and scores decline (Mithoefer et al. 2009). This also highlights the importance of using large animal models with anatomy similar to the human knee allowing orthopaedic surgeons to undergo procedures similar to those in human practice and therefore making possible to assess the performance of novel implants in situ using minimally invasive approaches. Due to its size and anatomy, sheep arises as a relevant translational animal model for this type of research and, in fact, it has been previously used in several other studies for the treatment of chondral and osteochondral lesions [as comprehensively reviewed by Ahern and collaborators (Ahern et al. 2009)].

Finally, we conclude that the use of expanded cells from cartilage, BM and ASC in combination with PLGA scaffolds for cell therapy of osteochondral defects is safe even after 1 year post-administration and that cartilage of hyaline quality is observed principally after using cells derived from cartilage and BM. Further work is needed in order to evaluate dose–effect relationships, improvement of integration to adjacent tissue by optimising scaffold design and to explore the mechanisms involved in the regeneration process, which may uncover additional advantages of the use of MSC in contrast to chondrocytes, such as MSC's anti-inflammatory effects.

Acknowledgments The authors would like to acknowledge Anna Garrit and Cristian de la Fuente for technical assistance; and José Luís Ruiz, Ramón Costa and the crew of the "Servei de Granges i Camps Experimentals" of the Universitat Autònoma de Barcelona (Bellaterra, Spain) for their careful assistance to animal management. This work was supported by "Ministerio de Economía y Competitividad" (Grant Number IPT-300000-2010-0017), "Ministerio de Ciencia e Innovación" (Grant Numbers PSE-010000-2007-4//PSE-010000-2008-4, BIO2008-01985), "Programa de suport a grups d'investigació DGR/DIUE" (Grant number 2009SGR1038) and by the European Regional Development Fund (ERDF), within the National Plan for Scientific Research, Development and Innovation 2008-2011.

References

Ahern BJ, Parvizi J, Boston R, Schaer TP (2009) Preclinical animal models in single site cartilage defect testing: a systematic review. Osteoarthr Cartil 17:705–713. doi:10.1016/j.joca.2008.11.008

Alford JW, Cole BJ (2005) Cartilage restoration, part 1: basic science, historical perspective, patient evaluation, and treatment options. Am J Sports Med 33:295

Barry F, Boynton RE, Liu B, Murphy JM (2001) Chondrogenic differentiation of mesenchymal stem cells from bone marrow: differentiation-dependent gene expression of matrix components. Exp Cell Res 268:189–200. doi:10.1006/excr.2001.5278

Batty L, Dance S, Bajaj S, Cole BJ (2011) Autologous chondrocyte implantation: an overview of technique and outcomes. ANZ J Surg 81:18–25. doi:10.1111/j.1445-2197.2010.05495.x

Caminal M, Fonseca C, Peris D, Moll X, Rabanal RM, Barrachina J, Codina D, García F, Cairó JJ, Gòdia F, Pla A, Vives J (2014a) Use of a chronic model of articular cartilage and meniscal injury for the assessment of long-term effects after autologous mesenchymal stromal cell treatment in sheep. N Biotechnol 31:492–498. doi:10.1016/j.nbt.2014.07.004

Caminal M, Moll X, Codina D, Rabanal RM, Morist A, Barrachina J, Garcia F, Pla A, Vives J (2014b) Transitory improvement of articular cartilage characteristics after implantation of polylactide:polyglycolic acid (PLGA) scaffolds seeded with autologous mesenchymal stromal cells in a sheep model of critical-sized chondral defect. Biotechnol Lett. doi:10.1007/s10529-014-1585-3

Capito RM, Spector M (2003) Scaffold-based articular cartilage repair. IEEE Eng Med Biol Mag 22:42–50

Caplan AI (1991) Mesenchymal stem cells. J Orthop Res 9:641–650. doi:10.1002/jor.1100090504

De Bie C (2007) Genzyme: 15 years of cell and gene therapy research. Regen Med 2:95–97. doi:10.2217/17460751.2.1.95

Erggelet C, Neumann K, Endres M, Haberstroh K, Sittinger M, Kaps C (2007) Regeneration of ovine articular cartilage defects by cell-free polymer-based implants. Biomaterials 28:5570–5580. doi:10.1016/j.biomaterials.2007.09.005

Fonseca C, Caminal M, Peris D, Barrachina J, Fàbregas PJ, Garcia F, Cairó JJ, Gòdia F, Pla A, Vives J (2014) An arthroscopic approach for the treatment of osteochondral focal defects with cell-free and cell-loaded PLGA scaffolds in sheep. Cytotechnology 66:345–354. doi:10.1007/s10616-013-9581-3

Huey DJ, Hu JC, Athanasiou KA (2012) Unlike bone cartilage regeneration remains elusive. Science 338:917–921. doi:10.1126/science.1222454

Hurtig MB, Buschmann MD, Fortier LA, Hoemann CD, Hunziker EB, Jurvelin JS, Mainil-Varlet P, McIlwraith CW, Sah RL, Whiteside RA (2011) Preclinical studies for cartilage repair. Cartilage 2:137–152. doi:10.1177/1947603511401905

Lee JS, Im GI (2010) Influence of chondrocytes on the chondrogenic differentiation of adipose stem cells. Tissue Eng Part A 16:3569–3577. doi:10.1089/ten.TEA.2010.0218

Liu TM, Martina M, Hutmacher DW, Hui JH, Lee EH, Lim B (2007) Identification of common pathways mediating differentiation of bone marrow- and adipose tissue-derived human mesenchymal stem cells into three mesenchymal lineages. Stem Cells 25:750–760. doi:10.1634/stemcells.2006-0394

Mainil-Varlet P, Aigner T, Brittberg M, Bullough P, Hollander A, Hunziker E, Kandel R, Nehrer S, Pritzker K, Roberts S, Stauffer E (2003) Histological assessment of cartilage repair: a report by the Histology Endpoint Committee of the International Cartilage Repair Society (ICRS). J Bone Joint Surg Am 85(Suppl 2):45–57

Middleton JC, Tipton AJ (2000) Synthetic biodegradable polymers as orthopedic devices. Biomaterials 21:2335–2346

Mithoefer K, McAdams T, Williams RJ, Kreuz PC, Mandelbaum BR (2009) Clinical efficacy of the microfracture technique for articular cartilage repair in the knee: an evidence-based systematic analysis. Am J Sports Med 37:2053–2063. doi:10.1177/0363546508328414

Niederauer GG, Slivka MA, Leatherbury NC, Korvick DL, Harroff HH, Ehler WC, Dunn CJ, Kieswetter K (2000) Evaluation of multiphase implants for repair of focal osteochondral defects in goats. Biomaterials 21:2561–2574

Oldershaw RA (2012) Cell sources for the regeneration of articular cartilage: the past, the horizon and the future. Int J Exp Pathol 93:389–400. doi:10.1111/j.1365-2613.2012.00837.x

Pittenger MF, Mackay AM, Beck SC, Jaiswal RK, Douglas R, Mosca JD, Moorman MA, Simonetti DW, Craig S, Marshak DR (1999) Multilineage potential of adult human mesenchymal stem cells. Science 284:143–147

Schnabel M, Marlovits S, Eckhoff G, Fichtel I, Gotzen L, Vecsei V, Schlegel J (2002) Dedifferentiation-associated changes in morphology and gene expression in primary human articular chondrocytes in cell culture. Osteoarthr Cartil 10:62–70. doi:10.1053/joca.2001.0482

Schop D, Janssen FW, van Rijn LD, Fernandes H, Bloem RM, de Bruijn JD, van Dijkhuizen-Radersma R (2009) Growth, metabolism, and growth inhibitors of mesenchymal stem cells. Tissue Eng Part A 15:1877–1886. doi:10.1089/ten.tea.2008.0345

Sittinger M, Reitzel D, Dauner M, Hierlemann H, Hammer C, Kastenbauer E, Planck H, Burmester GR, Bujia J (1996) Resorbable polyesters in cartilage engineering: affinity and biocompatibility of polymer fiber structures to chondrocytes. J Biomed Mater Res 33:57–63

Tang QO, Carasco CF, Gamie Z, Korres N, Mantalaris A, Tsiridis E (2012) Preclinical and clinical data for the use of mesenchymal stem cells in articular cartilage tissue engineering. Expert Opin Biol Ther 12:1361–1382. doi:10.1517/14712598.2012.707182

Uematsu K, Hattori K, Ishimoto Y, Yamauchi J, Habata T, Takakura Y, Ohgushi H, Fukuchi T, Sato M (2005) Cartilage regeneration using mesenchymal stem cells and a three-dimensional poly-lactic-glycolic acid (PLGA) scaffold. Biomaterials 26:4273–4279. doi:10.1016/j.biomaterials.2004.10.037

Vanlauwe J, Saris DB, Victor J, Almqvist KF, Bellemans J, Luyten FP (2011) Five-year outcome of characterized chondrocyte implantation versus microfracture for symptomatic cartilage defects of the knee: early treatment matters. Am J Sports Med 39:2566–2574. doi:10.1177/0363546511422220

Vélez R, Hernández-Fernández A, Caminal M, Vives J, Soldado F, Fernández A, Pla A, Aguirre M (2012) Treatment of femoral head osteonecrosis with advanced cell therapy in sheep. Arch Orthop Trauma Surg 132:1611–1618. doi:10.1007/s00402-012-1584-6

Veronesi F, Maglio M, Tschon M, Aldini NN, Fini M (2014) Adipose-derived mesenchymal stem cells for cartilage tissue engineering: State-of-the-art in in vivo studies. J Biomed Mater Res A 102:2448–2466. doi:10.1002/jbm.a.34896

Villalobos Córdoba FE, Velasquillo Martínez C, Martínez López V, Lecona Butrón H, Reyes Marín B, Estrada Villaseñor E, Villegas CH, Solís Arrieta L, Espinosa Morales R, Ponce de León CI (2007) Resultados en la reparación experimental de lesiones osteocondrales en un modelo porcino mediante ingeniería de tejidos. Acta Ortop Mex 21:217–223

Zaslav K, Cole B, Brewster R, DeBerardino T, Farr J, Fowler P, Nissen C (2009) A prospective study of autologous chondrocyte implantation in patients with failed prior treatment for articular cartilage defect of the knee: results of the Study of the Treatment of Articular Repair (STAR) clinical trial. Am J Sports Med 37:42–55. doi:10.1177/0363546508322897

5.3- STUDY 3

USE OF A CHRONIC MODEL OF ARTICULAR CARTILAGE AND MENISCAL INJURY FOR THE ASSESSMENT OF LONG-TERM EFFECTS AFTER AUTOLOGOUS MESENCHYMAL STROMAL CELL TREATMENT IN SHEEP.

Caminal M, Fonseca C, Peris D, Moll X, Rabanal RM, Barrachina J, Codina D, García F, Cairó JJ, Gòdia F, Pla A, Vives J.

New Biotechnology. 2014 Sep 25; 31(5):492-8.

RESEARCH PAPER

New Biotechnology • Volume 31, Number 5 • September 2014

Research Paper

Use of a chronic model of articular cartilage and meniscal injury for the assessment of long-term effects after autologous mesenchymal stromal cell treatment in sheep

Marta Caminal[1], Carla Fonseca[2], David Peris[3], Xavier Moll[2], Rosa M. Rabanal[2], Josep Barrachina[4], David Codina[4], Félix García[2], Jordi J. Cairó[3], Francesc Gòdia[3], Arnau Pla[1] and Joaquim Vives[1]

[1] Divisió de Teràpies Avançades/XCELIA, Banc de Sang i Teixits, Edifici Dr. Frederic Duran i Jordà, Passeig Taulat, 116, Barcelona 08005, Spain
[2] Departament de Medicina i Cirurgia Animals, Àrea de Medicina i Cirurgia Animal, Facultat de Veterinària, Universitat Autònoma de Barcelona, Edifici V, Campus de la UAB, 08193 Bellaterra, Cerdanyola del Vallès, Spain
[3] Grup d'Enginyeria Cel·lular i Tissular, Departament d'Enginyeria Química, Escola d'Enginyers, Universitat Autònoma de Barcelona, Edifici Q, Campus de la UAB, 08193 Bellaterra, Cerdanyola del Vallès, Spain
[4] Hospital ASEPEYO, Avinguda Alcalde Barnils, 54-60, Sant Cugat del Vallès, Barcelona 08174, Spain

Regenerative therapies using adult stem cells have attracted great interest in the recent years and offer a promising alternative to current surgical practices. In this report, we evaluated the safety and efficacy of an autologous cell-based treatment of osteoarthritis using mesenchymal stromal cells expanded from bone marrow aspirates that were administered intra-articularly.

Ten 2-year old ewes were divided in two groups (for analysis at 6 and 12 months, respectively). Full thickness articular cartilage defects of approximately 60 mm^2 were created arthroscopically in the medial femorotibial condyles and a meniscal tear in the anterior horn of the medial meniscus in the 20 hind legs. Intra-articular injection of 4 mL of either treatment (a suspension of cells) or control (same as treatment, without cells) were applied one month after generating a chronic condition similar to human pathology. Animals were monitored radiographically, by MRI and ultrasound scanning; and macroscopic and histological analyses were conducted at 6 and 12 months. Furthermore a full necropsy was performed at 12 months post-treatment. The intra-articular injection of autologous MSC was safe, as judged by the lack of local or systemic adverse effects during the clinical follow-up and by a full necropsy performed at 12 months post-treatment. Evidence of regeneration of articular cartilage and meniscus was case-dependent but statistically significant improvement was found in specific macroscopic and histological parameters. Such parameters included colour, rigidity, cell distribution and hyaline quality of the refill tissue as well as the structure of subchondral bone.

Introduction

Articular cartilage is a unique functional tissue comprising a narrow layer of specialised connective tissue that permits smooth, near-frictionless joint movement [1]. Damage to cartilage is very common in patients suffering from sports injuries, joint dysfunction, and osteoarthritis. However, its restoration represents a major clinical and scientific challenge. The limited healing potential of cartilage is due to its low chondrocytical proliferative activity and avascularity, and current clinical strategies (e.g. abrasion arthroplasty, chondrocyte implantation, or the use of perichondreal autografts) result in the formation of mechanically inferior fibrocartilage [2].

Corresponding author: Vives, J. (jvives@bst.cat, joaquim.vives@gmail.com)

http://dx.doi.org/10.1016/j.nbt.2014.07.004

Initial attempts in cell-based therapy were based on the use of *in vitro* cultured autologous chondrocytes that were implanted in articular cartilage defects on the femoral condyles [3]. As a cell source for cartilage tissue engineering, autologous chondrocytes have limited doubling potential, easily lose their phenotype after multiple passages on culture dishes, cease to produce extracellular matrix (ECM) and degradation of repaired tissue is detected in the long-term clinical follow-up [4,5]. In addition to the poor results obtained with cultured chondrocytes, which may be due to the complexity of the surgical approach for its implantation on the damaged area, there is a limitation in donor material for cell expansion and associated donor site morbidity, which represent a major drawback of this approach [6,7]. This makes other cell sources, such as mesenchymal stromal cells (MSC), more attractive for use in cell therapy [8]. Indeed, multipotent MSC are considered a promising cell type for cartilage repair by virtue of their straightforward isolation, extensive expansion potential, and high chondrogenic potential [9].

In the present work, we developed a translational animal model of chronic joint damage condition in which the long-term effects of the intra-articular injection of autologous MSC were studied with regard to safety and efficacy.

Material and methods

Study design

The surgical procedures were first developed in cadavers that were euthanized for reasons unrelated to the current study to reduce the number of animals used and to refine the technique in line with the 3Rs principles. Ten healthy 2-year old ewes of the Ripollesa-Lacona breed were supplied by *Servei de Granges i Camps Experimentals* (SGCE, Bellaterra, Spain). Animals were housed together, fed a standard diet and allowed access to water *ad libitum*. All animal procedures were performed in accordance with the guidelines of the local animal research committee and with national laws.

The chronogram of the study is described in Table 1. Two surgery steps were performed: (1) harvesting of bone marrow for *in vitro* expansion and generation of condylar and meniscal injuries (in the 20 knees); and (2) intra-articular injection of 4 mL of either treatment (a suspension of MSC) or control (same as treatment, without cells) (Fig. 1). The animals were further divided in two groups, being represented the two treatments: (A) 6-month follow-up (5 animals, 10 knees); (B) 12-month follow-up (5 animals, 10 knees) (Table 2).

TABLE 1

Chronogram. Experimental procedures performed to the animals included in the study

Time (days)	Procedure
−60 to −31	Animal selection Blood test and abdominal ecography Radiological, ecographic and MRI analysis of the knees
−30	Blood extraction for serum purification
0	Arthroscopy for the generation of the defect Bone marrow aspiration
7	Ecographic and MRI control
30	Treatment (ecoguided intraarticular infiltration)
37	Post-infiltration ecographic control
210	Blood test for sanitary control Radiological, ecographic and MRI analysis of the knees
211	Euthanasia and processing of specimens for histological analysis (Group A: 6-month follow-up)
280	Blood test for sanitary control (Group B: 12-month follow-up)
390	Blood test for sanitary control (Group B: 12-month follow-up) Radiological, ecographic and MRI analysis of the knees
391	Euthanasia, full necropsy and processing of specimens for histological analysis (Group B: 12-month follow-up)

Isolation and culture of mesenchymal stromal cells

Mesenchymal stromal cells were isolated and expanded as reported previously [10]. Briefly, sternal bone marrow aspirates from adult sheep were diluted 1:1 with phosphate buffered saline (PBS, Gibco). Bone marrow mononucleated cells (MNC) were isolated using a density gradient solution (Histopaque®-1077, Sigma–Aldrich) and MSC were selected by their capacity to adhere

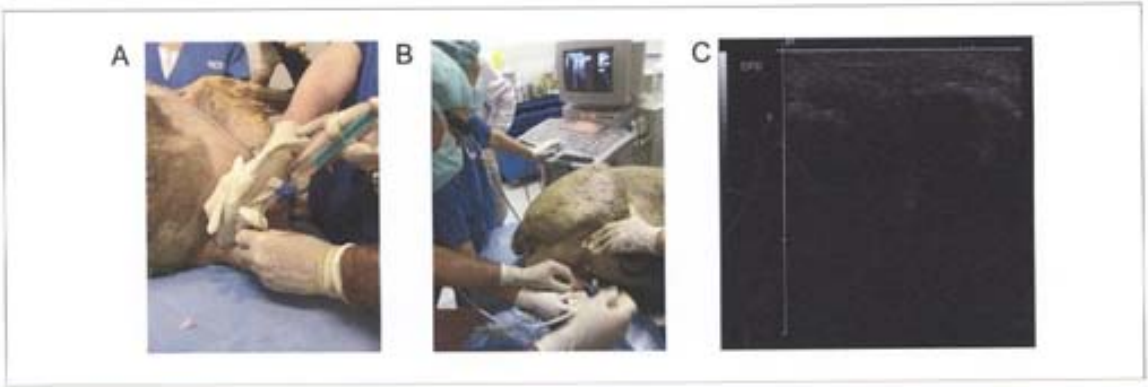

FIGURE 1

Ecoguided intra-articular injection procedure. Images **(a)** and **(b)** show the needle-tube-syringe system designed specifically for this study that allowed simultaneous ultrasound monitoring (probe enveloped in a sterile glove). In **(c)**, the needle appears as a hyperecogenic vertical line. This procedure ensured the delivery of the either MSC treatment or cell-free control solution within the articular capsule and therefore minimising the risk of extravasation.

TABLE 2

Study design. A total number of 10 sheep were included in the study. Model injuries were performed arthroscopically in all the medial condyles of femorotibial joints and each joint was randomly assigned to either MSC treatment or cell-free control group and final clinical follow-up endpoint

Animal ID	Treatment		Clinical follow-up
	Left knee	Right knee	
F55	Cell-free control	Cell-free control	6 months
F54	MSC treatment	MSC treatment	6 months
F46	MSC treatment	MSC treatment	6 months
425	MSC treatment	MSC treatment	6 months
F62	Cell-free control	MSC treatment	6 months
F51	MSC treatment	MSC treatment	12 months
F56	MSC treatment	Cell-free control	12 months
433	Cell-free control	MSC treatment	12 months
434	MSC treatment	Cell-free control	12 months
F43	MSC treatment	MSC treatment	12 months

to plastic cell culture dishes. Cells were cultured up to passage 3 in Dulbecco's modified Eagle's medium (DMEM, Gibco) supplemented with 10% autologous pooled sheep serum containing 2 mM glutamine. All cultures were maintained at 37°C and 5% CO_2 in humidified incubators. Differentiation assays were performed using StemPro differentiation media (Gibco) and Safranin O, Oil Red O and Von Kossa stainings were performed to determine the outcome of the differentiation assays. FACS analysis was performed to evaluate expression of CD44 (G44-26, BD Biosciences), CD45 (HI30, BD Biosciences), CD90 (5E10, BD Biosciences) and HLA-DR (TU36, BD Biosciences) in a FACSCalibur flow cytometer (BD Biosciences). PE-conjugated IgG1 (X40, BD Biosciences) and FITC-conjugated IgG2bk (27-35, BD Biosciences) antibodies were used as isotype controls. Glucose and lactate concentrations in supernatants were determined using an YSI 2700 automated analyser (Yellow Springs Instruments).

Anaesthesia, OA induction and post-operative care

All procedures were performed using aseptic techniques and under general anaesthesia. After premedication with an intramuscular (IM) injection of 0.01 mg/kg of buprenorphine (Buprex, Schering-Plough SA) and 0.2 mg/kg of midazolam (Dormicum, Roche Farma), intravenous (IV) access was established at cephalic vein. Sheep were pre-oxygenated and induced with 4 mg/kg IV propofol (Propofol-Lipuro 1%, BBraun Melsungen AG). The animals were endotracheal intubated and maintained on isoflurane 2% (Isoflo, Abbott laboratories Ltd) mixed with oxygen. Esophagic intubation was made to prevent ruminal bloat. A continuous infusion of Ringer lactate (Ringer lactate, BBraun Melsungen AG) was administered at 10 mL/kg/hour during surgery. Intra-operative monitoring consisted of electrocardiography, pulse oximetry, noninvasive blood pressure and capnography.

The arthroscopic approach for OA modelling was adapted to enable the generation of chondral-only defects based on a technique developed previously by our group [11]. Briefly, at the time of bone marrow aspiration, arthroscopically guided chondral lesions of approximately 60 mm^2 were generated in both femoral medial condyles by rotating a 5 mm-diameter Michel's trephine (Insorvet SL) in three contiguous areas. Each joint was approached via a stab incision lateral to the distal aspect of the patellar ligament, allowing the insertion of an arthroscope with camera for the visualization of the medial condyle. A mechanical shaver was used to remove the fat pad allowing a clearer view. For this purpose, a second stab incision was made medial to the distal aspect of the patellar ligament to allow the shaver insertion. Once cleaned, the shaver was removed. The joints were irrigated with saline solution (Grifols) using a two-way arthroscopic irrigation system (*Fluxisol®*, Grifols) at room temperature during surgery. The anterior horn of the medial meniscus was also pierced in both posterior legs using a Basket punch straight 1 mm scoop (ConMed Corp) generating a radial tear in the non-vascularised zone.

All animals received subcutaneous (SC) meloxicam (Metacam, Boehringer Ingelheim) 0.2 mg/kg for 10 days and transdermal fentanyl (Durogesic, Janssen-Cilag SA) 100 μg for post-operative pain relief. For peri-operative infection prophylaxis, animals received 22 mg/kg of cefazolin IM (Kurgan, Laboratorios Normon) every 12 hours for 10 days.

Animal monitoring

Blood samples were taken periodically for a flow cytometry analysis using ADVIA 120 Analyzer (Bayer Lab) and on an Olympus AU400 auto analyzer.

Ecographic assessment was performed using a Sequoia Acuson ultrasound scan (Siemens-Acuson) with a 10 MHz multiplane probe.

Radiographic (X-ray) imaging was performed in the latero-lateral and antero-posterior planes using Sedecal APR-Vet Console (Sedecal) at 50 kVp/5 mAs/100 mA/0.05 s with a digital flat-panel detector system (Regius cassette 14 × 17, Konica Minolta).

Magnetic resonance imaging (MRI) examination was performed on both knees of each animal under general anaesthesia, using a 0.2 T unit with open permanent magnet (Vet-MR, Esaote SA) as described elsewhere [11]. Animals were positioned in sternal recumbency with the leg extended and symmetrically placed inside a dual phased array coil.

Macroscopic assessment

After sedation with an IM injection of 0.02 mg/kg of midazolam, animals were euthanized by IV injection of pentobarbital

(Dolethal 20 g/100 mL, Vetoquinol SA). Both stifle joints from each animal were then harvested, grossly evaluated and photographed with a digital camera. The gross appearance of repaired tissues was assessed in accordance with the *International Cartilage Repair Society* (ICRS) classification (Supplemental Table 1), for cartilage repair [12]; and the criteria described by Kon and collaborators [13], for meniscus repair (Supplemental Table 2). Samples were excised in blocks including all the implanted tissue and the surrounding native tissue, and were fixed in a 4% paraformaldehyde (PFA, Sigma–Aldrich) solution, for histological analysis.

Histological evaluation and immunohistochemical procedures

Condyles and menisci were decalcified in 5% formic acid for 4–6 weeks and embedded in paraffin for subsequent histological and immunohistochemical procedures. 4 μm-thick microtome sections were cut in the sagittal plane and stained with Haematoxylin and Eosin (H&E) and Safranin O (Sigma–Aldrich). The success of the treatment was evaluated blindly on at least 4 sequential histological sections following the histological scoring grading scale recommended by the *International Cartilage Repair Society* (ICRS) for articular cartilage [14], and the criteria described previously by Frisbie and collaborators [15], Hollander and collaborators [16] and Kon and collaborators [13] for the assessment of the quality of articular cartilage matrix and meniscus, respectively (Supplemental Tables 3–5).

The presence of type II collagen was detected by immnunohistochemical techniques (MAB 8887, Chemicon). Briefly, paraffin sections were deparaffinised, hydrated, and treated with 0.1% Pepsin in 0.01 N HCl for 20 min. Endogenous peroxidase activity was blocked with 3% hydrogen peroxide in distilled water for 30 min and washed in 3% bovine serum albumin (BSA, Sigma–Aldrich) in PBS. Antibody (dilution 1:200) incubations were performed overnight at 4°C. Antibody binding was visualized by using Universal LSAB^{TM}2 Kits in combination with diaminobenzidine according to the manufacturer's instructions (Dako). The sections were counterstained with Haematoxylin.

Statistical analysis

Statistical significance was assessed by the *t*-test using GraphPad Prism program (GraphPad software). Statistical significance was set at $^{*}p < 0.05$.

Results

After complete inspection of the joints to rule out any pre-existing injury, 10 healthy animals were included in the study and experimental lesions were successfully created arthroscopically in weight-bearing areas of the medial femoral condyles and the anterior horn of the medial meniscus of both hind legs (Supplemental Video 1). On the same surgical procedure, sternal bone marrow aspirates were harvested for subsequent MSC isolation. Ovine MSC were expanded *in vitro* yielding a dose of 1.1×10^7 MSC for the 6-month follow-up group and 1.2×10^7 MSC for the 12-month follow-up group. The method used for cell expansion proved to retain chondrogenic, adipogenic and osteogenic differentiation potential of the cells as assayed *in vitro* (Fig. 2). Ovine MSC were morphologically large adherent cells resembling

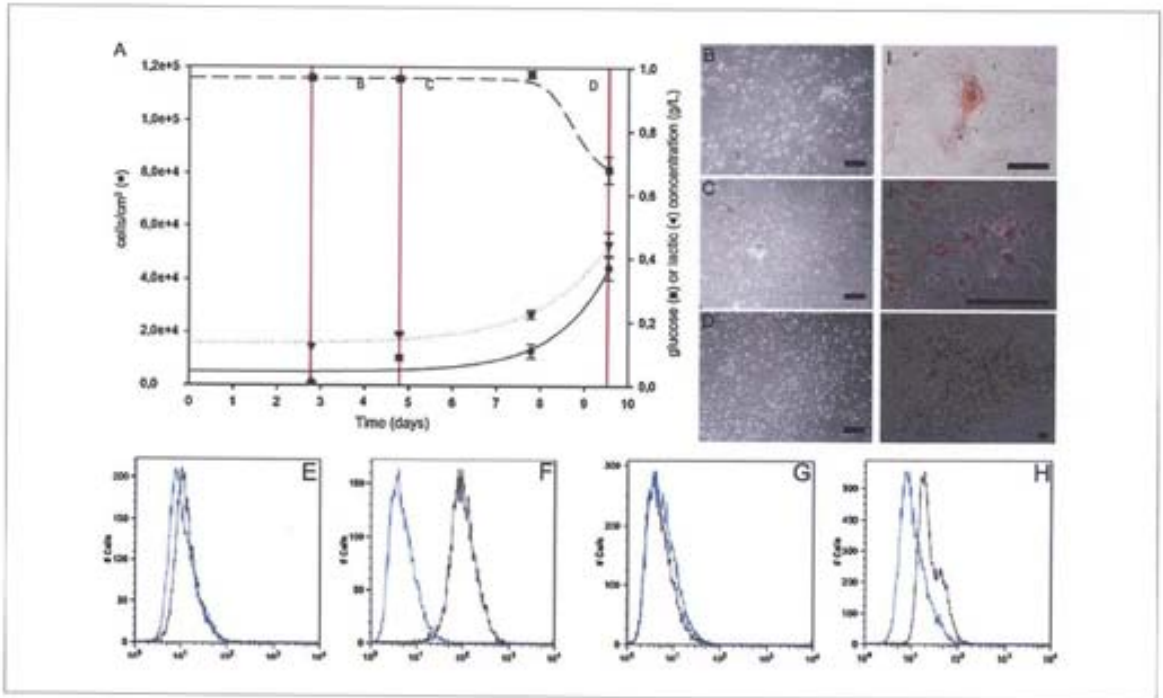

FIGURE 2

MSC expansion and characterisation. **(a)** Growth profile, glucose consumption and lactate production along with morphology of cultured cells at days 3 **(b)**, 5 **(c)** and 10 **(d)**. Phenotype of MSC was assessed by FACS for CD45 **(e)**, CD44 **(f)**, HLA-DR **(g)** and CD90 **(h)** antigen markers. Multipotentiality of expanded MSC is shown in I (chondrogenesis, Safranin O staining), J (adipogenesis, Oil Red O staining) and K (osteogenesis, Von Kosa staining). Scale bar = 200 μm.

fibroblasts and uniformly displayed a high level expression of the hyaluronate receptor CD44, low expression of CD90 and lacked expression of CD45 and HLA-DR (Fig. 2). The combination of differentiation assays, growth profiles, morphology assessment and cytometric phenotype confirmed the MSC nature of the cells used in this study.

The chronic condition of the injuries in condyles and menisci was confirmed by non-invasive techniques before applying the treatments (Supplemental Fig. 1). Then, at one month after injuring the joints, ecoguided intra-articular injections with cell treatment and cell-free control solutions were performed using a needle-tube-syringe system designed specifically for this purpose in order to avoid extravasation (Fig. 1). All animals were monitored following the procedures described in Table 1 to assess the clinical outcome by performing periodical blood tests, and radiological, ecographical (ultrasound scanning) and magnetic resonance analysis. No toxic effect was observed after injection in any of the experimental groups. None of the animals showed any sign of pain, lameness or local inflammation.

The full necropsy conducted in all animals from the 12-month follow-up group ruled out any adverse reaction at both macroscopic and histological levels. However, several acute macroscopic and microscopic spontaneous alterations were observed, although none of the sheep included in the study exhibited a lesion in any organ or femorotibial joints that could be caused by the treatment.

Gross assessment of cartilage repair evidenced high variability among specimens. At 6 months after treatment, the presence of fissures, fragmentation or depression of the surface of the defect site was observed in all condyles, therefore giving low scores (Fig. 3; Supplemental Tables 6 and 7). In most of the specimens, the gaps in the fissures appeared filled with a hyaline matrix of scarce cellularity, without proteoglycans or type II collagen, partially or totally integrated to the adjacent tissue. In all samples, the articular cartilage adjacent to the edges of the fissures presented groups of a variable number of viable chondrocytes. The amount of proteoglycans and type II collagen in the ECM varied widely from sample to sample. In most of the samples, with the exception of the right condyle of animal F46 (cell-based treatment group), focuses of chondroid metaplasia were observed in the subchondral bone, promoting its remodelation, which could develop to endochondral ossification and increasing subchondral bone size.

With respect to menisci analysed at 6 months post-treatment, all of them presented some degree of erosion and fissures in either tibial or femoral surfaces, except in the right knees from animals F46 and F54 and left knee of animal F54 (all three from the treatment group).

The first obvious observation at 12 months post-treatment was that the restoration of normal structure of cartilage could be observed in some specimens (Supplemental Fig. 2). However, high variability was still observed among specimens and even some of the condyles treated with MSC (left condyles from animals F56 and F43) presented a wide extension of damaged cartilage within the 12-month group along with a condyle from the cell-free control group (right knee from animal 434) therefore lowering the overall scores. Despite of this, it was possible to find cartilage of hyaline nature grown on the defect site, with areas of basophilic ECM where chondrocytes were embedded. There was also presence of variable number of chondrocytes with viable aspect distributed both in columns or groups and in acidophilic areas with less cellularity in the articular cartilage adjacent to the edge of the fissures. Proteoglycan and type II collagen content in the ECM varied within the same sample. Statistical analysis of subgroups of parameters included in the grading scales evidenced an improvement of several macroscopic and histological features in the MSC-treated group compared to controls (Fig. 3).

At 12 months post-treatment, 4 out of the 8 medial menisci treated with MSC presented features of healthy tissue (right knees from animals F43 and F51; and left knees from animals F51 and 434) (Supplemental Fig. 3, Fig. 3). The rest of the menisci presented some areas of erosion on the inner edge of the femoral side.

Discussion

The development of a novel pharmaceutical requires the characterisation of its pharmacological and toxicological properties according to its intended use in humans. In this sense, most previous studies have investigated the use of MSC for therapy of acute defects, in which generation and reconstruction of the defects were conducted simultaneously. However, chronic defects are more in line with the type of lesions found in clinical practice, since patients have a lengthy course following trauma to the cartilage, which results in altered intra-articular homeostasis [17]. This may explain why the encouraging and reproducible data obtained in experimental studies *in vivo* have been unattainable in the clinical setting [18–22]. Significant efforts have been made in the development of relevant chronic animal models of articular cartilage disease [23]. The translational animal model used in the present study mimicked an osteoarthritis condition of grade III in articular cartilage according to the ovine adaptation of the Outerbridge classification [24] and incorporated a further lesion on the anterior horn of the medial meniscus. The 4 weeks required for chronic degeneration of the defects were spent in the isolation and *ex vivo* expansion of MSC from bone marrow.

After treatment, MRI, ecographic or X-ray monitoring did not show any progression of the degenerative process, and the macroscopic, histological and immunohystochemical analyses (at 6 and 12 months) permitted to evaluate more accurately the extent of the refill tissue and hyaline nature of the regenerated cartilage of the condyles.

A case-dependent efficacy of the treatment was observed among animals from both experimental groups with respect to macroscopic and histological ICRS scores. A further examination of each individual parameter assessed in the macroscopic and histological analyses provided evidence of statistical significant improvement in the MSC-treated group compared to controls. Macroscopically, these parameters included the colour, rigidity and aspect of sagittal section. Likewise histological parameters displaying statistically significant differences between treatment and control groups included cell distribution, subchondral bone structure and proteoglycan/type II collagen content. Meniscal lesions were also partially repaired in some cases.

We concluded that the animal model used in the present study is relevant to pathological condition of joint disease found in humans and the results of intra-articular cell-based therapy suggest a safe and straightforward approach for the treatment of articular cartilage and meniscal injury, which may prevent the progression of osteoarthritis. However, further work is required to

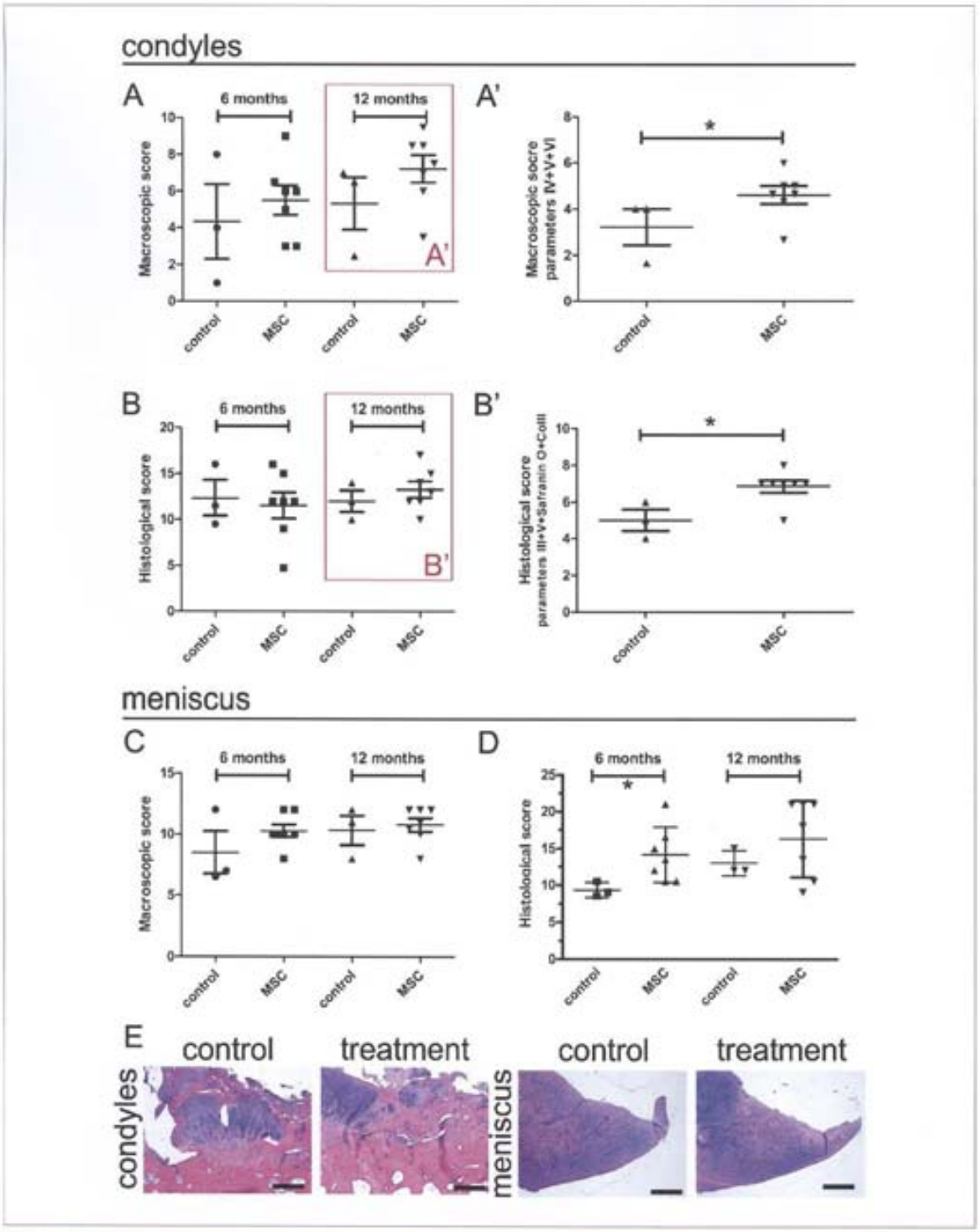

FIGURE 3

Graphical representation of macroscopic and histological scores. The graphs show the effects of the treatments on macroscopic damage to the articular cartilage **(a)** and meniscus **(c)** at 6 and 12 months; and histological scores for articular cartilage **(b)** and meniscal repair **((d)**; *$p = 0.0378$) at 6 and 12 months post-treatment (in total number of points). Further analysis of individual parameters from each grading scale is shown in **(a)'** (macroscopic assessment of colour, rigidity and aspect of sagittal section; *$p = 0.0337$) and **(b)'** (histological assessment of cell distribution, subchondral bone structure and proteoglycan/type II collagen content; *$p = 0.0331$) for the 12 months endpoint. Representative images taken from middle histological results are shown in **(e)**. Scale bars: cartilage = 500 μm; meniscus = 1 mm.

enhance the regenerative properties of MSC, understand the mechanisms involved, evaluate the use of scaffolds for cell delivery in focal lesions that otherwise may progress to osteoarthritis and to determine dose–effect relationships.

Acknowledgements

The authors would like to acknowledge Anna Morist, for veterinarian assistance; José Luís Ruiz, Ramón Costa and the crew of 'Servei de Granges i Camps Experimentals' (Universitat Autònoma de Barcelona, Bellaterra, Spain), for their careful assistance to animal management. This work was supported by 'Ministerio de Economía y Competitividad' (Grant number IPT-300000-2010-0017), 'Ministerio de Ciencia e Innovación' (Grant numbers PSE-010000-2007-4//PSE-010000-2008-4, BIO2008-01985) and 'Programa de soporte a grupos de investigación DGR/DIUE' (Grant number 2009SGR1038).

Appendix A. Supplementary data

Supplementary material related to this article can be found, in the online version, at http://dx.doi.org/10.1016/j.nbt.2014.07.004.

References

[1] Huey DJ, Hu JC, Athanasiou KA. Unlike bone, cartilage regeneration remains elusive. Science 2012;338(November (6109)):917–21.
[2] Widuchowski W, Widuchowski J, Trzaska T. Articular cartilage defects: study of 25,124 knee arthroscopies. Knee 2007;14(June (3)):177–82.
[3] Brittberg M, Lindahl A, Nilsson A, Ohlsson C, Isaksson O, Peterson L. Treatment of deep cartilage defects in the knee with autologous chondrocyte transplantation. N Engl J Med 1994;331(October (14)):889–95.
[4] Liu Y, Chen F, Liu W, Cui L, Shang Q, Xia W, et al. Repairing large porcine full-thickness defects of articular cartilage using autologous chondrocyte-engineered cartilage. Tissue Eng 2002;8(August (4)):709–21.
[5] Johnstone B, Alini M, Cucchiarini M, Dodge GR, Eglin D, Guilak F, et al. Tissue engineering for articular cartilage repair—the state of the art. Eur Cell Mater 2013;25:248–67.
[6] Saris DB, Vanlauwe J, Victor J, Almqvist KF, Verdonk R, Bellemans J, et al. Treatment of symptomatic cartilage defects of the knee: characterized chondrocyte implantation results in better clinical outcome at 36 months in a randomized trial compared to microfracture. Am J Sports Med 2009;37(November (Suppl 1)):10S–9S.
[7] Zaslav K, Cole B, Brewster R, DeBerardino T, Farr J, Fowler P, et al. A prospective study of autologous chondrocyte implantation in patients with failed prior treatment for articular cartilage defect of the knee: results of the Study of the Treatment of Articular Repair (STAR) clinical trial. Am J Sports Med 2009;37(January (1)):42–55.
[8] Prockop DJ. Marrow stromal cells as stem cells for nonhematopoietic tissues. Science 1997;276(April (5309)):71–4. PubMed PMID: 9082988. Epub 1997/04/04.eng.
[9] Mackay AM, Beck SC, Murphy JM, Barry FP, Chichester CO, Pittenger MF. Chondrogenic differentiation of cultured human mesenchymal stem cells from marrow. Tissue Eng 1998;4(Winter (4)):415–28.
[10] Velez R, Hernandez-Fernandez A, Caminal M, Vives J, Soldado F, Fernandez A, et al. Treatment of femoral head osteonecrosis with advanced cell therapy in sheep. Arch Orthop Trauma Surg 2012;132(November (11)):1611–8.
[11] Fonseca C, Caminal M, Peris D, Barrachina J, Fabregas PJ, Garcia F, et al. An arthroscopic approach for the treatment of osteochondral focal defects with cell-free and cell-loaded PLGA scaffolds in sheep. Cytotechnology 2014;66(March (2)):345–54.
[12] van den Borne MPJ, Raijmakers NJH, Vanlauwe J, Victor J, de Jong SN, Bellemans J, et al. International Cartilage Repair Society (ICRS) and Oswestry macroscopic cartilage evaluation scores validated for use in Autologous Chondrocyte Implantation (ACI) and microfracture. Osteoarthritis Cartilage 2007;15(12):1397–402.
[13] Kon E, Chiari C, Marcacci M, Delcogliano M, Salter DM, Martin I, et al. Tissue engineering for total meniscal substitution: animal study in sheep model. Tissue Eng Part A 2008;14(June (6)):1067–80.
[14] Mainil-Varlet P, Aigner T, Brittberg M, Bullough P, Hollander A, Hunziker E, et al. Histological assessment of cartilage repair: a report by the Histology Endpoint Committee of the International Cartilage Repair Society (ICRS). J Bone Joint Surg Am 2003;85A(Suppl 2):45–57.
[15] Frisbie DD, Kawcak CE, Trotter GW, Powers BE, Walton RM, McIlwraith CW. Effects of triamcinolone acetonide on an in vivo equine osteochondral fragment exercise model. Equine Vet J 1997;29(September (5)):349–59.
[16] Hollander AP, Pidoux I, Reiner A, Rorabeck C, Bourne R, Poole AR. Damage to type II collagen in aging and osteoarthritis starts at the articular surface, originates around chondrocytes, and extends into the cartilage with progressive degeneration. J Clin Invest 1995;96(December (6)):2859–69.
[17] Saris DB, Dhert WJ, Verbout AJ. Joint homeostasis. The discrepancy between old and fresh defects in cartilage repair. J Bone Joint Surg Br 2003;85(September (7)):1067–76.
[18] Wasiak J, Clar C, Villanueva E. Autologous cartilage implantation for full thickness articular cartilage defects of the knee. Cochrane Database Syst Rev 2006;3:CD003323.
[19] Buzano-Ravina A, Jato Diaz M. Autologous chondrocyte implantation: a systematic review. Osteoarthritis Cartilage 2006;14(January (1)):47–51.
[20] Knutsen G, Engebretsen L, Ludvigsen TC, Drogset JO, Grontvedt T, Solheim E, et al. Autologous chondrocyte implantation compared with microfracture in the knee. A randomized trial. J Bone Joint Surg Am 2004;86A(March (3)):455–64.
[21] Horas U, Pelinkovic D, Herr G, Aigner T, Schnettler R. Autologous chondrocyte implantation and osteochondral cylinder transplantation in cartilage repair of the knee joint. A prospective, comparative trial. J Bone Joint Surg Am 2003;85A(February (2)):185–92.
[22] Krishnan SP, Skinner JA, Carrington RWJ, Flanagan AM, Briggs TWR, Bentley G. Collagen-covered autologous chondrocyte implantation for osteochondritis dissecans of the knee: two- to seven year results. J Bone Joint Surg Br 2006;88B(February (2)):203–5.
[23] Hepp P, Osterhoff G, Niederhagen M, Marquass B, Aigner T, Bader A, et al. Perilesional changes of focal osteochondral defects in an ovine model and their relevance to human osteochondral injuries. J Bone Joint Surg Br 2009;91(August (8)):1110–9.
[24] Burger C, Mueller M, Wlodarczyk P, Goost H, Tolba RH, Rangger C, et al. The sheep as a knee osteoarthritis model: early cartilage changes after meniscus injury and repair. Lab Anim 2007;41(October (4)):420–31.

5.4- STUDY 4

REFINEMENT STRATEGIES FOR CHONDRAL EXPERIMENTAL LESION INDUCTION AND LONGITUDINAL ASSESSMENT ON THE SHEEP MODEL OF CARTILAGE REPAIR: KNEE ARTHROSCOPY AND ULTRA-SONOGRAPHY AS VALUABLE TOOLS.

Fonseca C, Caminal M, Peris D, Espada Y, Domínguez E, Barrachina J, Codina D, Moll X, de la Fuente C, Pla A, Gòdia F, Vives J , Cairó JJ, García F.

Paper submitted to the journal: BMC Musculoskeletal Disorders

REFINEMENT STRATEGIES FOR CHONDRAL EXPERIMENTAL LESION INDUCTION AND LONGITUDINAL ASSESSMENT ON THE SHEEP MODEL OF CARTILAGE REPAIR: KNEE ARTHROSCOPY AND ULTRASONOGRAPHY AS VALUABLE TOOLS.

Carla Fonseca[1], Marta Caminal[2], David Peris[3], Yvone Espada[1], Elisabet Dominguez[1], Josep Barrachina[4], David Codina[4], Xavier Moll[1], Christian de la Fuente[1], Arnau Pla[2], Francesc Gòdia[3], Joaquim Vives[2], Jordi J. Cairó[3], Félix García[1].

1- Departament de Medicina i Cirurgia Animals, Àrea de Medicina i Cirurgia Animal, Facultad de Veterinària, Edifici V, Campus de la UAB, Universitat Autonoma de Barcelona, 08193 Bellaterra, Cerdanyola del Vallès, Spain.

2- Divisió de Terapies Avançades/XCELIA, Banc de Sang I Teixits, Edifici Dr Frederic Duran i Jordà, Passeig Taulat, 116, 08005 Barcelona, Spain.

3- Grup d'Enginyeria Cellular i Tissular, Departament d'Enginyeria Química, Escola d'Enginyers, Universitat Autonoma de Barcelona, Edifici Q, Campus de la UAB, 08193 Bellaterra, Cerdanyola del Vallès, Spain.

4- Hospital Asepeyo Sant Cugat Hospital, Avinguda Alcalde Barnils, 54-60, Sant Cugat del Vallès, 08174 Barcelona, Spain.

Short title: A refined ovine model of chondral and meniscal injury by arthroscopy, with longitudinal assessment by US

Corresponding author: Carla Fonseca.
e-mail: carla.ribeirodafonseca@gmail.com

ABSTRACT

Background: Sheep are widely used as a preclinical model on cartilage repair studies. Refining this animal model is mandatory, as bibliography highlights the common use of invasive procedures for chondral defect modelling and to assess their progression. Here, we describe a minimally invasive surgical approach to perform partial thickness cartilage lesions on the knee and we describe non invasive longitudinal assessment of the lesions.

Methods: Bilateral knee arthroscopy was performed on 10 sheep (n=20 stifle joints) in order to model partial-thickness chondral lesions on the medial femoral condyle and a tear on the medial meniscus. For longitudinal assessment was used magnetic resonance imaging (MRI) and ultrasound imaging (US) to characterize and to assess the progression of the lesions at several time-points.

Results: Reproducible experimental lesions were successfully achieved by arthroscopy without complications on the postoperative period. Lesion evolution was successfully assessed by the combination of the used non-invasive diagnostic methods. Ultrasound revealed the ability to detect cartilage lesions and to evaluate the joint as a whole organ.

Conclusions: The arthroscopic approach presented here yields good exposure of the target structures, with low postoperative morbidity. We found ultrasound imaging to be a promising tool for longitudinal assessment on cartilage repair in the preclinical model.

The application of the developed refined techniques promotes animal welfare, and increases research quality as translational methodology is apllied.

Key words:

chondral lesion, meniscal lesion, arthroscopy, ultrasound, magnetic resonance imaging, sheep knee, preclinical model.

BACKGROUND

Articular cartilage damage frequently results from injury or diseases such as rheumatoid arthritis or osteoarthritis. It has a significant social and economic impact on the aging population.

The articular cartilage response to injury depends on the severity and depth of the injury [1, 2] . The avascular nature of articular cartilage means that pure cartilage injuries do not cause haemorrhage or fibrin-clot formation. The chondrocytes respond by proliferating and increasing the synthesis of matrix macromolecules near the injury location, but they cannot restore the surface [1].

Animal models have been the mainstay of cartilage repair research for decades and continue to be required for regulatory approval for clinical use of biologics, devices, and methods [3-7]. Among the several available animal models, large animal models are the ones typically required for regulatory approval of any cartilage repair strategy [7].

The ovine experimental model is widely used as a preclinical experimental model in articular cartilage regeneration and repair [4, 8] being the stifle joint an important location. Improving the 3R´s guidelines in this model is imperative, as published research in the area highlights the habitual use of invasive methodology (arthrotomy) for experimental lesion induction and treatment assessment [9-11].

The use of imaging modalities holds significant potential for the assessment of disease pathogenesis and therapeutic efficiency overtime in animal models of musculoskeletal disorders, minimising the use of conventional invasive methods and animal redundancy [12].

MRI is a non-invasive imaging technology extensively used in clinics for assessment of articular cartilage in joint disorders, and has also been used in the ovine model of cartilage repair [13-15].

In humans, musculoskeletal ultrasound (US) plays an important role in detecting the minimal soft tissue changes [16-19]. US has the

ability to differentiate intra and extra-articular soft tissue structures, is a quick, readily available, inexpensive and non-invasive imaging technique [20] which is particularly adapted in longitudinal in vivo experimental model studies [21] . However, to date, we could not found any report of US use in the study of the ovine knee under experimental manipulation.

The purpose of this study is to present our experience refining the generation and assessment of chondral and meniscal lesions in the ovine knee for posterior testing the therapeutic potential of new approaches in regenerative medicine. In order to refine our research we developed minimally invasive surgical procedures for experimental lesion induction and we used non-invasive diagnostic methods (ultrasonography and magnetic resonance imaging) to characterize the lesion, assess the progression of the lesion and to assess the safety of the arthroscopic surgery.

METHODS

All experimental procedures and animal care were conducted in full compliance with the Universitat Autonoma de Barcelona's Ethical Committee on Human and Animal Experimentation in accordance with current European, Spanish and Catalan Legislation regarding laboratory animal use.

Animals

Ten healthy 2-year old ewes of Ripollesa-Lacona breed, weighting 50 ± 6 kg obtained from the Servei de Granges i Camps Experimentals (SGCE, Bellaterra, Spain), were used on this study. Animals were housed together, fed a standard diet and allowed access to water *ad libitum*.

Study design

Each animal underwent bilateral knee arthroscopy under general anesthesia, for the induction of a chondral lesion in the medial femoral condyle and on the medial meniscus of each knee joint. Before arthroscopy, all 20 stifle joints were examined by ultrasound and by magnetic resonance imaging, to obtain basal images. After one week of arthroscopy, ultrasound and magnetic resonance imaging were repeated to all knees, to assess the experimental lesions. Four weeks after arthroscopy, it was injected a solution containing mesenchymal stem cells or non-cellular vehicle in each randomized knee, by ultrasound-guided percutaneous injection. Five weeks after arthroscopy, all stifle joints were imaged by ultrasonography to assess the experimental lesions evolution.

Anaesthesia

All surgeries were performed using aseptic techniques and under general anaesthesia. MRI examination was also performed under general anaesthesia. Animals were premedicated with an intramuscular injection of 0,01 mg/kg of buprenorphine (Buprex®, Schering-Plough, S.A.) and 0,2 mg/kg of midazolam (Dormicum®, Roche). After pre-oxygenation with a face mask, they were induced with 4 mg/kg intravenous propofol (Propofol®-Lipuro 1%, BBraun Melsungen AG). The animals had endotracheal intubation and were maintained on isoflurane 2% (Isoflo, Abbott laboratories Ltd) with 100% oxygen. Esophageal intubation was used to prevent ruminal bloat. A continuous infusion of Ringer lactate (Ringer lactate, BBraun Melsungen AG) was administered at 10 ml/kg/h during surgery. Intra-operative monitoring consisted of electrocardiography, pulse oximetry, noninvasive blood pressure and capnography (VetCare® multiparametric monitor, BBraun Germany).

Arthroscopy for the induction of the experimental chondral lesion on the femoral condyle and on the meniscus

All surgical procedures were developed in a preliminary study in sheep cadaver, in order to achieve accurate arthroscopic techniques. For this purpose 3 animals were euthanized at the end of other experimental procedures, with no previous experimental manipulation of knee articulation.

The experimental lesions were made by using arthroscopic surgery, in both knees of each animal. With the articulation positioned in flexion, each joint was approached via two stab incisions of 3 mm: one lateral and another medial to the distal aspect of the patellar ligament. The lateral arthroscopic portal allowed the insertion of the arthroscope (and the optics) for the visualization of the medial condyle as well as the joint irrigation. During surgery, the joints were irrigated by saline solution (Grifols) of 3000 ml with the irrigation set with double silicone terminal (Fluxisol®, Grífols) at room temperature. A mechanical shaver was introduced by the medial arthroscopic portal, being used to remove the fat pad, allowing a clearer view. Once cleaned, the shaver was removed.

In all animals a chondral lesion was performed. For this purpose, a Michelle punch (Insorvet SL) with a diameter of 5 mm (Figure 1) was inserted through the medial arthroscopic portal (Figure 2). The extremity of this instrument was pressed against the articular surface of the medial femoral condyle, applying a rotation movement in 3 contiguous areas. This way, the indentations of 1mm of this canula rubbed the cartilage eroding the articular cartilage, in a surface area of 60 mm^2, without reaching the subchondral bone.

Meniscal lesion was induced in both hind limbs using a Basket punch straight 1mm scoop (ConMed Corp)generating a radial tear in the non-vascularised zone of the anterior horn of the medial meniscus.

The skin incisions were closed with 2 surgical staples.

Figure 1- Surgical instrument (Michelle throcar) used to induce the experimental chondral lesión. Detail on the tip of the throcar, with edentations.

Figure 2- Arthroscopic surgery in the ovine experimental model, for chondral lesion induction. The knee joint is in full flexion, and through the lateral portal it is inserted the arthroscope with the optics and the irrigation set. Through the medial arthroscopic portal it is inserted the Michelle throcar.

Post-operative care

All animals were allowed to move freely and without restrictions after the surgery. Animals were submitted to daily clinical examination by a veterinarian, to assess general health status, surgical wound evolution and possible joint surgical complications as patellar luxation. For post-operative analgesia it was administered subcutaneously meloxicam (Metacam, Boehringer Ingelheim) 0,2 mg/kg for 10 days and transdermal fentanyl patch 100 µg (Durogesic, janssen-Cilag SA). For the prophylaxis of peri-operative infection the animals received intravenously 22 mg/kg of cefazolin (Kurgan, Normon Laboratories) in the induction of anesthesia and every 12 hours during 10 days. The skin staples were removel 10 days after arthroscopy.

Imaging the knee

Magnetic resonance imaging (MRI):

MRI was performed on the knees of all animals before the experimental lesion induction for basal examination, and one week after the arthroscopy for global examination of the stifle joint after the experimental lesion induction. MRI was conducted using a 0,2 T unit with open permanent magnet (Vet-MR, Esaote S.p.a., Genoa, Italy). This exam was performed under general anaesthesia with the animal positioned in sternal recumbency with the leg extended and symmetrically placed inside a dual phased array coil (Figure 3), as described elsewhere [15]. Sequences included axial, coronal and sagital in SE, FE and FSE in T1, T2 and STIR.

The structures evaluated were the articular cartilage surface, the menisci, the cruciate ligaments, the lateral ligaments, the digital extensor tendon, the patellar tendon and the presence of intra-articular fluid.

Figure 3- Sheep under general anaesthesia during MRI examination. The animal is on lateral/sternal recumbency, with the plevic limb in extensión and symmetrically placed inside a dual phased array coil.

Ultrasound (US) imaging

After thorough clipping of the knee, the joint echography was performed using a 10 MHz lineal transducer (Ultrasound apparatus Acuson®, Siemens). This examination was performed under light sedation with 0,2 mg/kg midazolam IM (Dormicum, Roche Farma) and gentle handling of the animals. Basal images were taken before experimental manipulation, one week after lesion induction and finally five weeks after lesion induction. This last examination correspond to the examination which followed the assay-product (cellular therapy) or vehicle infiltration, which composition was described elsewhere [14]. All the examinations were performed as blind-examinations, without previous knowledge of which treatment was applied to the articulation. To visualize the structures, the stifle joint was positioned in full flexion. The medial femoral condyle and the medial meniscus were visualized from a medial and sagittal portal, placing the transducer longitudinally and transversally (Figure 4). The Baker's cyst presence was investigated placing the

transducer on the popliteal area of the stifle joint. Images and time required for US examination were systematically recorded.

Figure 4- Placement of the ultrasound transducer on the ovine knee for visualization of the medial femoral condyle on longitudinal (A) and transversal (B) views.

RESULTS:

Arthroscopy procedure took a mean time of 35±8 minutes. Reproducible experimental lesions in the cartilage of the medial femoral condyle and on the medial meniscus were successfully achieved by arthroscopy (Figure 5). No intra-operatory complications as haemorrhage or ligaments lesion occurred.

Animals were ambulatory immediately after anaesthesia recovery, and lameness was gone after 4 days post-surgery. Neither infection nor surgical wound dehiscence or clinical signs of patellar luxation were observed.

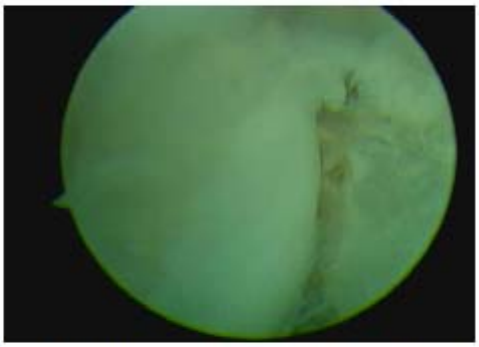

Figure 5- Arthroscopic image of the medial femoral condyle, after the induction of the chondral lesion.

MRI took a median time of 40± 7minutes per knee. At basal examination, the images obtained were compatible with normality on 19 knees. In one articulation it was observed an osteochondral lesion on the medial femoral condyle and joint effusion.

One week after arthroscopy, on the medial femoral condyle it was observed irregularity of the articular surface on 11 stifle joints, STIR increased signal not accompanied of detectable cartilage surface irregularity on 6 stifle joints and articular surface irregularity accompanied with subchondral increased signal on 5 knees. Those findings were compatible with cartilaginous erosion with underlying moderate subchondral bone oedema. The medial meniscus in the anterior horn presents an increased signal on all knees. Joint effusion was observed on all stifle joints. Cruciate ligaments, lateral ligaments, and digital extensor and patellar tendon had no alterations. No osteofitosis was detected.

US examination of the sheep knees (Table 1) took 8 ± 3minutes in each stifle joint and was easily performed. All animals tolerated well, under light sedation, the manipulation needed to complete the exam. Full flexion of the knee allowed a correct examination of the medial femoral

condyle cartilage and medial meniscus. Basal US (made before surgical intervention) revealed femoral condyle cartilage as a well-defined homogeneously hypoecogenic band comprised between the condrosynovial and the osteochondral sharp hyperecogenic margins (Figure 6A and Figure 7A). Medial meniscus appeared as a triangle with moderate ecogenicity and heterogeneous appearance (Figure 8A). It was not observed effusion on the knees. Only one articulation revealed effusion and alteration of cartilage layer echogenicity and contour, compatible with osteochondral lesion which presence was confirmed by MRI and arthroscopy.

One week after the arthroscopy for experimental lesions induction, the medial femoral condyle cartilage band showed an altered echogenicity, being observable an increased echogenicity, a heterogeneous global appearance and altered thickness. Alteration on the sharpness of the chondrosynovial margin was detected on all knees (Figure 6B and Figure 7B). Alteration was detected on the osteochondral margin on 4 knees at this moment (including the knee with basal osteochondral lesion).

The medial meniscus appeared as a triangle with moderate ecogenicity and heterogeneous appearance on all stifle joints (Figure 8B). The presence of intra-articular fluid was detected on all stifle joints. The presence of Baker's cyst was observed on 10 knees.

After five weeks of arthroscopy for experimental lesion induction, the cartilage band of the medial femoral condyle presented globally a more hipoecogenic appearance considering the anterior examination. The condrosynovial margin maintained an irregular shape on all knees. The osteochondral margin presents increased echogenicity and a blurred delineation on 17 stifle joints (Figure 6C and Figure 7C). The medial meniscus exhibits a slightly heterogeneous appearance (Figure 8C).

Intra-articular fluid was detected on 5 stifle joints. Baker's cyst (poplyteal cyst) was detected on 5 knees (Figure 9). At cranial level of the articulation, a cyst was detected on 3 stifle joints.

	Popliteal cyst	Intra-articular effusion	Condrosynovial line		Osteochondral line		Cartilage layer		Cysts in anterior area
			Regular	Irregular	Regular	Irregular	Homogeneous echogenicity	Heterogenous echogenicity	
Basal	0	1	19	1	19	1	19	1	0
One week after arthroscopy	10	20	0	20	16	4	0	20	0
Five weeks after arthroscopy	5	5	0	20	3	17	0	20	3

Table 1- Summary of ultrasonographic alterations detected on the 20 stifle joints, at several time points.

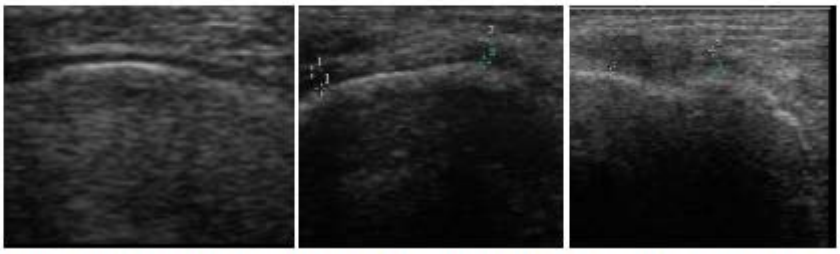

Figure 6- Ultrasound image of the medial femoral condyle in transversal view, at 3 different time points of the experiment. **A-** Image taken before surgical manipulation of the articulation was performed. On this basal image, the cartilage layer appears as a homogeneously hipoecogenic layer/band between two hiperecogenic lines, which correspond to the chondrosynovial and the osteochondral margins. **B-** Image obtained one week after arthroscopy for experimental chondral lesion induction. The cartilage layer presents an altered ecogenicity (more ecogenic) and a diminuished thickness, compatible with the inflicted chondral lesion. The chondrosynovial line presents an irregular contour, while the osteochondral line mantains the regular shape. **C-** Image obtained five weeks after arthroscopy for experimental chondral lesion induction. The cartilage band presents an altered appearance, with heterogeneous ecogenicity with several hyperecogenic areas.The chondrosynovial line presents an irregular countour, as observed previously observed in the anterior time point. The osteochondral margin presents an evident irregular shape, not previously found (Animal F46 D).

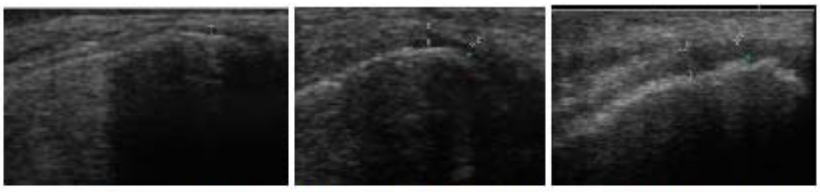

Figure 7- Ultrasound image of the medial femoral condyle in longitudinal view, at 3 different time points of the experiment. **A-** Image taken before surgical manipulation of the articulation was performed. On this basal image, the cartilage layer appears as a homogeneously hipoecogenic layer/band between two hiperecogenic lines, which correspond to the chondrosynovial and the osteochondral margins. **B-**Image obtained one week after arthroscopy for experimental chondral lesion induction. The cartilage layer presents an altered ecogenicity (more ecogenic) and a diminuished thickness, compatible with the inflicted chondral lesion. The chondrosynovial line presents an irregular contour, while the osteochondral line mantains the regular shape. **C-** Image

obtained five weeks after arthroscopy for experimental chondral lesion induction. The cartilage band presents an altered appearance, with heterogeneous ecogenicity.The chondrosynovial and osteochondral lines presents a blurred and an irregular countours (Animal F46D).

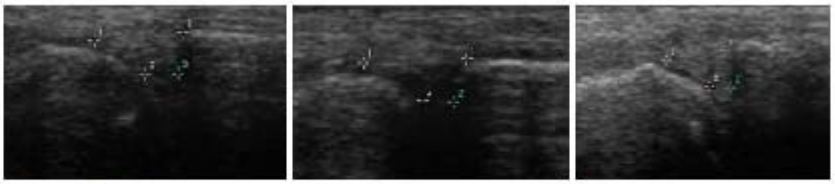

Figure 8- Ultrasound image of the medial meniscus, at 3 different time points of the experiment. **A-** Image taken before surgical manipulation of the articulation was performed. On this basal image, **B-**Image obtained one week after arthroscopy for experimental chondral lesion induction. **C-** Image obtained five weeks after arthroscopy for experimental chondral lesion induction.

Figure 9- Ultrasound image of a popliteal cyst, found one week after arthroscopy (Animal F62RI).

DISCUSSION

In the present study, a minimally invasive surgical approach was successfully performed for modelling partial-thickness chondral lesions on the medial femoral condyles and meniscal tears on the sheep knee, without surgical complications on the post-operatory period. Arthroscopy was an effective, safe and quick technique to perform the experimental lesions on all the 20 stifle joints.

The sheep is a key animal as a preclinical experimental model of cartilage repair, being the stifle joint one of the preferred location for these studies due to anatomical similarities with human knee [4, 22]. Arthrotomy is the usual method to induce the experimental cartilage lesions, however it is recognized that arthrotomy in sheep has as a common post-operative complication patellar luxation. Recent work described a mini-arthrotomy without patellar luxation as a refinement of the usually performed technique [23]. However, as bilateral surgery is usually performed on animal models on cartilage research [24], a minimally invasive surgical technique (arthroscopy) should be preferred in order to minimize animal distress after the surgical approach. It is also expected that arthroscopic approach is accompanied of a lower risk of joint infection, as surgical exposure of the intraarticular tissues and surgical wounds are smaller than in arthrotomy exposure: this is especially important due to housing conditions of sheep, which are usually on a reduced antiseptic environment due to the nature of the animal model itself.

It is recognized that the implementation of preclinical imaging represents a keystone in the refinement of animal models allowing longitudinal studies and enabling a powerful, non-invasive and clinically translatable way for monitoring disease progression in real time [12]. In this sense, it was used on this study magnetic resonance imaging and US

imaging for lesion longitudinal assessment. On the present study MRI was especially useful to detect meniscal tears and subchondral alterations and to discard lesions on tendons or ligaments. The fact that we used a 0,2 T unit limited the ability to detect cartilage lesions that didn´t produce a reaction of the subchondral bone.

US is emerging as a viable imaging modality in the diagnosis and assessment of the musculoskeletal system, and as a valuable additional diagnostic modality for the evaluation of the knee joint in the clinical practice [25].

Human hyaline cartilage is described as a well-defined anechogenic or homogeneously hypoechogenic band between the chondrosynovial and osteochondral margins [26, 27]. In our study, we found that normal articular cartilage of sheep stifle joint has a similar aspect. The lack of echoes is due to uniform transmission of sound wave in cartilage with high water content and densely packed and organized collagen [17, 19]. The absence of echoes of the cartilage layer and the sharpness of the margins are its principal features in healthy subjects, corresponding the sharp margin to smooth surface of healthy cartilage [26-28].

On the present study, one week after the experimental lesion induction the cartilage band of the medial femoral condyle presented altered echogenicity with alteration on the sharpness of the chondrosynovial margin, which correspond to fibrillations and erosion of the cartilage induced previously on the arthroscopy for chondral lesion induction. At this moment, no alteration was detected on the osteochondral margin of the majority of the condyles, suggesting that the surgical methodology to partial-thickness chondral lesion induction respected the calcified cartilage layer. Five weeks after the chondral lesion induction, it was already noticeable alteration in the osteochondral margin.

This alteration on the osteochondral margin 5 weeks after the lesion induction, which was not consistently present on the previous examination (4 weeks before) can be due to the natural evolution of the lesion: the underlying subchondral bone suffers alteration due to abnormal mechanical forces which are no longer attenuated by the eroded cartilage. The highly specific microscopic anatomy and interdependent physiology of articular cartilage can be disrupted by small, superficial injuries, even without immediate cartilage loss. Superficial damage will injure chondrocytes, limit their metabolic capacity for repair, and lead to decreased proteoglycan concentration, increased hydration, and altered fibrillar organization of collagen. Proteoglycan loss, increased water content, decreased cartilage stiffness, and increased hydraulic permeability lead to increased force transmission to the underlying subchondral bone, which increases its stiffness and, in turn, causes impact loads to be more readily transmitted to the partially damaged cartilage. This vicious cycle is thought to contribute to the progression of partial-thickness articular cartilage injuries [2].

Though the US examination at 5 weeks was performed one week after assay-product or saline vehicle intra-articular infiltration, we believe that at this moment it is not noticeable alteration of the lesion status due to the injected products. The cellular treatment effects over the lesions are expected to be noticed at long-time period. Moreover, identical lesion images were obtained between the knees injected with saline or MSC. The total volume of 4 ml is small to consider a lavage procedure.

The described earlier US features of osteoarthritis in humans are loss of clarity of the cartilage band and loss of sharpness of the margins. The loss of sharpness of the interface is due to scattering of sound by a rough surface. The increased echogenicity may represent structural alteration such as fibrillation of cartilage and cleft formation. In the later stages, an asymmetric narrowing of the cartilaginous layer occurs [27]. In

our study we found difficult to correctly measure by US the cartilage band thickness. It is recognized on the clinical settings that the loss of sharpness of the interface can make the placement of markers, for thickness measurement, difficult [17, 19]. The overlying soft tissue may influence the appearance of the underlying cartilage band. Synovial fluid in patients with synovitis may impair the visualization of the synovial-cartilage interface [19, 28]. Varying thickness of the overlying tissue may also verify the image echogenicity [17, 28]. Because of this, clarity and sharpness of the cartilage images are considered the best predictors of cartilage alteration, correlating significantly with gross findings of the specimen in the clinics [17].

The main limitation of US is the inability of the beam to penetrate the bony cortex. Thus, US visualization of the articular cartilage is restricted by the acoustic windows, their width being determined by the anatomy of the joint under examination [27]. The bone alterations that can be detected by US are loss of continuity of the bone profile or an increased intensity of the posterior bone-cartilage interface, that may reflect subchondral bone sclerosis or loss of overlying cartilage [19]. Difficulty to measure cartilage thinning and the fact that US is an operator-dependent imaging technique are also important limitations, as the recorded US images largely display the subjective selection of findings observed by the individual performing the examination [27]. In order to minimize this limitation, we defined a standardized examination protocol, we took basal images and we performed blind examination of the articulations.

The basal US images on our study were also important to diagnosis naturally occurring chondral lesions on the sheep. Naturally occurring osteoarthritis exists in ageing sheep, and prevalent cartilage defects should be take into account at baseline in studies using ovine models [29].

On our study, US assessment after arthroscopy revealed the presence of popliteal cysts on 50% of the stifle joints. This represents the channel of communication with the joint space, and the route for potential decompression of large intra-articular fluid collections, of any etiology, and are frequently associated with internal meniscal tears [25].

The cysts on our study didn´t required surgical treatment and desapeared spontaneously some weeks after. We hypothetized that these cysts appeared as a consequence of the meniscal tear sor as a mechanism of descompresion of the joint after arthroscopy, due to articulation irrigation during the surgery.

The consideration of all articular tissues with respect to treatment of cartilage pathology is vitally important, but often overlooked. The joint is an organ and even early focal cartilage defects are associated with pathology of perilesional and apposing articular cartilage, subchondral bone and synovium, as well as other tissues such meniscus, intra-articular ligaments, and labrum in respective joints. If the whole joint is not taken into consideration when developing and assessing cartilage repair strategies, clinical applicability of the data will be severely limited, especially with respect to pain relief, level or function attained and effects on disease progression [7]. Therefore on the preclinical studies longitudinal assessment of lesion evolution should include whole-joint assessments [7]. Demonstration of inflammation requires sensitive modalities like MRI or US. US has the advantage over MRI in that is cheaper, convenient and easier to use, is dynamic [30] and does not require general anaesthesia on the preclinical studies. US is a valuable tool on the clinical settings, and can be a valuable tool on longitudinal assessment on the preclinical ovine model of cartilage repair. For many years, studies in animal models relied on histological analysis of tissues and/or organs post-mortem. These destructive methods limited the ability of researchers to study the progression of the disease on a single animal serially over time as well as assessing therapeutic efficiency overtime

[12]. It is possible that US imaging could enable the reduction of the total number of animals on cartilage repair studies, if each animal could be studied serially over time.

CONCLUSIONS

Arthroscopy was an appropriate and safe surgical technique for partial-thickness chondral experimental lesion induction on the medial femoral condyle and in the medial meniscus of the ovine knee.

This was the first description of US assessment in vivo of experimental chondral lesions in the sheep knee.

US revealed to be a useful non-invasive technique in the assessment of the injured articular cartilage in the sheep knee, making possible the prediction of small alterations in the cartilage band, allowing effective longitudinal follow-up. MRI was important to detect deeper subchondral bone alterations, and to assess the safety of the surgical technique.

The application of the developed refined techniques in the field of cartilage repair promotes animal welfare and increases research quality. Refining the preclinical animal model facilitates the extrapolation of methodologies on assay-product application and diagnosis techniques in future clinic human trials.

ACKNOWLEDGEMENTS

The authors would like to acknowledge Anna Morist, for experiments technical assistance; José Luiz Ruiz de la Torre, Ramón Costa and all the crew of " Servei de Granjes I Camps Experimentals" (Universitat Autònoma de Barcelona, Bellaterra, Spain) for their careful assistance to animal management. This work was supported by

"Ministerio de Economia y Competitividad" (Grant number IPT-300000-2010-0017), "Ministerio de Ciencia e Innovación" (Grant numbers PSE-010000-2007-4/PSE-010000-2008-4, BIO2008-01985) and "Programa de soporte a grupos de investigación DGR/DIUE" (Grant number 2009SGR1038).

REFERENCES:

1. Mankin, H.J., *Current concepts review. The response of articular cartilage to mechanical injury*. J Bone Joint Surg Am, 1982. **64**(3): p. 460-6.
2. Alford, J.W. and B.J. Cole, *Cartilage restoration, part 1 basic science, historical perspective, patient evaluation, and treatment options*. The American journal of sports medicine, 2005. **33**(2): p. 295-306.
3. McGowan, K.B. and G. Stiegman, *Regulatory challenges for cartilage repair technologies*. Cartilage, 2013. **4**(1): p. 4-11.
4. Ahern, B.J., et al., *Preclinical animal models in single site cartilage defect testing: a systematic review*. Osteoarthritis and Cartilage, 2009. **17**(6): p. 705-713.
5. Hurtig, M.B., et al., *Preclinical Studies for Cartilage Repair Recommendations from the International Cartilage Repair Society*. Cartilage, 2011. **2**(2): p. 137-152.
6. Chu, C.R., M. Szczodry, and S. Bruno, *Animal models for cartilage regeneration and repair*. Tissue Engineering Part B: Reviews, 2010. **16**(1): p. 105-115.
7. Cook, J.L., et al., *Animal models of cartilage repair*. Bone and Joint Research, 2014. **3**(4): p. 89-94.

8. Martini, L., et al., *Sheep model in orthopedic research: a literature review.* Comparative medicine, 2001. **51**(4): p. 292-299.
9. Munirah, S., et al., *Articular cartilage restoration in load-bearing osteochondral defects by implantation of autologous chondrocyte-fibrin constructs: an experimental study in sheep.* Journal of Bone & Joint Surgery, British Volume, 2007. **89**(8): p. 1099-1109.
10. Jubel, A., et al., *Transplantation of de novo scaffold-free cartilage implants into sheep knee chondral defects.* The American journal of sports medicine, 2008. **36**(8): p. 1555-1564.
11. Milano, G., et al., *Repeated platelet concentrate injections enhance reparative response of microfractures in the treatment of chondral defects of the knee: an experimental study in an animal model.* Arthroscopy: The Journal of Arthroscopic & Related Surgery, 2012. **28**(5): p. 688-701.
12. Tremoleda, J.L., et al., *Imaging technologies for preclinical models of bone and joint disorders.* EJNMMI research, 2011. **1**(1): p. 1-14.
13. Goebel, L., et al., *Experimental scoring systems for macroscopic articular cartilage repair correlate with the MOCART score assessed by a high-field MRI at 9.4 Tâ€"comparative evaluation of five macroscopic scoring systems in a large animal cartilage defect model.* Osteoarthritis and Cartilage, 2012. **20**(9): p. 1046-1055.
14. Caminal, M., et al., *Use of a chronic model of articular cartilage and meniscal injury for the assessment of long-term effects after autologous mesenchymal stromal cell treatment in sheep.* New Biotechnology 2014. **(In press)**.
15. Fonseca, C., et al., *An arthroscopic approach for the treatment of osteochondral focal defects with cell-free and cell-loaded PLGA scaffolds in sheep.* Cytotechnology, 2014. **66**(2): p. 345-354.
16. Naredo, E., et al., *Ultrasonographic findings in knee osteoarthritis: a comparative study with clinical and radiographic assessment.* Osteoarthritis and Cartilage, 2005. **13**(7): p. 568-574.

17. McCune, W., et al., *Sonographic evaluation of osteoarthritic femoral condylar cartilage: correlation with operative findings.* Clinical orthopaedics and related research, 1990. **254**: p. 230-235.
18. Court-Payen, M., *Sonography of the knee: Intra-articular pathology.* Journal of Clinical Ultrasound, 2004. **32**(9): p. 481-490.
19. Grassi, W., et al. *Sonographic imaging of normal and osteoarthritic cartilage.* in *Seminars in arthritis and rheumatism.* 1999: Elsevier.
20. Abraham, A.M., et al., *Reliability and validity of ultrasound imaging of features of knee osteoarthritis in the community.* BMC musculoskeletal disorders, 2011. **12**(1): p. 70.
21. Boulocher, C., et al., *Knee joint ultrasonography of the ACLT rabbit experimental model of osteoarthritis: relevance and effectiveness in detecting meniscal lesions.* Osteoarthritis and Cartilage, 2008. **16**(4): p. 470-479.
22. Allen, M.J., et al., *The surgical anatomy of the stifle joint in sheep.* Veterinary Surgery, 1998. **27**(6): p. 596-605.
23. Orth, P. and H. Madry, *A low morbidity surgical approach to the sheep femoral trochlea.* BMC musculoskeletal disorders, 2013. **14**(1): p. 5.
24. Orth, P., et al., *Reduction of sample size requirements by bilateral versus unilateral research designs in animal models for cartilage tissue engineering.* Tissue Engineering Part C: Methods, 2013. **19**(11): p. 885-891.
25. Friedman, L., K. Finlay, and E. Jurriaans, *Ultrasound of the knee.* Skeletal radiology, 2001. **30**(7): p. 361-377.
26. Tsai, C.Y., et al., *The validity of in vitro ultrasonographic grading of osteoarthritic femoral condylar cartilage- a comparison with histologic grading.* Osteoarthritis and Cartilage, 2007. **15**(3): p. 245-250.
27. Möller, I., et al., *Ultrasound in the study and monitoring of osteoarthritis.* Osteoarthritis and Cartilage, 2008. **16**: p. S4-S7.

28. Lee, C.L., et al., *The validity of in vivo ultrasonographic grading of osteoarthritic femoral condylar cartilage: a comparison with in vitro ultrasonographic and histologic gradings*. Osteoarthritis and Cartilage, 2008. **16**(3): p. 352-358.
29. Vandeweerd, J.M., et al., *Prevalence of naturally occurring cartilage defects in the ovine knee*. Osteoarthritis and Cartilage, 2013. **21**(8): p. 1125-1131.
30. Iagnocco, A., *Imaging the joint in osteoarthritis: a place for ultrasound?* Best Practice & Research Clinical Rheumatology, 2010. **24**(1): p. 27-38.

DISCUSSION

6- DISCUSSION

In the studies performed for this thesis, we first focused on the development of an arthroscopic approach to the ovine stifle joint, which could enable the implantation of a tissue engineered therapy based on Co-MSC seeded on PLGA scaffolds to repair osteochondral defects on the femoral medial condyle.

After this study, and due to the limited source of cartilage and morbidity of donor site, we studied the ability of different MSC sources (adipose tissue, bone marrow in comparison with cartilage) to regenerate osteochondral defects in the stifle joint, using the arthroscopic approach previously developed.

On the third study, we used the most efficient MSC source found in the study 2 in a new model of chronic chondral lesion. This model was created to mimic the clinical condition found in human patients with OA in the clinical settings. The arthroscopic technique was adapted to induce the chondral lesion in the medial femoral condyle and medial meniscus of the ovine stifle joint. After evolution of the lesions, the BM-MSC therapy was applied as an intra-articular injection of cells.

Finally, in the fourth study we aimed to highlight the refinement strategies which were developed on the animal models on these studies. The ovine model is commonly used on preclinical studies of cartilage repair strategies, but the review of the published literature reveals the common use of invasive procedures for experimental lesion induction, for cellular therapies implantation and for longitudinal assessment. Ethical concerns relative to animal welfare during research procedures encourages the development of refined procedures, which have the advantage of decreased morbidity and in-

creased translational potential of the model itself. In this study we described in detail the minimally invasive surgical approach to the ovine stifle joint, and the non-invasive imaging techniques which allowed a comprehensive longitudinal follow-up of the lesions during the time.

6.1-Development of an arthroscopic approach to model osteochondral defects and to implant tissue engineered constructs using Co-MSC as cell source in the ovine stifle joint: Study 1

The use of tissue engineered approaches to cartilage repair involves the use of scaffolds and cells seeded in these scaffolds. The osteochondral defects are a challenging condition, as two different tissues types are involved: articular cartilage and subchondral bone.

The study of biocompatible scaffolds is a hot topic, and several research is performed using natural based polymers or synthetic materials for this purpose.

Also, due to the nature and characteristics of the both tissues involved in osteochondral defects, there is also studies describing the use of scaffolds with two distinct layers or gradients (Rodrigues, Gomes *et al.* 2011).

In the present study, a synthetic PLGA scaffold was chosen because it is one of the few synthetic materials approved by the FDA as scaffolding material for clinical applications. Furthermore, it was been previously used in articular cartilage treatment, emerging as a valuable chondrocyte and MSC delivery vehicle (Sittinger, Reitzel *et al*. 1996; Uematsu, Hattori *et al*. 2005).

The methodology followed for the manufacture of the scaffolds permitted to set a porosity level that allowed the ingrowth of host tissue as well as

supporting the preloading with *in vitro* expanded chondrocytes. Importantly, the scaffold structure allowed arthroscopic implantation making it an attractive material for clinical use. This highlights the need of the use of large animal models in the development of new cartilage repair techniques, in particular those species with size and physiology similar to humans.

We used skeletally mature 2-year old sheep (Kilborn, Trudel *et al*. 2002), and the osteochondral defects were modeled in weight bearing areas. For this purpose, the experimental defects were located in the central/posterior region of the medial femoral condyle, with the aim of represent the clinical situation faced in humans. We harvest donor cartilage cells from the shoulder, so both knees of each animal could be used in the study, in the same comparable conditions without additional lesions on the surrounding area that might influence the outcome of the treatments.

The use of chondrocytes allowed a significant improvement with respect to untreated controls at the macroscopic level, although this observation was not confirmed histologically, probably due to the short observation time. Therefore, it was not clear whether the addition of chondrocytes into the PLGA scaffolds could significantly accelerate the regeneration mechanisms.

To our knowledge, this is the first report of arthroscopic implantation of the PLGA scaffolds in the sheep knee. Published studies used arthrotomy procedures to implant the tissue engineered constructs (Niederauer, A Slivka *et al*. 2000; Córdoba, Martínez *et al.* 2007; Erggelet, Neumann *et al*. 2007), because of the difficulty of holding in place the implant without invasive procedures. The biomechanical characteristics of some of the constructs, as the ones made of chondrocytes and fibrin are too soft to hold in the defect site independently of the use of a periosteum patch. The need of development of this minimally invasive technique in the sheep knee has

been mentioned by some authors (Munirah, Samsudin *et al*. 2007; Sha'ban, Kim *et al*. 2008). Furthermore, the regulatory authorities require the use of the intended route of administration in humans and the intended delivery device in preclinical studies.

This surgical technique has the recognized advantage of decrease morbidity associated with arthrotomy, more ethical experimental procedure and a final study that matches the clinical situation faced in human patients.

On the other side there are two limitations that need to be acknowledged in the present study. Although the clinically accepted range of MRI covers from 0.2T to 3T (Ghazinoor, Crues *et al.* 2007), the use of low-field MRI in this study made the detection of small cartilage abnormalities very challenging. The second point concerns to the sample size and the proximity of the two time endpoints for the euthanasia, which gave similar results, making possible to combine data for each treatment from both the 12 and 20-week groups for the statistical analysis.

Cartilage has limitations as a cell source for osteochondral regeneration, which is related to the lesion that is inflicted to the donor site and the limited amount of tissue that can be extracted. Some studies discussed the possibility of using the debrided discarded cartilage tissue obtained from around the cartilage lesion itself, which could solve the problem of iatrogenic damage during the cartilage sourcing (Biant and Bentley 2007) . However, alternative cell sources should be investigated.

Future studies should evaluate the effects of a full regeneration process at later end-points (i.e., up to 12 months), other cell sources, and the appropriate therapeutic dose.

6.2- Comparing BM-MSC, ASC and Co-MSC as cell sources in a tissue engineering approach to regenerate osteochondral defects in the ovine stifle joint: Study 2

In the actuality only ex vivo expanded chondrocytes have been approved by the regulatory authorities for human use and have thus become the gold standard in cell therapy for cartilage resurfacing of focal injuries (Vanlauwe, Saris *et al.* 2011). However limitations of this technique include donor site limitation and morbidity, as well as low success rate.

Therefore there is the need to explore and study other cell sources to regenerate osteochondral defects.

In the present study, scaffolds of PLGA were used as a vehicle of three different cell types that were tested side-to-side under the same experimental conditions in order to assess cartilage resurfacing capacity at 6 and 12 months post-implantation on critical-size osteochondral defects. PLGA was chosen due to its proven biocompatibility and the feasibility of three-dimensional molding of the constructs in the shape of the experimental defects. Furthermore it allowed minimally invasive surgical implantation. The PLGA degradation rate, which was compatible with the deposition of extra cellular matrix (ECM) by the cells loaded on the scaffolds (Sittinger, Reitzel *et al.* 1996; Niederauer, A Slivka *et al*. 2000; Uematsu, Hattori *et al.* 2005; Córdoba, Martínez *et al*. 2007). The use of porous PLGA scaffolds permitted the retention of the cells at the defect site and promoted homogeneous distribution throughout the graft.

We observed that PLGA scaffolds at a ratio of 50 (PLA): 50 (PGA) preserved their integrity up to 5 weeks *in vitro*, which is compatible with the time taken by the cells to synthesize the new ECM (from 9 to 20 days, ac-

cording to the work performed by Barry and collaborators (Barry, Boynton *et al.* 2001)) that substitutes the scaffolding material (Middleton and Tipton 2000). Furthermore, PLGA-based constructs allow arthroscopic implantation, making this biomaterial even more attractive for clinical use, since the arthroscopic technique reduces morbidity, surgical time, secondary complications and improves patient recovery. The complications derived from open surgery which is routinely performed in tissue engineering strategies for cartilage repair (Niederauer, A Slivka *et al.* 2000; Córdoba, Martínez *et al.* 2007; Erggelet, Neumann *et al*. 2007).

Although in some samples the tide mark was faint or disappeared, it is remarkable that none of the specimens showed detachment of neocartilage from subchondral bone, indicating that the integration between the two layers resisted the load bearing forces in all treatment groups and highlighting the suitability of PLGA scaffolds in the treatment of osteochondral defects.

With respect to cell types, the differentiation potential of MSC into chondrocytes and osteoblasts makes these cells very attractive for the simultaneous regeneration of bone/cartilage lesions. Additionally, MSC can be expanded extensively *in vitro* whilst chondrocytes hold a limited culture growth capacity and display phenotypic instability during the course of their expansion in monolayer culture. Such phenotypic instability, also called dedifferentiation, is characterized by a shift of cellular morphology from a rounded to the typical fusiform fibroblastic shape, among other features (Schnabel, Marlovits *et al.* 2002), as we also observed in the present study. Considering the advantages of using BM-MSC and provided that both chondrocytes and BM-MSC gave similar results with respect to the quality of the new tissue, our results may suggest that BM-MSC as the preferred cell source in cell-therapies aiming at osteochondral repair using PLGA scaffolds. On the other hand, we observed that ASC were not as effective as

BM-MSC to regenerate osteochondral defects neither at 6 nor at 12 months post-treatment. Different expression profiles in ASC and BM-MSC may explain why the later differentiate more efficiently into bone and cartilage, whereas ASC differentiate better into adipocytes as reported previously by Liu and collaborators (Liu, Martina *et al.* 2007) thus supporting our observations in the present study.

The safety of the implantation of autologous cell- scaffold constructs was demonstrated by the absence of local or systemic adverse effects during the clinical follow-up and by a full necropsy performed at 12 months post-treatment.

With respect to the efficacy, the presence of cartilage of hyaline quality one year after treatment with either BM-MSC or chondrocytes is a key point since current surgical approaches typically result in a short-term clinical success but eventually fail due to poor mechanical properties of the mixed matrix that is generated. For example, even though fibrocartilaginous repair tissue from microfracture results in initially enhanced clinical knee-function scores at earlier assessment time points, it later degrades, and scores decline (Mithoefer, McAdams *et al.* 2009). This also highlights the importance of using large animal models with anatomy similar to the human knee allowing orthopaedic surgeons to undergo procedures similar to those in human practice and therefore making possible to assess the performance of novel implants *in situ* using minimally invasive surgical approaches. Due to its size and anatomy, sheep arises as a relevant translational animal model for this type of research and, in fact, it has been previously used in several other studies for the treatment of chondral and osteochondral lesions (Ahern, Parvizi *et al.* 2009).

Although the promising results obtained in this study, further work is needed in order to evaluate dose-effect relationships. Also scaffold design

should be optimized in order to improve the integration to the adjacent tissue. Mechanisms involved in the regeneration process should be explored, which may uncover additional advantages of the use of MSC in contrast to chondrocytes, such as MSC's anti-inflammatory effects.

To accurately translate the results to the clinics, the developed cell therapies should be further tested in an animal model of chronic cartilage injury. This would enable to assess the efficacy of this cell therapy on a joint condition that more truthfully simulate the pathological condition found in the clinics.

6.3- Assessment of BM-MSC long-term effects on a chronic model of chondral lesion in the ovine stifle joint: Study 3.

The development of a novel pharmaceutical requires the characterization of its pharmacological and toxicological properties according to its intended use in humans. In this sense, most previous studies have investigated the use of MSC for therapy of acute defects, in which generation and reconstruction of the defects were conducted simultaneously. However, chronic defects are more in line with the type of lesions found in clinical practice, since patients have a lengthy course following trauma to the cartilage, which results in altered intra-articular homeostasis (Saris, Dhert *et al.* 2003). This may explain why the encouraging and reproducible data obtained in experimental studies *in vivo* have been unattainable in the clinical setting (Horas, Pelinkovic *et al.* 2003; Krishnan, Skinner *et al.* 2006; Ruano-Ravina and Diaz 2006; Wasiak, Clar *et al*. 2006). Significant efforts have been made in the development of relevant chronic animal models of articular cartilage disease (Hepp, Osterhoff *et al.* 2009). The translational animal model used on this

study mimicked an osteoarthritis condition of grade III in articular cartilage according to the ovine adaptation of the Outerbridge classification (Burger, Mueller *et al.* 2007)and incorporated a further lesion on the anterior horn of the medial meniscus. The 4 weeks required for chronic degeneration of the defects were spent in the isolation and *ex vivo* expansion of MSC from bone marrow.

After treatment, MRI, ecographic or X-Ray monitoring did not show any progression of the degenerative process, and the macroscopic, histological and immunohystochemical analysis (at 6 and 12 months) permitted to evaluate more accurately the extent of the refill tissue and hyaline nature of the regenerated cartilage of the condyles.

A case-dependent efficacy of the treatment was observed among animals from both experimental groups with respect to macroscopic and histological International Cartilage Repair Society (ICRS) scores. A further examination of each individual parameter assessed in the macroscopic and histological analysis provided evidence of statistical significant improvement in the MSC-treated group compared to controls. Macroscopically, these parameters included the color, rigidity and aspect of sagittal section. Likewise histological parameters displaying statistically significant differences between treatment and control groups included cell distribution, subchondral bone structure and proteoglycan/ type II collagen content. Meniscal lesions were also partially repaired in some cases.

The animal model used in this study is relevant to pathological condition of joint disease found in humans and the results of intra-articular cell-based therapy suggest a safe and straightforward approach for the treatment of articular cartilage and meniscal injury, which may prevent the progression of osteoarthritis.

Further work is required in order to enhance the regenerative properties of MSC, understand the mechanisms involved, evaluate the use of scaffolds for cell delivery in focal lesions that otherwise may progress to OA and to determine dose-effect relationships.

6.4- Detailing the refinement strategies for chondral experimental lesion induction and longitudinal assessment on the ovine model of cartilage repair: Study 4

In the present study, a minimally invasive surgical approach was successfully performed for modelling partial-thickness chondral lesions on the medial femoral condyles and meniscal tears on the sheep knee, without surgical complications on the post-operatory period. Arthroscopy was an effective, safe and quick technique to perform the experimental lesions on all the 20 stifle joints.

The sheep is a key animal as a preclinical experimental model of cartilage repair, being the stifle joint one of the preferred location for these studies due to anatomical similarities with human knee (Allen, Houlton *et al*. 1998; Ahern, Parvizi *et al*. 2009). Arthrotomy is the usual method to induce the experimental cartilage lesions, however it is recognized that arthrotomy in sheep has as a common post-operative complication patellar luxation. Recent work described a mini-arthrotomy without patellar luxation as a refinement of the usually performed technique (Orth and Madry 2013). However, as bilateral surgery is usually performed on animal models on cartilage research (Orth, Zurakowski *et al*. 2013), a minimally invasive surgical technique (arthroscopy) should be preferred in order to minimize animal distress after the surgical approach. It is also expected that arthroscopic approach is

accompanied of a lower risk of joint infection, as surgical exposure of the intraarticular tissues and surgical wounds are smaller than in arthrotomy exposure: this is especially important due to housing conditions of sheep, which are usually on a reduced antiseptic environment due to the nature of the animal model itself.

It is recognized that the implementation of preclinical imaging represents a keystone in the refinement of animal models allowing longitudinal studies and enabling a powerful, non-invasive and clinically translatable way for monitoring disease progression in real time (Tremoleda, Khalil *et al*. 2011). In this sense, it was used on this study magnetic resonance imaging and US imaging for lesion longitudinal assessment. On the present study MRI was especially useful to detect meniscal tears and subchondral alterations and to discard lesions on tendons or ligaments. The fact that we used a 0,2 T unit limited the ability to detect cartilage lesions that didn´t produce a reaction of the subchondral bone.

US is emerging as a viable imaging modality in the diagnosis and assessment of the musculoskeletal system, and as a valuable additional diagnostic modality for the evaluation of the knee joint in the clinical practice (Friedman, Finlay *et al.* 2001).

Human hyaline cartilage is described as a well-defined anechogenic or homogeneously hypoechogenic band between the chondrosynovial and osteochondral margins (Tsai, Lee *et al.* 2007; Möller, Bong *et al*. 2008). In our study, we found that normal articular cartilage of sheep stifle joint has a similar aspect. The lack of echoes is due to uniform transmission of sound wave in cartilage with high water content and densely packed and organized collagen (McCune, Dedrick *et al.* 1990; Grassi, Lamanna *et al*. 1999). The absence of echoes of the cartilage layer and the sharpness of the margins are its principal features in healthy subjects, corresponding the sharp margin

to smooth surface of healthy cartilage (Tsai, Lee *et al.* 2007; Lee, Huang *et al*. 2008; Möller, Bong *et al*. 2008).

On the present study, one week after the experimental lesion induction the cartilage band of the medial femoral condyle presented altered echogenicity with alteration on the sharpness of the chondrosynovial margin, which correspond to fibrillations and erosion of the cartilage induced previously on the arthroscopy for chondral lesion induction. At this moment, no alteration was detected on the osteochondral margin of the majority of the condyles, suggesting that the surgical methodology to partial-thickness chondral lesion induction respected the calcified cartilage layer. Five weeks after the chondral lesion induction, it was already noticeable alteration in the osteochondral margin.

This alteration on the osteochondral margin 5 weeks after the lesion induction, which was not consistently present on the previous examination (4 weeks before) can be due to the natural evolution of the lesion: the underlying subchondral bone suffers alteration due to abnormal mechanical forces which are no longer attenuated by the eroded cartilage. The highly specific microscopic anatomy and interdependent physiology of articular cartilage can be disrupted by small, superficial injuries, even without immediate cartilage loss. Superficial damage will injure chondrocytes, limit their metabolic capacity for repair, and lead to decreased proteoglycan concentration, increased hydration, and altered fibrillar organization of collagen. Proteoglycan loss, increased water content, decreased cartilage stiffness, and increased hydraulic permeability lead to increased force transmission to the underlying subchondral bone, which increases its stiffness and, in turn, causes impact loads to be more readily transmitted to the partially damaged cartilage. This vicious cycle is thought to contribute to the progression of partial-thickness articular cartilage injuries (Alford and Cole 2005).

Though the US examination at 5 weeks was performed one week after assay-product or saline vehicle intra-articular infiltration, we believe that at this moment it is not noticeable alteration of the lesion status due to the injected products. The cellular treatment effects over the lesions are expected to be noticed at long-time period. Moreover, identical lesion images were obtained between the knees injected with saline or MSC. The total volume of 4 ml is small to consider a lavage procedure.

The described earlier US features of osteoarthritis in humans are loss of clarity of the cartilage band and loss of sharpness of the margins. The loss of sharpness of the interface is due to scattering of sound by a rough surface. The increased echogenicity may represent structural alteration such as fibrillation of cartilage and cleft formation. In the later stages, an asymmetric narrowing of the cartilaginous layer occurs (Möller, Bong *et al.* 2008). In our study we found difficult to correctly measure by US the cartilage band thickness. It is recognized on the clinical settings that the loss of sharpness of the interface can make the placement of markers, for thickness measurement, difficult (McCune, Dedrick *et al.* 1990; Grassi, Lamanna *et al*. 1999). The overlying soft tissue may influence the appearance of the underlying cartilage band. Synovial fluid in patients with synovitis may impair the visualization of the synovial-cartilage interface (Grassi, Lamanna *et al*. 1999; Lee, Huang *et al*. 2008). Varying thickness of the overlying tissue may also verify the image echogenicity (McCune, Dedrick *et al*. 1990; Lee, Huang *et al*. 2008). Because of this, clarity and sharpness of the cartilage images are considered the best predictors of cartilage alteration, correlating significantly with gross findings of the specimen in the clinics (McCune, Dedrick *et al*. 1990).

The main limitation of US is the inability of the beam to penetrate the bony cortex. Thus, US visualization of the articular cartilage is restricted by

the acoustic windows, their width being determined by the anatomy of the joint under examination (Möller, Bong *et al.* 2008). The bone alterations that can be detected by US are loss of continuity of the bone profile or an increased intensity of the posterior bone-cartilage interface, that may reflect subchondral bone sclerosis or loss of overlying cartilage (Grassi, Lamanna *et al*. 1999). Difficulty to measure cartilage thinning and the fact that US is an operator-dependent imaging technique are also important limitations, as the recorded US images largely display the subjective selection of findings observed by the individual performing the examination (Möller, Bong *et al.* 2008). In order to minimize this limitation, we defined a standardized examination protocol, we took basal images and we performed blind examination of the articulations.

The basal US images on our study were also important to diagnosis naturally occurring chondral lesions on the sheep. Naturally occurring osteoarthritis exists in ageing sheep, and prevalent cartilage defects should be take into account at baseline in studies using ovine models (Vandeweerd, Hontoir *et al.* 2013).

On our study, US assessment after arthroscopy revealed the presence of popliteal cysts on 50% of the stifle joints. This represents the channel of communication with the joint space, and the route for potential decompression of large intra-articular fluid collections, of any etiology, and are frequently associated with internal meniscal tears (Friedman, Finlay *et al.* 2001).

The cysts on our study didn´t required surgical treatment and desapeared spontaneously some weeks after. We hypothesized that these cysts appeared as a consequence of the meniscus tears or as a mechanism of decompression of the joint after arthroscopy, due to articulation irrigation during the surgery.

The consideration of all articular tissues with respect to treatment of cartilage pathology is vitally important, but often overlooked. The joint is an organ and even early focal cartilage defects are associated with pathology of peri-lesional and apposing articular cartilage, subchondral bone and synovium, as well as other tissues such meniscus, intra-articular ligaments, and labrum in respective joints. If the whole joint is not taken into consideration when developing and assessing cartilage repair strategies, clinical applicability of the data will be severely limited, especially with respect to pain relief, level or function attained and effects on disease progression (Cook, Hung *et al.* 2014). Therefore on the preclinical studies longitudinal assessment of lesion evolution should include whole-joint assessments (Cook, Hung *et al*. 2014). Demonstration of inflammation requires sensitive modalities like MRI or US. US has the advantage over MRI in that is cheaper, convenient and easier to use, is dynamic (Iagnocco 2010) and does not require general anaesthesia on the preclinical studies. US is a valuable tool on the clinical settings, and can be a valuable tool on longitudinal assessment on the preclinical ovine model of cartilage repair. For many years, studies in animal models relied on histological analysis of tissues and/or organs post-mortem. These destructive methods limited the ability of researchers to study the progression of the disease on a single animal serially over time as well as assessing therapeutic efficiency overtime (Tremoleda, Khalil *et al*. 2011). It is possible that US imaging could enable the reduction of the total number of animals on cartilage repair studies, if each animal could be studied serially over time.

CONCLUSIONS

7- CONCLUSIONS

- Arthroscopic techniques are feasible and appropriate to model osteochondral and chondral experimental lesions on the ovine stifle joint.
- The used PLGA scaffolds resisted successfully to arthroscopic surgical manipulation.
- The use of Co-MSC in combination with PLGA scaffolds improves osteochondral regeneration on the ovine model at 20 weeks end-point.
- Comparing efficacy on cartilage resurfacing of Co-MSC, BM-MSC and ASC in combination with PLGA scaffolds on osteochondral lesions, cartilage of hyaline quality is observed principally after using cells derived from cartilage and bone marrow.
- The use of expanded cells from cartilage, bone marrow and adipose tissue in combination with PLGA scaffolds for cell therapy of osteochondral defects is safe at one year post-implantation.
- After using BM-MSC on the treatment of chondral defects in the ovine knee it was found significant improvement in colour, rigidity, cell distribution, hyaline quality of the refill tissue and on the structure of the subchondral bone.
- The use of BM-MSC for the treatment of chondral defects in the ovine stifle joint is safe at one year post-implantation.
- US revealed to be a useful non-invasive technique in the assessment of the injured articular cartilage in the ovine knee, making possible the prediction of small alterations in the cartilage band, allowing effective longitudinal follow-up.

- The application of the developed refined techniques in the field of cartilage repair promotes animal welfare and increases research quality.
- Refining the preclinical animal model facilitates the extrapolation of methodologies on assay-product application and diagnosis techniques in future clinic human trials.
- The developed preclinical studies using the refined ovine model allowed the set-up of clinical studies in humans using autologous BM-MSC as cellular therapy on knee cartilage repair.

BIBLIOGRAPHY

8- BIBLIOGRAPHY

Abraham, A. M., I. Goff, et al. (2011). "Reliability and validity of ultrasound imaging of features of knee osteoarthritis in the community." BMC musculoskeletal disorders **12**(1): 70.

Abumaree, M., M. Al Jumah, et al. (2012). "Immunosuppressive properties of mesenchymal stem cells." Stem Cell Reviews and Reports **8**(2): 375-392.

Ahern, B. J., J. Parvizi, et al. (2009). "Preclinical animal models in single site cartilage defect testing: a systematic review." Osteoarthritis and Cartilage **17**(6): 705-713.

Alford, J. W. and B. J. Cole (2005). "Cartilage restoration, part 1 basic science, historical perspective, patient evaluation, and treatment options." The American journal of sports medicine **33**(2): 295-306.

Alford, J. W. and B. J. Cole (2005). "Cartilage Restoration, Part 1: Basic Science, Historical Perspective, Patient Evaluation, and Treatment Options." The American Journal of Sports Medicine **33**(2): 295.

Allen, M. J., J. E. Houlton, et al. (1998). "The surgical anatomy of the stifle joint in sheep." Veterinary Surgery **27**(6): 596-605.

An, Y. H. and R. J. Freidman (1998). Animal models in orthopaedic research, CRC Press.

An, Y. H. and R. J. Friedman (1999). Animal models in orthopaedic research, CRC Press.

Anraku, Y., H. Mizuta, et al. (2009). "Analyses of early events during chondrogenic repair in rat full-thickness articular cartilage defects." Journal of bone and mineral metabolism **27**(3): 272-286.

Anraku, Y., H. Mizuta, et al. (2008). "The chondrogenic repair response of undifferentiated mesenchymal cells in rat full-thickness articular cartilage defects." Osteoarthritis and Cartilage **16**(8): 961-964.

Baksh, D., L. Song, et al. (2004). "Adult mesenchymal stem cells: characterization, differentiation, and application in cell and gene therapy." Journal of cellular and molecular medicine **8**(3): 301-316.

Barry, F., R. E. Boynton, et al. (2001). "Chondrogenic differentiation of mesenchymal stem cells from bone marrow: differentiation-dependent gene expression of matrix components." Experimental cell research **268**(2): 189-200.

Bendele, A., J. McComb, et al. (1999). "Animal models of arthritis: relevance to human disease." Toxicologic pathology **27**(1): 134-142.

Biant, L. C. and G. Bentley (2007). "Stem cells and debrided waste. Two alternative sources of cells for transplantation of cartilage." Journal of Bone & Joint Surgery, British Volume **89**(8): 1110-1114.

Boulocher, C., M. E. Duclos, et al. (2008). "Knee joint ultrasonography of the ACLT rabbit experimental model of osteoarthritis: relevance and effectiveness in detecting meniscal lesions." Osteoarthritis and Cartilage **16**(4): 470-479.

Bourget, J. L., D. W. Mathes, et al. (2001). "Tolerance to Musculoskeletal Allografts With Transient Lymphocyte Chimerism in Miniature Swine1." Transplantation **71**(7): 851-856.

Bouwmeester, P. S. J. M., R. Kuijer, et al. (2002). "A retrospective analysis of two independent prospective cartilage repair studies: autogenous perichondrial grafting versus subchondral drilling 10 years post-surgery." Journal of Orthopaedic Research **20**(2): 267-273.

Brehm, W., B. Aklin, et al. (2006). "Repair of superficial osteochondral defects with an autologous scaffold-free cartilage construct in a caprine

model: implantation method and short-term results." Osteoarthritis and Cartilage **14**(12): 1214-1226.

Breinan, H. A., T. Minas, et al. (2001). "Autologous chondrocyte implantation in a canine model: change in composition of reparative tissue with time." Journal of Orthopaedic Research **19**(3): 482-492.

Breinan, H. A., T. O. M. Minas, et al. (1997). "Effect of Cultured Autologous Chondrocytes on Repair of Chondral Defects in a Canine Model." The Journal of Bone & Joint Surgery **79**(10): 1439-51.

Brooks, P. (2003). "Inflammation as an important feature of osteoarthritis." Bulletin of the World Health Organization **81**(9): 689-690.

Buma, P., J. S. Pieper, et al. (2003). "Cross-linked type I and type II collagenous matrices for the repair of full-thickness articular cartilage defects - a study in rabbits." Biomaterials **24**(19): 3255-3263.

Burger, C., M. Mueller, et al. (2007). "The sheep as a knee osteoarthritis model: early cartilage changes after meniscus injury and repair." Laboratory Animals **41**(4): 420-431.

Butnariu-Ephrat, M., D. Robinson, et al. (1996). "Resurfacing of goat articular cartilage by chondrocytes derived from bone marrow." Clinical orthopaedics and related research **330**: 234-243.

Caplan, A. I. (2005). "Mesenchymal stem cells: cell-based reconstructive therapy in orthopedics." Tissue engineering **11**(7-8): 1198-1211.

Clar, C., E. Cummins, et al. (2005). "Clinical and cost-effectiveness of autologous chondrocyte implantation for cartilage defects in knee joints: systematic review and economic evaluation." Health Technology Assessment **9**(7).

Convery, F. R., W. H. Akeson, et al. (1972). "The repair of large osteochondral defects. An experimental study in horses." Clinical orthopaedics and related research **82**: 253-262.

Cook, J. L., C. T. Hung, et al. (2014). "Animal models of cartilage repair." Bone and Joint Research **3**(4): 89-94.

Cook, S. D., L. P. Patron, et al. (2003). "Repair of articular cartilage defects with osteogenic protein-1 (BMP-7) in dogs." The Journal of Bone & Joint Surgery **85**(suppl_3): 116-123.

Córdoba, F. E. V., C. V. Martínez, et al. (2007). "Resultados en la reparación experimental de lesiones osteocondrales en un modelo porcino mediante ingeniería de tejidos." Acta Ortopédica Mexicana **21**(4): 217-223.

Court-Payen, M. (2004). "Sonography of the knee: Intra-articular pathology." Journal of Clinical Ultrasound **32**(9): 481-490.

Chiang, H., T.-F. Kuo, et al. (2005). "Repair of porcine articular cartilage defect with autologous chondrocyte transplantation." Journal of Orthopaedic Research **23**(3): 584-593.

Chu, C. R., R. D. Coutts, et al. (1995). "Articular cartilage repair using allogeneic perichondrocyte-seeded biodegradable porous polylactic acid (PLA): A tissue-engineering study." Journal of biomedical materials research **29**(9): 1147-1154.

Chu, C. R., J. S. Dounchis, et al. (1997). "Osteochondral repair using perichondrial cells: a 1-year study in rabbits." Clinical orthopaedics and related research **340**: 220-229.

Chu, C. R., M. Szczodry, et al. (2010). "Animal models for cartilage regeneration and repair." Tissue Engineering Part B: Reviews **16**(1): 105-115.

Dausse, Y., L. Grossin, et al. (2003). "Cartilage repair using new polysaccharidic biomaterials: macroscopic, histological and biochemical approaches in a rat model of cartilage defect." Osteoarthritis and Cartilage **11**(1): 16-28.

Dhandayuthapani, B., Y. Yoshida, et al. (2011). "Polymeric scaffolds in tissue engineering application: a review." International Journal of Polymer Science **2011**: 1-19.

Dorotka, R., U. Windberger, et al. (2005). "Repair of articular cartilage defects treated by microfracture and a three-dimensional collagen matrix." Biomaterials **26**(17): 3617-3629.

Erggelet, C., K. Neumann, et al. (2007). "Regeneration of ovine articular cartilage defects by cell-free polymer-based implants." Biomaterials **28**(36): 5570-5580.

FDA Cellular, T., and Gene Therapies Advisory Committee (2005). Cellular Products for Joint Surface Repair, FDA**:** 1-41.

Feczkó, P., L. Hangody, et al. (2003). "Experimental results of donor site filling for autologous osteochondral mosaicplasty." Arthroscopy: The Journal of Arthroscopic & Related Surgery **19**(7): 755-761.

Ferretti, M., K. G. Marra, et al. (2006). "Controlled in vivo degradation of genipin crosslinked polyethylene glycol hydrogels within osteochondral defects." Tissue engineering **12**(9): 2657-2663.

Flik, K. R., N. Verma, et al. (2007). Cartilage Repair Strategies. Articular Cartilage Structure, Biology, and Function, Humana Press, Totowa, NJ.

Friedenstein, A. J., K. V. Petrakova, et al. (1968). "Heterotopic of bone marrow. Analysis of precursor cells for osteogenic and hematopoietic tissues." Transplantation **6**(2): 230-247.

Friedman, L., K. Finlay, et al. (2001). "Ultrasound of the knee." Skeletal radiology **30**(7): 361-377.

Frisbie, D. D., M. W. Cross, et al. (2006). "A comparative study of articular cartilage thickness in the stifle of animal species used in human preclinical studies compared to articular cartilage thickness in the human knee." Vet Comp Orthop Traumatol **19**(3): 142-146.

Frosch, K.-H., A. Drengk, et al. (2006). "Stem cell-coated titanium implants for the partial joint resurfacing of the knee." Biomaterials **27**(12): 2542-2549.

Furukawa, T., D. R. Eyre, et al. (1980). "Biochemical studies on repair cartilage resurfacing experimental defects in the rabbit knee." J Bone Joint Surg **62**(1): 79-89.

Ghazinoor, S., J. V. Crues, et al. (2007). "Low-field musculoskeletal MRI." Journal of Magnetic Resonance Imaging **25**(2): 234-244.

Goebel, L., P. Orth, et al. (2012). "Experimental scoring systems for macroscopic articular cartilage repair correlate with the MOCART score assessed by a high-field MRI at 9.4 T. Comparative evaluation of five macroscopic scoring systems in a large animal cartilage defect model." Osteoarthritis and Cartilage **20**(9): 1046-1055.

Goldberg, V. M. and A. I. Caplan (1998). "Biologic restoration of articular surfaces." Instructional course lectures **48**: 623-627.

Gotterbarm, T., S. J. Breusch, et al. (2008). "The minipig model for experimental chondral and osteochondral defect repair in tissue engineering: retrospective analysis of 180 defects." Laboratory Animals **42**(1): 71-82.

Grassi, W., G. Lamanna, et al. (1999). Sonographic imaging of normal and osteoarthritic cartilage. Seminars in arthritis and rheumatism, Elsevier.

Guo, X., H. Park, et al. (2010). "Repair of osteochondral defects with biodegradable hydrogel composites encapsulating marrow mesenchymal stem cells in a rabbit model." Acta biomaterialia **6**(1): 39-47.

Han, C. W., C. R. Chu, et al. (2003). "Analysis of rabbit articular cartilage repair after chondrocyte implantation using optical coherence tomography." Osteoarthritis and Cartilage **11**(2): 111-121.

Hancock, W. W. (1997). "Beyond hyperacute rejection: strategies for development of pig--> primate xenotransplantation." Kidney international. Supplement **58**: S36-40.

Hardingham, T. E., R. A. Oldershaw, et al. (2006). "Cartilage, SOX9 and Notch signals in chondrogenesis." Journal of anatomy **209**(4): 469-480.

Harwin, S. F. (1999). "Arthroscopic debridement for osteoarthritis of the knee: predictors of patient satisfaction." Arthroscopy: The Journal of Arthroscopic & Related Surgery **15**(2): 142-146.

Helminen, H. J., K. Kiraly, et al. (1993). "An inbred line of transgenic mice expressing an internally deleted gene for type II procollagen (COL2A1). Young mice have a variable phenotype of a chondrodysplasia and older mice have osteoarthritic changes in joints." Journal of Clinical Investigation **92**(2): 582.

Helminen, H. J., A.-M. Säämänen, et al. (2002). "Transgenic mouse models for studying the role of cartilage macromolecules in osteoarthritis." Rheumatology **41**(8): 848-856.

Hendrickson, D. A., A. J. Nixon, et al. (1994). "Chondrocyte-fibrin matrix transplants for resurfacing extensive articular cartilage defects." Journal of Orthopaedic Research **12**(4): 485-497.

Hennig, T., H. Lorenz, et al. (2007). "Reduced chondrogenic potential of adipose tissue derived stromal cells correlates with an altered TGFbeta receptor and BMP profile and is overcome by BMP-6." Journal of cellular physiology **211**(3): 682-691.

Hepp, P., G. Osterhoff, et al. (2009). "Perilesional changes of focal osteochondral defects in an ovine model and their relevance to human osteochondral injuries." Journal of Bone & Joint Surgery, British Volume **91**(8): 1110-1119.

Hidaka, C., L. R. Goodrich, et al. (2003). "Acceleration of cartilage repair by genetically modified chondrocytes over expressing bone morphogenetic protein-7." Journal of Orthopaedic Research **21**(4): 573-583.

Hollister, S. J. (2005). "Porous scaffold design for tissue engineering." Nature materials **4**(7): 518-524.

Horas, U., D. Pelinkovic, et al. (2003). "Autologous chondrocyte implantation and osteochondral cylinder transplantation in cartilage repair of the knee joint." The Journal of Bone & Joint Surgery **85**(2): 185-192.

Hunziker, E. B. (2002). "Articular cartilage repair: basic science and clinical progress. A review of the current status and prospects." Osteoarthritis and Cartilage **10**(6): 432-463.

Iagnocco, A. (2010). "Imaging the joint in osteoarthritis: a place for ultrasound?" Best Practice & Research Clinical Rheumatology **24**(1): 27-38.

Im, G.-I., D.-Y. Kim, et al. (2001). "Repair of cartilage defect in the rabbit with cultured mesenchymal stem cells from bone marrow." Journal of Bone & Joint Surgery, British Volume **83**(2): 289-294.

Jackson, D. W., P. A. Lalor, et al. (2001). "Spontaneous Repair of Full-Thickness Defects of Articular Cartilage in a Goat Model A Preliminary Study." The Journal of Bone & Joint Surgery **83**(1): 53-53.

Jackson, W. M., T. P. Lozito, et al. (2010). "Differentiation and regeneration potential of mesenchymal progenitor cells derived from traumatized muscle tissue." Journal of cellular and molecular medicine **15**(11): 2377-2388.

Jiang, C.-C., H. Chiang, et al. (2007). "Repair of porcine articular cartilage defect with a biphasic osteochondral composite." Journal of Orthopaedic Research **25**(10): 1277-1290.

Jones, B. A. and M. Pei (2012). "Synovium-derived stem cells: a tissue-specific stem cell for cartilage engineering and regeneration." Tissue Engineering Part B: Reviews **18**(4): 301-311.

Jones, E. A., A. Crawford, et al. (2008). "Synovial fluid mesenchymal stem cells in health and early osteoarthritis: Detection and functional evaluation at the single-cell level." Arthritis & Rheumatism **58**(6): 1731-1740.

Jubel, A., J. Andermahr, et al. (2008). "Transplantation of de novo scaffold-free cartilage implants into sheep knee chondral defects." The American journal of sports medicine **36**(8): 1555-1564.

Kandel, R. A., M. Grynpas, et al. (2006). "Repair of osteochondral defects with biphasic cartilage-calcium polyphosphate constructs in a sheep model." Biomaterials **27**(22): 4120-4131.

Kangarlu, A. and H. K. Gahunia (2006). "Magnetic resonance imaging characterization of osteochondral defect repair in a goat model at 8T." Osteoarthritis and Cartilage **14**(1): 52-62.

Kawamura, S., S. Wakitani, et al. (1998). "Articular cartilage repair: rabbit experiments with a collagen gel-biomatrix and chondrocytes cultured in it." Acta Orthopaedica **69**(1): 56-62.

Khan, W. S., A. A. Malik, et al. (2009). "Stem cell applications and tissue engineering approaches in surgical practice." Journal of perioperative practice **19**(4): 130-135.

Kilborn, S. H., G. Trudel, et al. (2002). "Review of growth plate closure compared with age at sexual maturity and lifespan in laboratory animals." Journal of the American Association for Laboratory Animal Science **41**(5): 21-26.

Koch, T. G. and D. H. Betts (2007). "Stem cell therapy for joint problems using the horse as a clinically relevant animal model." Expert opinion on biological therapy **7**(11): 1621-6.

Koga, H., T. Muneta, et al. (2008). "Comparison of mesenchymal tissues-derived stem cells for in vivo chondrogenesis: suitable conditions for cell therapy of cartilage defects in rabbit." Cell and tissue research **333**(2): 207-215.

Krishnan, S. P., J. A. Skinner, et al. (2006). "Collagen-covered autologous chondrocyte implantation for osteochondritis dissecans of the knee: Two-to seven -year results." Journal of Bone & Joint Surgery, British Volume **88**(2): 203-205.

Lammi, P. E., M. J. Lammi, et al. (2001). "Strong hyaluronan expression in the full-thickness rat articular cartilage repair tissue." Histochemistry and cell biology **115**(4): 301-308.

Lee, C. L., M. H. Huang, et al. (2008). "The validity of *in vivo* ultrasonographic grading of osteoarthritic femoral condylar cartilage: a comparison with *in vitro* ultrasonographic and histologic gradings." Osteoarthritis and Cartilage **16**(3): 352-358.

Liu, T. M., M. Martina, et al. (2007). "Identification of common pathways mediating differentiation of bone marrow- and adipose tissue- derived human mesenchymal stem cells into three mesenchymal lineages." Stem cells **25**(3): 750-760.

Liu, X., J. M. Holzwarth, et al. (2012). "Functionalized synthetic biodegradable polymer scaffolds for tissue engineering." Macromolecular bioscience **12**(7): 911-919.

Lu, L., S. J. Peter, et al. (2000). "In vitro and in vivo degradation of porous poly (DL-lactic-co-glycolic acid) foams." Biomaterials **21**(18): 1837-1845.

Lu, Y., K. Hayashi, et al. (2000). "The effect of monopolar radiofrequency energy on partial-thickness defects of articular cartilage." Arthroscopy: The Journal of Arthroscopic & Related Surgery **16**(5): 527-536.

Majumdar, M. K., R. Askew, et al. (2007). "Double-knockout of ADAMTS-4 and ADAMTS-5 in mice results in physiologically normal animals and prevents the progression of osteoarthritis." Arthritis & Rheumatism **56**(11): 3670-3674.

Mankin, H. J. (1982). "Current concepts review. The response of articular cartilage to mechanical injury." J Bone Joint Surg Am **64**(3): 460-6.

Mankin, H. J. (1982). The response of articular cartilage to mechanical injury, JBJS. **64:** 460-466.

Mankin, H. J., V. C. Mow, et al. (1994). "Form and function of articular cartilage." Orthopaedic Basic Science. Rosemont, Ill: American Academy of Orthopaedic Surgeons: 1-44.

Mano, J. F. and R. L. Reis (2007). "Osteochondral defects: present situation and tissue engineering approaches." Journal of tissue engineering and regenerative medicine **1**(4): 261-273.

Martini, L., M. Fini, et al. (2001). "Sheep model in orthopedic research: a literature review." Comparative medicine **51**(4): 292-299.

Matsumoto, T., S. Kubo, et al. (2008). "The influence of sex on the chondrogenic potential of muscleâ€• derived stem cells: Implications for cartilage regeneration and repair." Arthritis & Rheumatism **58**(12): 3809-3819.

McCune, W., D. Dedrick, et al. (1990). "Sonographic evaluation of osteoarthritic femoral condylar cartilage: correlation with operative findings." Clinical orthopaedics and related research **254**: 230-235.

Middleton, J. C. and A. J. Tipton (2000). "Synthetic biodegradable polymers as orthopedic devices." Biomaterials **21**(23): 2335-2346.

Milano, G., L. Deriu, et al. (2012). "Repeated platelet concentrate injections enhance reparative response of microfractures in the treatment of chondral defects of the knee: an experimental study in an animal

model." Arthroscopy: The Journal of Arthroscopic & Related Surgery **28**(5): 688-701.

Mithoefer, K., T. McAdams, et al. (2009). "Clinical Efficacy of the Microfracture Technique for Articular Cartilage Repair in the Knee An Evidence-Based Systematic Analysis." The American journal of sports medicine **37**(10): 2053-2063.

Mizuno, H., M. Tobita, et al. (2012). "Adipose-derived stem cells as a novel tool for future regenerative medicine." Stem cells **30**(5): 804-810.

Möller, I., D. Bong, et al. (2008). "Ultrasound in the study and monitoring of osteoarthritis." Osteoarthritis and Cartilage **16**: S4-S7.

Mow, V. C., L. A. Setton, et al. (1990). "Structure-function relationships of articular cartilage and the effects of joint instability and trauma on cartilage function." Cartilage Changes in Osteoarthritis: 22-42.

Munirah, S., O. C. Samsudin, et al. (2007). "Articular cartilage restoration in load-bearing osteochondral defects by implantation of autologous chondrocyte-fibrin constructs: an experimental study in sheep." Journal of Bone & Joint Surgery, British Volume **89**(8): 1099-1109.

Murphy, J. M., D. J. Fink, et al. (2003). "Stem cell therapy in a caprine model of osteoarthritis." Arthritis & Rheumatism **48**(12): 3464-3474.

Murray, R. C., S. Vedi, et al. (2001). "Subchondral bone thickness, hardness and remodelling are influenced by short-term exercise in a site-specific manner." Journal of Orthopaedic Research **19**(6): 1035-1042.

Naredo, E., F. Cabero, et al. (2005). "Ultrasonographic findings in knee osteoarthritis: a comparative study with clinical and radiographic assessment." Osteoarthritis and Cartilage **13**(7): 568-574.

Nehrer, S., M. Spector, et al. (1999). "Histologic analysis of tissue after failed cartilage repair procedures." Clinical orthopaedics and related research **365**: 149-162.

Newman, E., A. S. Turner, et al. (1995). "The potential of sheep for the study of osteopenia: current status and comparison with other animal models." Bone **16**(4): S277-S284.

Niederauer, G. G., M. A Slivka, et al. (2000). "Evaluation of multiphase implants for repair of focal osteochondral defects in goats." Biomaterials **21**(24): 2561-2574.

Nixon, A. J., L. A. Fortier, et al. (2004). "Arthroscopic reattachment of osteochondritis dissecans lesions using resorbable polydioxanone pins." Equine veterinary journal **36**(5): 376-383.

Nukavarapu, S. P. and D. L. Dorcemus (2013). "Osteochondral tissue engineering: current strategies and challenges." Biotechnology advances **31**(5): 706-721.

Oates, K. M., A. C. Chen, et al. (1995). "Effect of tissue culture storage on the in vivo survival of canine osteochondral allografts." Journal of Orthopaedic Research **13**(4): 562-569.

Okamoto, M. and B. John (2013). "Synthetic biopolymer nanocomposites for tissue engineering scaffolds." Progress in Polymer Science **38**(10): 1487-1503.

Oldershaw, R. A. (2012). "Cell sources for the regeneration of articular cartilage: the past, the horizon and the future." International journal of experimental pathology **93**(6): 389-400.

Orth, P. and H. Madry (2013). "A low morbidity surgical approach to the sheep femoral trochlea." BMC musculoskeletal disorders **14**(1): 5.

Orth, P., D. Zurakowski, et al. (2013). "Reduction of sample size requirements by bilateral versus unilateral research designs in animal models for cartilage tissue engineering." Tissue Engineering Part C: Methods **19**(11): 885-891.

Pagnotto, M. R., Z. Wang, et al. (2007). "Adeno-associated viral gene transfer of transforming growth factor-beta1 to human mesenchymal stem cells improves cartilage repair." Gene therapy **14**(10): 804-813.

Pan, Y., Z. Li, et al. (2003). "Hand-held arthroscopic optical coherence tomography for in vivo high-resolution imaging of articular cartilage." Journal of biomedical optics **8**(4): 648-654.

Pearce, S. G., M. B. Hurtig, et al. (2001). "An investigation of 2 techniques for optimizing joint surface congruency using multiple cylindrical osteochondral autografts." Arthroscopy: The Journal of Arthroscopic & Related Surgery **17**(1): 50-55.

Pittenger, M. F., A. M. Mackay, et al. (1999). "Multilineage potential of adult human mesenchymal stem cells." Science **284**(5411): 143-147.

Place, E. S., J. H. George, et al. (2009). "Synthetic polymer scaffolds for tissue engineering." Chemical Society Reviews **38**(4): 1139-1151.

Puppi, D., F. Chiellini, et al. (2010). "Polymeric materials for bone and cartilage repair." Progress in Polymer Science **35**(4): 403-440.

Räsänen, T. and K. Messner (1996). "Regional variations of indentation stiffness and thickness of normal rabbit knee articular cartilage." Journal of biomedical materials research **31**(4): 519-524.

Rodrigues, M. T., M. E. Gomes, et al. (2011). "Tissue-engineered constructs based on SPCL scaffolds cultured with goat marrow cells: functionality in femoral defects." Journal of tissue engineering and regenerative medicine **5**(1): 41-49.

Ruano-Ravina, A. and M. J. Diaz (2006). "Autologous chondrocyte implantation: a systematic review." Osteoarthritis and Cartilage **14**(1): 47-51.

Saris, D. B. F., W. J. A. Dhert, et al. (2003). "Joint homeostasis. The discrepancy between old and fresh defects in cartilage repair. ." Journal of Bone & Joint Surgery, British Volume **85**(7): 1067-1076.

Schnabel, M., S. Marlovits, et al. (2002). "Dedifferentiation-associated changes in morphology and gene expression in primary human articular chondrocytes in cell culture." Osteoarthritis and Cartilage **10**(1): 62-70.

Serra, R., M. Johnson, et al. (1997). "Expression of a truncated, kinase-defective TGF-beta type II receptor in mouse skeletal tissue promotes terminal chondrocyte differentiation and osteoarthritis." The Journal of cell biology **139**(2): 541-552.

Sha'ban, M., S. H. Kim, et al. (2008). "Fibrin and poly(lactic-co-glycolic acid) hybrid scaffold promotes early chondrogenesis of articular chondrocytes: an in vitro study." Journal of Orthopaedic Surgery and Research **3**: 17.

Shapiro, F., S. Koide, et al. (1993). "Cell origin and differentiation in the repair of full-thickness defects of articular cartilage." The Journal of Bone & Joint Surgery **75**(4): 532-553.

Shirasawa, S., I. Sekiya, et al. (2006). "In vitro chondrogenesis of human synovium-derived mesenchymal stem cells: Optimal condition and comparison with bone marrow-derived cells." Journal of cellular biochemistry **97**(1): 84-97.

Shortkroff, S., L. Barone, et al. (1996). "Healing of chondral and osteochondral defects in a canine model: the role of cultured chondrocytes in regeneration of articular cartilage." Biomaterials **17**(2): 147-154.

Siebert, C. H., O. Miltner, et al. (2003). "Healing of osteochondral grafts in an ovine model under the influence of bFGF." Arthroscopy: The Journal of Arthroscopic & Related Surgery **19**(2): 182-187.

Singhvi, R., A. Kumar, et al. (1994). "Engineering cell shape and function." Science **264**(5159): 696-698.

Sittinger, M., D. Reitzel, et al. (1996). "Resorbable polyesters in cartilage engineering: affinity and biocompatibility of polymer fiber structures to chondrocytes." Journal of biomedical materials research **33**(2): 57-63.

Strauss, E. J., L. R. Goodrich, et al. (2005). "Biochemical and biomechanical properties of lesion and adjacent articular cartilage after chondral defect repair in an equine model." The American journal of sports medicine **33**(11): 1647-1653.

Swindle, M. M., A. C. Smith, et al. (1988). "Swine as models in experimental surgery." Investigative Surgery **1**(1): 65-79.

Tang, Q. O., C. F. Carasco, et al. (2012). "Preclinical and clinical data for the use of mesenchymal stem cells in articular cartilage tissue engineering." Expert opinion on biological therapy **12**(10): 1361-1382.

Tibesku, C. O., T. Szuwart, et al. (2004). "Hyaline cartilage degenerates after autologous osteochondral transplantation." Journal of Orthopaedic Research **22**(6): 1210-1214.

Timmins, N. E., M. Kiel, et al. (2012). "Closed system isolation and scalable expansion of human placental mesenchymal stem cells." Biotechnology and bioengineering **109**(7): 1817-1826.

Tremoleda, J. L., M. Khalil, et al. (2011). "Imaging technologies for preclinical models of bone and joint disorders." EJNMMI research **1**(1): 1-14.

Tsai, C. Y., C. L. Lee, et al. (2007). "The validity of *in vitro* ultrasonographic grading of osteoarthritic femoral condylar cartilage- a comparison with histologic grading." Osteoarthritis and Cartilage **15**(3): 245-250.

Tytherleigh-Strong, G., M. Hurtig, et al. (2005). "Intra-articular hyaluronan following autogenous osteochondral grafting of the knee." Arthroscopy: The Journal of Arthroscopic & Related Surgery **21**(8): 999-1005.

Uematsu, K., K. Hattori, et al. (2005). "Cartilage regeneration using mesenchymal stem cells and a three-dimensional poly-lactic-glycolic acid (PLGA) scaffold." Biomaterials **26**(20): 4273-4279.

Uhl, M., A. Lahm, et al. (2005). "Experimental autologous osteochondral plug transfer in the treatment of focal chondral defects: magnetic resonance imaging signs of technical success in sheep." Acta Radiologica **46**(8): 875-880.

Vacanti, C. A. and J. Upton (1994). "Tissue-engineered morphogenesis of cartilage and bone by means of cell transplantation using synthetic biodegradable polymer matrices." Clinics in plastic surgery **21**(3): 445-462.

van Dyk, G. E., L. M. Dejardin, et al. (1998). "Cancellous bone grafting of large osteochondral defects: an experimental study in dogs." Arthroscopy: The Journal of Arthroscopic & Related Surgery **14**(3): 311-320.

Vandeweerd, J. M., F. Hontoir, et al. (2013). "Prevalence of naturally occurring cartilage defects in the ovine knee." Osteoarthritis and Cartilage **21**(8): 1125-1131.

Vanlauwe, J., D. B. F. Saris, et al. (2011). "Five-Year Outcome of Characterized Chondrocyte Implantation Versus Microfracture for Symptomatic Cartilage Defects of the Knee Early Treatment Matters." The American journal of sports medicine **39**(12): 2566-2574.

Vasara, A. I., M. M. Hyttinen, et al. (2006). "Immature porcine knee cartilage lesions show good healing with or without autologous chondrocyte transplantation." Osteoarthritis and Cartilage **14**(10): 1066-1074.

Veronesi, F., M. Maglio, et al. (2013). "Adipose-derived mesenchymal stem cells for cartilage tissue engineering: State-of-the-art in *in vivo* studies." Journal of Biomedical Materials Research Part A **102**(7): 2448-2466.

Von Rechenberg, B., M. K. Akens, et al. (2003). "Changes in subchondral bone in cartilage resurfacingâ€"an experimental study in sheep using different types of osteochondral grafts." Osteoarthritis and Cartilage **11**(4): 265-277.

Wasiak, J., C. Clar, et al. (2006). "Autologous cartilage implantation for full thickness articular cartilage defects of the knee." The Cochrane Library.

Wei, X., J. Gao, et al. (1997). "Maturation-dependent repair of untreated osteochondral defects in the rabbit knee joint." Journal of biomedical materials research **34**(1): 63-72.

Wilke, M. M., D. V. Nydam, et al. (2007). "Enhanced early chondrogenesis in articular defects following arthroscopic mesenchymal stem cell implantation in an equine model." Journal of Orthopaedic Research **25**(7): 913-925.

Woolf, A. D. and B. Pfleger (2003). "Burden of major musculoskeletal conditions." Bulletin of the World Health Organization **81**(9): 646-656.

Wu, Q., K.-O. Kim, et al. (2008). "Induction of an osteoarthritis-like phenotype and degradation of phosphorylated Smad3 by Smurf2 in transgenic mice." Arthritis & Rheumatism **58**(10): 3132-3144.

Yang, P. J. and J. S. Temenoff (2009). "Engineering orthopedic tissue interfaces." Tissue Engineering Part B: Reviews **15**(2): 127-141.

Yang, S., S. Huang, et al. (2012). "Umbilical cord-derived mesenchymal stem cells: strategies, challenges, and potential for cutaneous regeneration." Frontiers of medicine **6**(1): 41-47.

Yang, Y.-G. and M. Sykes (2007). "Xenotransplantation: current status and a perspective on the future." Nature Reviews Immunology **7**(7): 519-531.

Yoshimura, H., T. Muneta, et al. (2007). "Comparison of rat mesenchymal stem cells derived from bone marrow, synovium, periosteum, adipose tissue, and muscle." Cell and tissue research **327**(3): 449-462.

Yousefi, A.-M., M. E. Hoque, et al. (2014). "Current strategies in multiphasic scaffold design for osteochondral tissue engineering: A review." Journal of Biomedical Materials Research Part A.

Zelle, S., T. Zantop, et al. (2007). "Arthroscopic techniques for the fixation of a three-dimensional scaffold for autologous chondrocyte transplantation: structural properties in an in vitro model." Arthroscopy: The Journal of Arthroscopic & Related Surgery **23**(10): 1073-1078.

Zhou, G., W. Liu, et al. (2006). "Repair of porcine articular osteochondral defects in non-weightbearing areas with autologous bone marrow stromal cells." Tissue engineering **12**(11): 3209-3221.